GIS-BASED QUARRY SITE SELECTION AND SUITABILITY ASSESSMENT OF THE ROCK FOR CONCRETE AGGREGATE: CASE STUDY OF ADAMA TOWN

YEABSERA WORKU GENET

A THESIS SUBMITTED TO THE DEPARTMENT OF APPLIED GEOLOGY

PRESENTED IN PARTIAL FULFILLMENT OF THE REQUIREMENT FOR THE DEGREE OF MASTER'S IN ENGINEERING GEOLOGY

SCHOOL OF APPLIED NATURAL SCIENCE

OFFICE OF GRADUATE STUDIES

ADAMA SCIENCE AND TECHNOLOGY UNIVERSITY

June, 2022

Adama, Ethiopia

GIS-BASED QUARRY SITE SELECTION AND SUITABILITY ASSESSMENT OF THE ROCK FOR CONCRETE AGGREGATE: CASE STUDY OF ADAMA TOWN

Yeabsera worku Genet

Advisor

Yadeta Chemdesa (PhD.)

Co-advisor

Shankar Karuppannan (PhD.)

A Thesis Submitted to the Department of Applied Geology
School of Applied Natural Science

Presented in partial fulfillment of the requirement for the degree of master's in Applied Geology (specialization in engineering geology)

Office of Graduate Studies
Adama Science and Technology University

June, 2021

Adama,Ethiopia

DECLARATION

I hereby declare that this Master Thesis entitled "**GIS-Based Quarry Site Selection and Suitability Assessment of the Rock for Concrete Aggregate: Case Study Of Adama Town**" is my original work. That is, it has not been submitted for the award of any academic degree, diploma or certificate in any other university. All sources of materials that are used for this thesis have been duly acknowledged through citation.

Name of the Student	Signature	Date

RECOMMENDATION OF ADVISORS

we, the advisor(s) of this thesis, hereby certify that we have read the revised version of the thesis entitled "**GIS-Based Quarry Site Selection and Suitability Assessment of the Rock for Concrete Aggregate: Case Study Of Adama Town**" prepared under our guidance by Yeabsera Worku submitted in partial fulfillment of the requirements for the degree of Mater's of Science in Engineering geology. Therefore, we recommend the submission of a revised version of the thesis to the department following the applicable procedures.

______________________	______________________	______________
Major-Advisor	Signature	Date
______________________	______________________	______________
Co-advisor	Signature	Date

APPROVAL SHEET

I/we, the advisors of the thesis entitled "**GIS-Based Quarry Site Selection and Suitability Assessment of the Rock for Concrete Aggregate: Case Study of Adama Town**" and developed by Yeabsera Worku, hereby certify that the recommendation and suggestions made by the board of examiners are appropriately incorporated into the final version of the thesis.

______________________ ______________________ _______________

Major Advisor Signature Date

______________________ ______________________ _______________

Co-advisor Signature
Date

We, the undersigned, members of the Board of Examiners of the thesis by Yeabsera Worku have read and evaluated the thesis entitled "**GIS-Based Quarry Site Selection and Suitability Assessment of the Rock for Concrete Aggregate: Case Study of Adama Town**" and examined the candidate during the open defense. This is, therefore, to certify that the thesis is accepted for partial fulfillment of the requirement of the degree of Master of Science in engineering geology.

______________________ ______________________ _______________

Chairperson Signature Date

______________________ ______________________ _______________

Reviewer1 Signature Date

______________________ ______________________ _______________

Reviewer2 Signature Date

Final approval and acceptance of the thesis proposal is contingent upon the submission of its final copy to the Office of Postgraduate Studies (OPGS) through the Department Graduate Council (DGC) and School Graduate Committee (SGC).

______________________ ______________________ _______________

Department-Head Signature Date

______________________ ______________________ _______________

School-Dean Signature Date

______________________ ______________________ _______________

Office of Postgraduate Studies, Dean Signature Date

ACKNOWLEDGMENT

First and foremost, I would like to convey my sincere gratitude to my advisor, Dr. Yadeta Chemdesa, for his unwavering support throughout my MSC studies and research, as well as his encouragement, Supervision and guidance. I would also like to thank my co-advisor Dr. Shankar Karuppannan. Apart from my advisors, I would like to thank Mr. Abity for his assistance during the laboratory portion of these studies; I couldn't imagine doing the lab work without his help.

I would like to show my gratitude to Mr. liben Sisay who has been supportive of my thesis work and I would also like to express my deepest appreciation to my family and friends for their motivation and support throughout my study.

Finally, I would like to thank Adama Science and Technology, Applied Geology department, for giving me this opportunity and providing the necessary support for my thesis.

Contents

List of Table

List of Figures

List of Acronyms

ASTU…..Adama Science and Technology University

GIS……...Geographical Information System

DEM…….Digital Elevation Model

IDW……..Inverse Distance Weighted

AHP……..Analytical Hierarchy Process

ACV……..Aggregate crushing value

LAAV……Los Angeles abrasion value

AIV………Aggregate impact value

SSSV…….Sodium sulphate soundness value

WFB……...Wenji fault belt

MER………Main Ethiopian Rift

LULC………Land use land cover

CI…………. Consistency index

CR…………Consistency ratio

Abstract

Aggregates are construction materials derived from primary resources either by crushing sound rock (crushed stone aggregates) or naturally occurring unbound clastic sediments (natural sand and gravel aggregates). It is one of the main constituents of the construction industry. It is used to produce concrete, which is one of the versatile and widely used building materials in the construction industry. Consequently, the aggregate demand is escalating related to the rapid development of high-rise buildings, road & railway construction, etc. (Adinkrah-Appiah et al., 2016). They are produced by a process called quarrying, which is one of the processes that highly affect the environment, so for their production, a suitable quarry site that has less influence on the environment and that is economically feasible must be selected. Aggregate quality assessment is also important to ensure aggregate good performance for the intended use. This study aims to select a suitable quarry site that qualifies as a concrete aggregate for various construction projects in Adama town and surrounding areas. The most suitable quarry sites were identified by using integrated GIS and AHP approaches in two stages. In the first stage, the selection was carried out based on criteria that govern the economic and environmental aspects of the quarry site, such as land use and land-cover, distance to the built-up area, depth to ground water, distance to streams/water bodies, distance to roads, relative relief, and slope angle. Then, the suitable quarry sites were further refined, considering the availability of suitable lithology for aggregate. The result suggests that 72.5% of the study area is unsuitable, 0.53% of the study area has low suitability, 3.24% of the study area is moderately suitable, and 23.64% highly suitable for crushed stone aggregate. After the suitable sites were identified, rock samples were collected from highly suitable sites for quality assessment. Aggregate physical property tests; strength tests, including aggregate crushing value (ACV), Los Angeles abrasion value (LAAV), aggregate impact value (AIV); chemical characterization for soundness, and petrographical analysis were the parameters considered in the study. Based on the result, the ignimbrite rock Q1, the basalt rock in Q6, and the basalt rock in Q7 exhibit a remarkable quality that complies with the standard to be used as a crushed stone aggregate.

Key words: Aggregate, Quarry site, GIS, Quality assessment, Petrography

CHAPTER ONE

1. INTRODUCTION

1.1 Background of the study

Buildings of residential, commercial, industrial and other functions as well as transportation networks are more demanded as the economy and population of the country grows. Therefore exploration, production and consumption of locally available geological materials for construction are thus critical for the development of a country. In the construction industry, aggregate is a major component used for the production of concrete which is a versatile and widely used construction material. Natural aggregates are thus the world's most valuable non-fuel mineral commodity and are the third most utilized resource after air and water (Lüttig, 1994). The rising demand for these resources necessitates more investigation in areas rich in rock minerals in order to find new possible source of rocks. However, like all industrial operations, this activity has the potential to have an environmental impact primarily related to biodiversity, ecosystems and landscape. Therefore, exploration must be carried out in an environmentally sustainable manner because quarry activities, by their very nature, pose a threat to the landscape and ecosystem (Langer, 2001).

The selection of quarry sites, as well as their operations and administration in most African countries does not take environmental sustainability into account (Darwish *et al*., 2011) which results in land collapse, land conversion and environmental contamination (Pal and Mandal, 2017). Poor resource extraction and quarry closer to residential areas may also have an impact on people living in surrounding communities. As a result, for effective quarry operations, competent site selection, quarry planning and management is necessary in addition to quality control and long-term environmental management (Egesi & Nwosu, 2018; Gudissa *et al*., 2021). Hence, suitable quarry site selection depends on multiple factors that govern the economic and environmental aspect of the quarry site, such as weathering grade, the thickness of overburden at the proposed quarry site, land use and land-cover, accessibility, distance to the built-up area, distance to streams/water bodies, distance to roads, relative relief and slope angle (Bayisa *et al*., 2015;Gudissa *et al*., 2021).

Technical, social, economic and environmental issues shall be considered for suitable quarry site selection (Ming'ate & Mohamed, 2016). This in turn, makes quarry site selection more challenging and places significant limits on decision-makers when it comes to selecting a good quarry site particularly for large areas. In such circumstances, multi analytical approaches, such as AHP (Analytical hierarchy process), can be used in a GIS (Geographic information system) system to select suitable sites considering various factors. Previous works have used the technique to select suitable quarry sites (Gudissa *et al*., 2021) and landfill sites (Dimopoulou *et al*., 2013; Akanwa *et al*., 2017).

Following the identification of a suitable quarry site, the subsequent stage in the evaluation process is to assess the quality of the aggregate using various physical and mechanical parameters of the source rock (Raisanen *et al*., 2006). Since, the aggregate performance and applicability is primarily influenced by the type and physio-mechanical properties of the rock and the aggregates themselves (Smith and Collis, 2001; Naeem *et al*., 2014; Engidasew and Abay, 2016; Khaleghi *et al*., 2019). Therefore, aggregate quality assessment is important to ensure aggregate good performance for the intended use. It has to meet a number of specifications related to strength and durability. The mechanical properties, physical properties and qualities of aggregates are commonly evaluated by using different laboratory tests (Waltham, 1994; Abd & Ahmed, 2015), such as aggregate crushing test, aggregate impact test, aggregate abrasion resistance test, aggregate water absorption, soundness, flakiness Index, elongation Index, specific gravity, density test, etc. The current study aims to select suitable quarry sites around Adama-Dera area and apply standard laboratory tests to assess physico-mechanical properties of the rocks, in terms of their suitability as concrete aggregates.

1.2 Statement of the Problem

Adama town, which is located in the Main Ethiopian Rift valley, is one of the major and densely populated towns in Ethiopia. The urbanization and infrastructure developments in the town and surrounding areas are increasing very rapidly which would undoubtedly demand high tonnage and quality construction material. Crushed stone aggregate is the major construction material that makes up most of the engineering works. It accounts for 70% of the volume of the concrete and 90% of the volume of the pavement. Therefore, it is important to identify in-situ hard-rock aggregate sources that could potentially be developed into quarries in the near future in order to meet this demand.

The decision on the suitability of aggregate for any utilization needs both comprehensive physical and mechanical characterization and a detailed petrological study. There was no proper characterization of the rocks around the town towards their physical and mechanical properties for which purpose they are best suitable and preferable. Hence, it is important to assess the future potential sites and existing quarries currently used as aggregate source with regard to its suitability in view of the current tight standards and specifications. Otherwise, the long-lasting performance of the structures may be affected by poor aggregate quality. Therefore, the present work aimed at select suitable quarry site around Adama town in terms of its suitability, economic feasibility, and adherence to environmental standards.

1.3 Objective of the Study

1.3.1 General objective

The overall objective of this research work is to investigate the suitability of rocks around Adama town as a potential source of crushed stone aggregates for various construction projects.

1.3.2 Specific objectives

- To identify suitable quarry sites (preliminary quarry site selection) using multi-criteria selection approach in GIS environment;
- To determine the physico-mechanical properties of crushed stone aggregate from suitable and existing quarry sites;
- To evaluate the physical and mechanical properties of aggregates with reference to standards, specifications and assess their suitability as a concrete aggregate;
- To conduct petrographic analysis of the rock samples and correlate this with the engineering geological behaviors of rocks.

1.4 Significance of the Study

The rapid development of construction in Ethiopia, including the study area, has created high demand for crushed stone aggregate. Therefore, with the current increasing demand for rocks as construction materials, it is critically important to explore, produce and utilize locally available geological materials for construction. This study will select the most suitable quarry sites based on multiple criteria that govern the economic and environmental aspect of quarrying activity. In addition, a detail investigation of aggregate properties is very important to assure that the best type of rocks with high quality aggregate is selected for the construction of engineering structures which in turn ensures the long-lasting performance of engineering structures.

CHAPTER TWO

2. LITERATURE REVIEW

2.1 Aggregate

The construction and building industries, which are vital to the development of any modern society, rely significantly on mined and quarried raw materials such as gravel, sands and crushed rocks (aggregates) (Langer, 1988; Langer, 1993; Bolen and Tepordei, 2001). Aggregates are construction materials made from primary resources such as sound rock masses which are broken into aggregates (crushed stone aggregates) or naturally occurring unbound clastic deposits (natural sand and gravel aggregates). Aggregates are a critical component in the production of concrete, road materials, railway ballast and other ancillary goods in the construction sector (Adinkrah-Appiah *et al*., 2016). Natural aggregates are the world's most valuable non-fuel mineral commodity and are the third most utilized resource after air and water (Lüttig, 1994). It is currently the most abundant mineral raw material used by human beings (Fookes, 1991; Přikryl, 2017). The rising demand for these resources necessitates more investigation in areas rich in rock minerals in order to find new possible source rocks. They are produced by a process called quarrying.

2.2 Stone quarrying

Quarrying began in the early twentieth century and was carried out near water sources, farming, and human settlements rather than in isolated regions (Kakulu, 2003). Stone quarrying is a type of land use in which non-fuel and non-metal materials are extracted from rocks (Lad and Samant, 2014). It is commonly done in an open-cast method with rock drills, dynamite explosions, and other ways (Lad and Samant, 2014). Gamal El-Dine *et al*., (2009) describes a quarry as a type of open-pit mine from which rock or minerals are extracted. Coppin and Bradshaw, (1982) also states that quarrying is an open cast excavation from which fairly massive and deep deposits of hard or soft rocks are extracted. Quarries are made when big deposits of commercially helpful minerals or rocks are found close to the earth’s surface and it is commonly done in an open-cast approach with rock drills, dynamite explosions and other ways (Lad & Samant, 2014). On the other hand, quarrying is a short-term activity with long-term consequences. It carries with it the promise of wealth and jobs, but it also has a tremendous environmental cost.

2.3 Environmental impact of quarrying

Stone quarrying is an important industry that mines and produces stone. For many individuals, stone mining is their primary source of income, and it plays a critical part in the economic growth of many countries. Nonetheless, like with all industrial operations, this activity has the potential to have an environmental impact (Ozcan *et al*., 2012; Gabarrón *et al*.,2019).

Quarrying has inevitable effects on the safety and sustainability of the environment. Sati, (2015) states that stone quarrying, whether small or large scale, is inherently disruptive to the environment, producing enormous quantities of waste that can have noxious impacts for decades and that the environmental deterioration caused by stone quarrying occurs mainly as a result of inappropriate and wasteful working practices and rehabilitation measures. Maponga and Munyanduri, (1998) argued that quarrying negatively affects the environment in a variety of ways during exploration and blasting, transportation and disposal of waste rocks. The level of land degradation caused by stone quarrying in Ghana has put forth questions as to whether or not the activity should be allowed to continue (Nartey *et al*., 2012).

Sreenivasa and Ravanu, (2014) hold the view that the major impacts of quarries to the environment are water pollution, land degradation, noise pollution, vibrations and landslides. To them, this could directly or indirectly affect human life and the environment. Chizoro *et al*., (1997) emphasize that quarrying has land use policy implications; it is agriculture vs. quarrying because coexistence of agriculture, often is a source of conflict over traditional uses of land. He also added that clearing land to develop access roads and open up mining sites destroys habitats for wild animals, reduces grazing, and reduces sources of plant life for human beings and animals.

Quarries can also be a cause for water table alterations where the quarries go deep enough to affect groundwater aquifers (Ajagbe *et al*., 2015). The formation of ponds at quarry sites is also a common feature in abandoned quarry sites. If the protective soil cover or unsaturated rock is removed, the hole created by the mining may move surface water to the groundwater system. As a result, the quantity and physical and chemical quality of surface water and groundwater may be affected and flows can be increased or decreased and may be contaminated by runoff or dust from the quarry (Abate, 2016).

Dust from quarry sites is a major source of air pollution, although the severity will depend on factors like the local microclimate, the concentration of dust particles in the ambient air, the size of the dust particles, and their chemistry (Emil, 2010). In fact, four million people have been reported to die yearly from acute respiratory problems in developing countries, the most part being aggravated by environmental pollution emanating from quarrying, sandblasting, and emission of dangerous chemicals (Carney, 1998; Langer , 2001 and Asante *et al*., 2014). Abate, (2016) also identifies fatal accidents, physical injuries, and respiratory diseases such as silicosis and tuberculosis as some health problems confronting workers in the quarry industry.

Nevertheless, with careful planning and management, it is possible to minimize the effect on the environment (Tanko, 2007). Therefore, to achieve the equilibrium between natural ecosystems, project planning, formulation and implementation are needed to avoid the impact of stone quarries on the environment and living community (Awoke *et al*., 2018).

2.4 Site suitability analysis

The term "Site suitability assessment" refers to an assessment of land performance to derive maximum benefits with minimum degradation when used for a specific purpose. This assessment involves many biophysical factors that directly or indirectly control the ability of this part of the land to host the land use under investigation. Performing land suitability evaluation and generating maps of land suitability for agricultural or non-agricultural uses will facilitate to reach sustainable agriculture (FAO, 1976; Vargahan *et al*., 2011; Rabia and Terribile, 2013). Dengiz *et al*., (2003) stated that land evaluation studies are of great importance in guiding decisions on land uses in terms of their potential and conserving natural resources for feature generations. Therefore, suitability is a function of land use requirements and land characteristics (Mustafa, *et al*., 2011). That's why suitability is a measure of how well the qualities of a land unit match the requirements of a particular form of land use (FAO, 1976).

2.4.1 Site Suitability Analysis using GIS

One of the most widely used GIS applications in urban planning and management is site suitability mapping and analysis (Brail and Klosterman, 2001). Site suitability analysis with GIS has been used in a range of areas additional to planning, such as land suitability for plant species, animals, agriculture, geological investigations, environmental impact assessments, and landscape planning and design (Malczewski, 2004).

GIS site suitability analysis has been a major instrument for planners to combine the components of environmental, regional, and urban planning development sectors throughout the previous fifty years (Braila and Klosterman, 2001). GIS overlay techniques were first employed as the major root of land suitability study approach by American planners in the late eighteenth century (Xu and Li, 2014). GIS overlay technique was enhanced by Woodfin, (1993) to, which maps with both human-made and natural data and qualities with dark and light coloring to highlight the suitability analysis to the area of interest. This method has been known as a classical overlay method in GIS. The overlay tool plays an important role in a lot of GIS applications that are related to site suitability, such as multi-criteria decision analysis (MCDA), visualization methods, artificial intelligence (AI) geo-computation methods, and Web-GIS (Xiao *et al*., 2002).

Site suitability analysis is not only the planners' point of view, but it is considered as a collective opinion for different parties such as citizens, professional interest groups, developers, policymakers, and others. It cannot be summarized that site suitability depends only on GIS procedure, but also it includes other professionals' and users' approaches (Jafari and Zaredar, 2010).

Finally, it can be summarized that GIS-based site suitability analysis is considered as a process of converting data into useful information that gives the decision maker great support to take the right planning decision. GIS overlay technique is also considered as one of the useful tools that support MCDM in site suitability analysis and has the capabilities of combining the data into map-based GIS operations to be helpful in answering questions related to the land-use suitability analysis (Broesamle *et al*., 2001).

2.4.2 Integration of multi-criteria decision making with GIS for site suitability analysis

MCDM has been integrated with GIS to create an overlay map approach and query the database of this overlay map by combining distinct views for all development sectors expertise (Xu and Yang, 2001). The combination of MCDM with GIS techniques has the capacity to transform both geographical and non-spatial data into a fully supported decision, which can be a useful tool for planners (Temiz and Tecim, 2009).This is given that the MCDM technique can support the GIS capabilities for data analysis, recapture, repository, manipulation and acquisition and GIS can successfully deal with combining different views for planner participants and reach the best decision from this combination. Site suitability analysis is one of the key issues that both MCDM and GIS can effectively address. MCDM is not only integrated with the GIS overlay vector application but it is also integrated with the raster analysis application for evaluating the site suitability analysis resulted in features using the weighted sum technique in order to assign successful weights to the various planning dimensions (Xu and Yang, 2001).

In site suitability analysis, recent researchers have developed approaches that integrate the GIS with MCDM throughout the last decade (Aydin *et al*., 2013). These approaches are fuzzy logic techniques, neural networks techniques, evolutionary algorithms and Cellular automata. Regarding the fuzzy logic technique, one of the main criticisms that face integrating both GIS with MCDM in the site suitability analysis field is importing the accurate input data for the area of interest, which is, of course, unrealistic (Ning *et al*., 2016).

From multi-criteria decision-making methods, value measurement approaches such as AHP, weighted sum method and weighted product method, which are basically utility-based models, are mainly used in site suitability analysis. Apparently, the weighted sum technique has the flaw of merely providing a basic estimate of one's preference function or failing to integrate numerous preferences. The weighted product technique, on the other hand, produces undesired results since it prioritizes or de-prioritizes the alternative that is not average (Dey *et al*., 2008). Thus, to apply multiple factors, the systematic framework through AHP technique which was initially developed by Saaty, (1977) can be applied in a GIS environment. It offers a flexible and simple method of assessing complex problems, allowing both subjective and objective aspects to be incorporated in to the decision-making process (Vaidya and Kumar, 2006; Dey and Ramcharan, 2008 ; Dimopoulou *et al*., 2013; Jablonsky, 2015; Kou *et al*., 2016; Haile and Suryabhagavan, 2019).

Lately, multi-attribute evaluation methods have been successfully implemented in the planning field using GIS as a successful tool to apply that kind of analytic hierarchy analysis to finally reach the optimum planning decisions (Brail and Klosterman, 2001). Analytic hierarchy analysis has a closed relationship to site suitability analysis as it can be implemented to assign the weights of suitability for map attribute that can be presented by means of raster data to be ready for the weighted sum technique. It can also help in determining the priority level of the planning points included in site suitability analysis (Chaudhary *et al*., 2016). The method has been adopted in previous works for a selection of mining methods (Ataei *et al*., 2008; Mandal and Mondal, 2016), land fill sites (Yoxas, *et al*., 2011; Zelenović *et al*.,2012; Ebistu and Minale, 2013 ; Dimopoulou *et al*., 2013; Khan and

Samadder, 2015; Chabuk *et al*., 2016a; Chabuk *et al*., 2017; Akanwa *et al*., 2017; Chabuk *et al*.,2019 and Alkaradaghi *et al*., 2019) and for groundwater recharge site (Rajasekhar, *et al*., 2019).

2.5 Quarry site selection

Quarry site selection is the process of selecting a suitable quarry site that qualifies various criteria set for economic feasibility and environmentally safe extraction of the geologic material.

Bayisa *et al*., (2015) conducted research on the selection of suitable quarry sites for Ambo-Ijaji Railway Project in Central Ethiopia. In this study, the selection criteria were formulated by considering parameters such as slope, distance of the site, overburden soil thickness, land use/land cover, general accessibility, and rock type with its degree of weathering. In total, six quarry sites were initially identified by considering the suitable rock type and optimum distance from the proposed rail line alignment. Later, the general selection criterion was formulated and was applied in the GIS environment to identify suitable quarry sites. And to determine the overall suitability of each quarry site based on the six evaluated parameters, equal weights were given to the parameters, and later their average value was calculated. According to the average evaluation results, all quarries were identified as suitable except for one quarry which is identified as highly suitable.

Barakat *et al*., (2016) have conducted similar work in the identification of potential areas of Tadla-Azilal Region hosting aggregate resources. Barakat *et al*., (2016) stated that many environmental, social, and economic factors, including rock lithology, land use, distance to cities and to roads, elevation, and slope, are considered in order to prevent conflicts between land users. These factors were mapped using the GIS technique and weighted by comparing them with each other according to their importance. Based on the results of this study, various aggregate potential areas in the Tadla-Azilal region have been selected, and each one has been assigned three categories (suitable, moderately suitable, and unsuitable), representing their suitability levels for future development in terms of the environmental constraints, availability of transport networks, current land use and availability of mineral reserves.

Gudissa *et al*., (2021) also conducted research on quarry site selection utilizing GIS and AHP methods around Harer and DireDawa. According to this study, optimal site selection for quarry operation is governed by factors such as the availability of suitable lithology, land form, nearness to demand centers, environment, and socio-economic considerations. Thus, seven criteria were formulated: lithology, land use and land cover, distance to buildup areas, distance to water bodies, distance to roads, relative relief and slope angle for preliminary quarry site selection. AHP method of pair-wise comparison matrix was used to assign the weights to each of the considered factors. And Arc GIS was used for weighted overlay analysis of maps by considering selected factors to produce the preliminary quarry site suitability map for the study area for all available lithologies. Gudissa *et al*., (2021) further conducted a detailed investigation on suitable preliminary areas to produce a total estimated suitability map. Different parameters, such as unconfined compressive strength, rock quality designation, and geometrical properties of discontinuity were collected during a detailed field survey from preliminary, highly, and moderately suitable sites. Rock mass classification systems such as rock mass rating (RMR) and slope mass rating (SMR) were used to assess rock mass quality and slope stability, respectively. The weighting scheme approach is then applied and the ratings assigned to each factor (RMR, SMR, reserve, depth to water table and overburden thickness) were summed up to produce a total estimated suitability (TES) map. The map showed that about 40.4% of the preliminary suitable sites are unsuitable, 20. 3% are moderately suitable, 14.7% are highly suitable and 24.7% are most suitable.

The physical, mechanical, and petrographic property of an aggregate affects their performance. Thus, after the selection of suitable quarry site the next component of evaluation is to determine the quality of ballast rock based on different physical, mechanical and photographic properties of the source ballast rock (Raisanen *et al*., 2006).

2.6 Correlation between the properties of an aggregate with the performance of concrete

Aggregate constitutes 75% of the total volume of the concrete mix (de Castro Pessoa *et al*., 2015). Thus the performance of the concrete highly depends on the property of the aggregate. Not only may the aggregate limit the strength of concrete but also greatly affect the durability and structural performance of concrete (Prajapati and Karanjit, 2019).

Lindqvist *et al*., (2007) stated that the engineering properties of rocks could be assessed through their intrinsic properties, including texture and mineralogy. Räisänen, (2004) reported that the mechanical properties of rocks are significantly influenced by the abundance of fine-grained minerals, grain-size distribution and degree of interlocking of grain boundaries of minerals. Similarly, Irfan, (1996) noted that the properties of rocks are influenced by the mineral composition, texture, fabric, and weathering state. On the other hand, Sajid and Arif, (2015) concluded that variations in the mechanical properties of rocks are largely associated with differences in their textures and modal mineralogical compositions.

The variations in the aggregate mechanical properties will in turn affect the performance of aggregate when used in concrete. According to Ajagbe *et al*., (2015), the quality of the coarse aggregates is essential when considering the quality of the concrete itself. Research indicated that changes in coarse aggregate can change the strength and fracture properties of concrete (Kozul and Darwin, 1997). Wei and Faguang, (2011) indicated that the mechanical properties of coarse aggregate have varying degrees of influence on drying, shrinkage, creep and temperature crack of concrete. The study confirmed the possibility of cracking of concrete prepared by aggregate with low density is much bigger than concrete prepared by aggregate with high density. The properties of coarse aggregates grossly affect the durability and structural performance of concrete.

CHAPTER THREE

3. MATERIAL AND METHOD

3.1 Methodology

The methods and approaches used for suitable quarry site selection and characterization include Data collection, reconnaissance survey, Preparation of thematic layer, assigning of weights to each layer and reclassification of the thematic layers, Weighted overlay analysis for the preparation of the preliminary quarry site suitability map without the inclusion of the lithology and map algebra for intersecting the areas with suitable lithology (consolidated rock) and preliminary suitable quarry site to produce the final quarry site suitability map. The procedures followed to identify the quarry suitability map is summarized in Figure 3.1 Finally, rock block samples were collected from a suitable quarry site, sample preparation (such as crushing and coring of the cylindrical sample) and laboratory test were conducted to determine the physico mechanical properties of the intact rock and crushed rock aggregate.

3.1.1 Data collection

Two different means are used to acquire the data needed to prepare the suitability map. That is, remotely sensed data such as satellite images with 10m resolution of the study area and Google earth images were used to generate data such as built-up area, road network, water body, and land use /land cover of the study area. The rest of the data for suitability map preparation were taken from previous literature, East Shewa water and mineral that is the lithology and the static water level of the study area respectively.

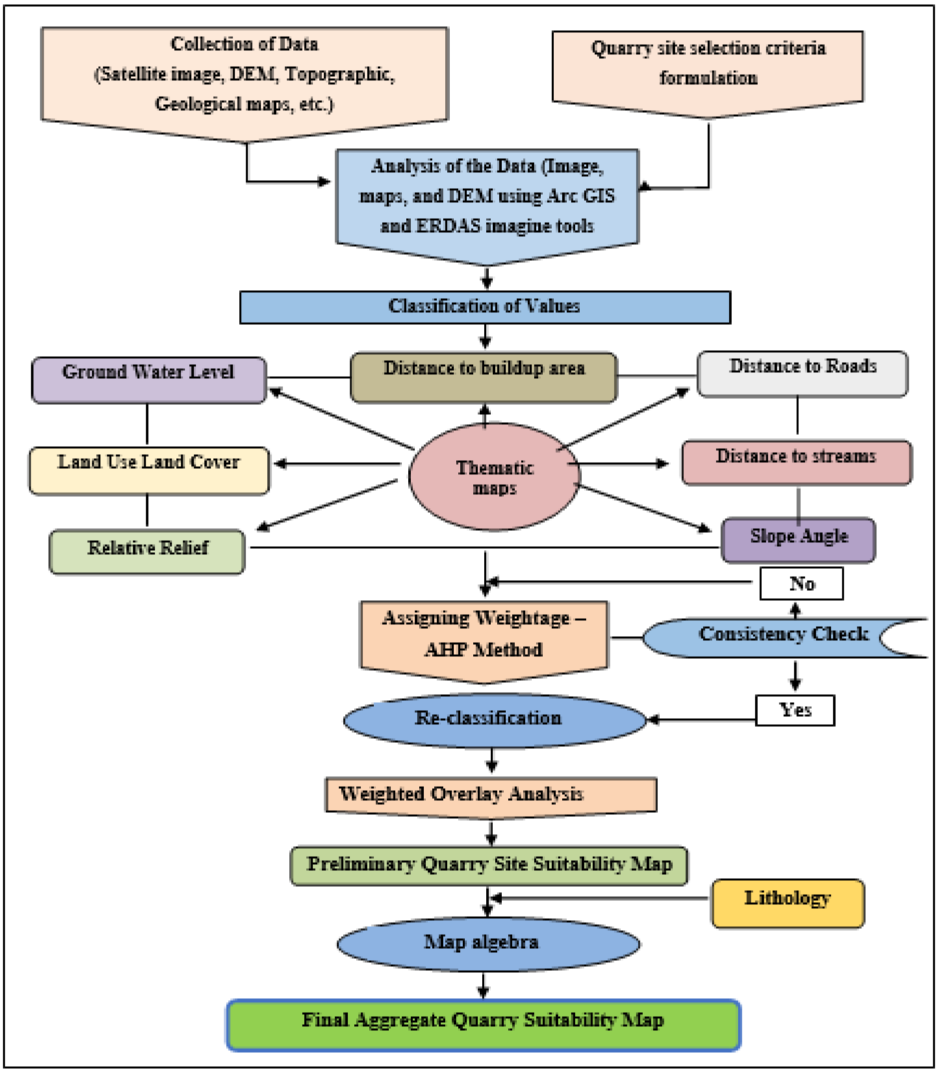

Figure 3.1: Flow chart showing the methodology followed in selecting suitable aggregate quarry site (Modified from Gudissa *et al*., 2021)

3.1.2 Data pre-processing

For suitable quarry site selection, eight parameters were considered that is lithology, land-use and land-cover, distance to the built-up area, distance to streams, water bodies, distance to roads, relative relief, depth to ground water, and slope angle. The data for lithology was prepared by digitizing Adama-Dera geological map of 1:50,000 scale from previous work done by Alula *et al*., (1992) and was later modified after field survey in order to prepare the geologic map of the study area. The land use land cover map was produced from a satellite image of 10m resolution by Supervised classification method in which training sample of the pixels representing each land use land cover class present in the study area was assigned and then the image was classified using Maximum likelihood classification method to produce the final Land use land cover model of the study area. The data collected from the satellite images and topo sheet (1:50,000 scale) in vector format that is the representative shape files such as built-up area, streams and road network are converted into raster data by using arc tool box spatial analyst tool that is Euclidean distance in order to create a thematic map of distance to build-up area, distance to water body and distance to road respectively. Aster DEM of 30m pixel size that is resampled in 10m resolution is used to extract the slope angle and the relative relief of the study area. The thematic map representing the static water level or ground water depth is generated using the borehole data obtained from East Shewa water and mineral and from previous work (Taye, 2007). The point data were added to the ArcMap platform, and continuous data of ground water depth (GWD) of the study area was created by interpolating the water points using IDW in the spatial analyst tool. The thematic maps were then projected with the same projection that is the Adindan UTM 37N zone and was produced in the same pixel size of 10 m resolution, and the vector layers were converted into raster to create favorable conditions for the overlay analysis.

3.1.3 Assigning of weights

For assigning weights, multi-criteria analytical approach called Analytical hierarchy process was used to support the decision. It is fundamentally based on complex calculations using matrix algebra. It was developed by Saaty, (1970) and allowed the decomposing of a complex problem into a hierarchical system, in which binary combinations are established at each level of the hierarchy (Ali *et al*., 2017). The combination of geographic information systems and the analytical hierarchy process is a powerful tool for developing future policies relevant to urban growth (Aburas *et al*., 2015) and greatly simplifies the decision-making process (Serbu *et al*., 2016). It is one of the most comprehensive systems designed for making multi-criteria decisions, as it allows problems to be developed hierarchically. This combination is versatile and strong method for the qualitative and quantitative examination of multi-criteria situations (Lyu *et al*., 2018)**.**

The complex multi-criteria decision-making problem was initially broken down into a hierarchy of interrelated decision elements (criteria, decision alternatives). Since with the AHP, the objectives, criteria, and alternatives are arranged in a hierarchical structure. Once the problem had been decomposed, and the hierarchy was constructed, prioritization of the criteria, in order to determine the relative importance of the criteria within each level, was established. That is Pair wise comparison matrix of each element within each level was constructed. In AHP, multiple pairwise comparisons are based on a standardized comparison scale of nine levels, Table 1. Let C = {Cj | j = 1, 2,.., n} be the set of criteria. The result of the pairwise comparison on n criteria can be summarized in an (n _ n) evaluation matrix A in which every element aij (i, j = 1,2, . . ., n) is the quotient of weights of the criteria, as shown in equation 3.1:

$$A = \begin{Bmatrix} a11 & a12 & \ldots & a1n \\ a21 & a22 & \ldots & a2n \\ M & M & 0 & M \\ & & & \\ an1 & an2 & \ldots & ann \end{Bmatrix} \quad aij=1,\ aji\text{-}1/\ aij,\ aij\neq 0 \ldots\ldots \text{Eqn (3.1)}$$

Table 3.1: Nine point's intensity of importance and their description

Definition	Intensity of importance
Equally important	1
Moderately more important	3
Strongly more important	5
Very strongly more important	7
Extremely more important	9
Intermediate value	2,4,6,8

This pair-wise comparison permits an independent rating of each factor's contribution, which simplifies the decision-making process (Adewumi *et al.*,2019). Pair-wise comparison was followed by the mathematical process that commences to normalize and find the relative weights for each matrix. And the relative weights are given by the right eigenvector (w) corresponding to the largest eigenvalue (λ-max), as:

$$Aw = \lambda \max w \ldots\ldots \text{Eqn (3.2)}$$

If the pairwise comparisons are completely consistent, the matrix A has rank 1 and λ max = n. In this case, weights were obtained by normalizing the rows or columns of 'A'.

The quality of the output of the AHP is strictly related to the consistency of the pairwise comparison judgments. Thus the consistency is defined by the relation between the entries of A: aij × ajk = aik. The consistency index (CI) is:

$CI = (\lambda\ max - n)/\ (n - 1)$…………………………………………………………...Eqn (3.3)

The consistency of the weight for various factors was checked through a single numerical value, the consistency ratio (CR), which measures the level of the inconsistency of the pair-wise comparison matrix (i.e. the likelihood of whether factor weights were randomly assigned). It is calculated as the ratio of the CI and the random index (RI), as indicated:

$CR = CI\ /\ RI$…………………………………………………………………….............Eqn (3.4)

The number 0.1 is the accepted upper limit for CR. If the final consistency ratio exceeds this value, the evaluation procedure has to be repeated to improve consistency. The measurement of consistency can be used to evaluate the consistency of decision-makers as well as the consistency of the overall hierarchy.

The considered factors for preliminary quarry site suitability map preparation, their significance, and relative order of importance is presented in Table 3.2.

Table 3.2: Factors for the selection of quarry sites and their order of importance modified after Gudissa *et al*., (2017).

S/n	Factors	Significance	Order of importance
1	Land use and Land cover	The environmental code of practices preserves and protects cultural heritages, archeological sites, parks, and built-up areas. Thus, LULC may totally prohibit the development of quarry site even when good quality and quantity material is available.	Extremely strong influence
2	Distance to build up area	Community safety is a sensitive issue that strongly influences quarry site suitability. However, it does not prohibit the development of quarry sites. Quarrying can be possible with appropriate environmental protection and by adopting suitable mitigation measures.	Very strong importance over the rest
3	Depth to ground water	Ground water is one of the major sources of water used for domestic purposes; thus, it should not be disturbed or polluted, so quarrying operation should be in the area where the ground water is present at a greater depth.	Strong influence
4	Distance to water body	Lakes and streams are more susceptible to pollution as runoff from quarry sites flows very rapidly into them. Thus, a safe distance to water bodies needs to be maintained from the quarry sites.	Moderately more important
5	Distance to road	Distance to roads is an important factor. The close proximity of the road to the quarry site may result in dangers of fly rock due to blasting and air pollution. Roads at far distances may result in additional project costs due to the development of new roads and increased transportation cost.	Least important but more important than Relative relief
6	Relative relief	Important from slope instability point of view, flooding potential, ease of excavation, and inaccessibility.	Moderately important than Slope angle
7	Slope angle	Induce slope instability but is not the sole factor that triggers the instability.	Relatively least effect

Table 3. 3: Pair wise comparison matrix and the weight assigned to the seven factors

LU-Land use land cover map, DB-Distance to build-up area, DGW-Depth to ground water, DW-Distance to a water body, DR-Distance to the road, RR-Relative relief, SA-Slope angle

Attributes	LU	DB	DGW	DW	DR	RR	SA	Eigenvector weights	Weights (%)
LU	1	2	3	4	5	6	7	0.350445	35
DB	0.5	1	2	3	4	5	6	0.237508	24
DGW	0.33	0.5	1	2	3	4	5	0.158804	16
DW	0.25	0.33	0.5	1	2	3	4	0.105463	10
DR	0.2	0.25	0.33	0.5	1	2	3	0.069586	7
RR	0.17	0.2	0.25	0.33	0.5	1	2	0.046308	5
SA	0.143	0.17	0.2	0.25	0.33	0.5	1	0.031886	3
Total Consistency Ratio (CR) value of 0.02 consistency is acceptable								1	100

After assigning appropriate weight to the seven criteria, the suitable condition for each criterion were identified and later used for the reclassification of each thematic map.

3.1.4 Reclassification of the thematic layers and weighted overlay

Reclassification of the thematic layers was done using the reclassification tool, which is a tool used to reclassify or change cell values to alternative values using a variety of methods. It is done to make a favorable condition for weighted overlay analysis as different types of raster data in different factor sub-classes may represent different conditions. Thus, by using reclassification for each thematic layer, a ranking scheme based on pre-defined weights was used to work out the least and most suitable conditions (Anbalagan, 1992). All the thematic maps were produced with the same projection and the same resolution or pixel size of 10m to make a favorable condition for weighted overlay analysis. After the layer was reclassified, all of the thematic layers except lithology were overlaid in the weighted overlay tool by integrating them with the weight assigned, and the weighted sum scheme was applied to produce the preliminary suitability map. Then map algebra was used to combine the pixels that were suitable in the preliminary suitability map with the pixels representing the existence of hard rock in the lithology thematic map to produce the final quarry site suitability map.

3.1.5 Detail field survey and sample collection

After the quarry site suitability map was produced, a field survey was conducted to validate the quarry site suitability model and to collect a sample for further laboratory examination of their physico-mechanical and petrographic property. The rock samples were collected from the highly suitable sites in the quarry site suitability model from nine different locations. Approximately 40 kg of rock samples for each site were collected to prepare the sample for the aggregate tests such as aggregate crushing, impact, abrasion, soundness, and shape test. An additional 2 block samples were taken for preparing a core sample for the uniaxial compressive strength test, and one small rock sample was taken for each site to prepare the thin section.

3.1.6 Engineering geological characterization of aggregate

To characterize the suitability of the rock, the samples collected from the nine sites were examined in the laboratory. The engineering properties tested to determine the suitability of the rock as an aggregate in the concrete structure include specific gravity, water absorption, bulk density, flakiness and elongation index, Aggregate Impact test, Aggregate Crushing test (ACV), Aggregate Abrasion Value (AAV) and UCS (uniaxial compressive strength).

3.1.6.1 Aggregate particle shape

The particle shape and surface texture of an aggregate are the major parameters that influence the properties of freshly mixed concrete**.** So, the rock used for an aggregate should examine its shape, that is, Flakiness and Elongation. In this study, aggregate particle shape that is flakiness and elongation was conducted as per BS:812-105.1:1989 and BS:812-105.2:1989, respectively.

The flakiness index of an aggregate sample is determined by separating the flaky particles and expressing their mass as a percentage of the mass of the sample tested. The elongation index is determined by separating the elongated particles and expressing their mass as a percentage of the mass of the sample tested. The test is inapplicable to material passing a 6.3 mm test sieve or retained on a 50 mm test sieve.

In this case, the sample collected from the sites were crushed and sieved, and the aggregate retained on 37.5mm, 28mm, 20mm, 14mm, 10mm, and 6.3mm were considered for the analysis of their shape that is flakiness and elongation and each particle size were weighted.

After weighing, each particle retained on the sieve was passed through the flakiness gauge representing that size then, the mass of the aggregate passing through the gauge was recorded and were used to calculate the flakiness index as shown in equation 3.5

Flakiness index = $\frac{M3}{M2} * 100\%$...Eqn (3.5)

Where,

M2 is the sum of the masses of size fractions that have a mass greater than 5% of the total mass; and

M3 is the mass of all the flaky particles.

For the elongation index, the particle retained on 37.5mm, 28mm, 20mm, 14mm, 10mm, and 6.3mm were passed through the elongation gauge by the elongated side of the aggregate, and the material retained by the gauge is weighted to find the elongation index as per equation 3.6**.**

Elongation index= $\frac{M3}{M2} * 100\%$...Eqn (3.6)

Where,

M2 is the sum of the masses of size fractions that have a mass greater than 5% of the total mass, and M3 is the mass of all the elongated particles.

Figure 3.2: Aggregate shape test instruments

3.1.6.2 Density testing

The bulk density of construction aggregate is expressed as the weight per unit volume, for example, kilograms per cubic meter (kg/m3). In this study the density is determined by water displacement method as per ASTM-D5030 standard. The rock sample was weighted, and a graduated cylinder containing a known volume of water was prepared, and the rock sample was inserted into the graduated cylinder. Then the volume change is observed for determination of the density of the rock, as shown in the equation below.

$V = V_2 - V_1$ ……………………………………………………………………………….Eqn (3.7)

Where V_2 is the volume of the water after the immersion of the test specimen and

V_1 is the volume of water before the immersion of the sample.

$\rho = \frac{M}{V}$, ……. Eqn (3.8), where ρ is the bulk density of the rock

M is the mass of the test specimen

V is the volume of the test specimen

3.1.6.3 Determination of water absorption

Water absorption is defined as the amount of water absorbed by a material and is calculated as the ratio of the weight of water absorbed to the weight of the dry material. In this study, water absorption is determined as per BS:812-2:1995 first, the sample is immersed in water for 24 hours, then the weight of the sample immersed is recorded and the sample is taken out, and water is filled to the full capacity of the container then it’s weighted. Finally, the samples were oven-dried for 24 hours and were left too cool for 2 hours and then weighed to determine the water absorption.

Water absorption= $\frac{C-D}{D} * 100$ ………………………………………………………….Eqn (3.9)

3.1.6.4 Aggregate Impact Value (AIV)

This is the measurement of the aggregate's resistance to repeated and sudden force. For this test, the aggregate samples passing a 14mm sieve and retained on a 10mm sieve were used according to BS 812-112:1990. The measure was filled until it overflowed with the aggregate comprising the test specimen by means of a scoop. The weight of the mold or cylindrical cap was measured. Then the aggregate was placed in the cylindrical steel cup in three layers by tamping with steel road 25 times after the placement of each layer then, the weight of the mold and sample was taken. The cylindrical cup containing the sample is then placed in the impact machine where the test specimen of aggregate were hit 15 times with a standard weight dropped from a fixed height. The aggregate impact value were determined from the proportion of material passing a 2.36mm sieve and mean value of two tests was be taken as shown equation 3.10.

Aggregate impact value = $\frac{M2}{M1} * 100\%$...Eqn (3.10)

Where,

M1 is the mass of the test specimen (in g); and

M2 is the mass of the material passing the 2.36 mm test sieve (in g).

Figure 3.3: Aggregate impact machine

3.1.6.5 Aggregate Crushing Value (ACV)

This is the measurement of the resistance of an aggregate to crushing by compressive force. As per BS 812-110:1990, for this test, aggregate passing 14mm sieve and retained on 10mm sieve were used. The samples were washed so that dust particles attached to the aggregates were removed and they were oven dried at 110^0c until constant mass was reached and then cooled to room temperature. After sample preparation was completed, the test sample was put in the measure and placed in the cylindrical cup in three layers by tamping each layer 25 times. Then the mold containing the sample is placed in a compression machine and was compressed at a constant rate up to 400 KN and the weight of the sample plus the mold is measured, the weight of the mold and weight aggregate passing through a 2.3mm sieve was used for determination of ACV as presented in equation 3.11.

ACV=$\frac{M2}{M1}$*100………………………………………………………………………...Eqn (3.11)

Where, M_2 is the mass of the material passing through a 2.36mm sieve and M_1 is the total mass of the test sample

3.1.6.6 Los Angeles Abrasion Value (LAAV)

Los Angeles abrasion value is a measurement of the resistance to attrition. This test method is a measure of degradation of mineral aggregates of standard grading resulting from a combination of actions including abrasion or attrition, impact and grinding in a rotating steel drum containing a specified number of steel spheres, the number depending upon the grading of the test sample. As the drum rotates, a shelf plate picks up the test sample and the steel spheres, carrying them around until they are dropped to the opposite side of the drum, creating an impact-crushing effect. The contents then roll within the drum with an abrading and grinding action until the shelf plate picks up the test sample and the steel spheres and the cycle is repeated. This test was performed as per BS:812-113:1990. In this study, standard grade B is taken, which is 2.5 Kg of aggregate having a size 20mm to 14mm and 2.5 Kg of 14mm to 10mm size are taken that is a total of 5Kg sample is taken for one test trial. This sample was washed and oven-dried, until it attains a constant mass and was inserted into the drum along with 11 cylindrical steel balls and the Los Angeles machine is rotated at a rate of 33rev/sec for a total of 500 revolutions. Then the weight of the sample retained on 1.7mm sieve is used to determine the Los Angeles abrasion value as in equation 3.11.

LAV=$\frac{M1-M2}{M1}$*100, ………………………………………………………….…………Eqn (3.11),

Where M1 is the total mass of the sample taken andM2 is the mass of the aggregate retained in 1.7mm sieve

Figure 3.4: Los Angeles abrasion machine

3.1.6.7 Soundness Value

Soundness testing is used to identify those aggregates that may be prone to degradation in saturated moisture conditions, elevated temperatures, or freezing conditions. This test method measures the aggregate's resistance to disintegration due to freezing and thawing. The soundness test was performed using an anhydrous sodium sulphate chemical following ASTM.C88-99a, 1999 procedure. First, the sodium sulphate solution is prepared by adding 215g per 1 liter of ionized or distilled water. Then the aggregate of two sizes was prepared, that is 19mm to 12.5mm and 12.5mm to 10mm, having a mass of 670g & 330 g, respectively and were washed and oven-dried until constant mass is reached. The aggregate sample prepared is then socked in the saturated sodium sulphate solution for about 17 hours, then drained, and then oven-dried for 4 hours at 110^0 C to complete the first cycle. A total of 5 cycles of immersion and drying took place as per the standard .After the completion of the last cycle the aggregates were washed with water until the cloudiness of the water clears, and then the sample was dried again in an oven at 110^0C until constant mass has been reached. Then the aggregate was sieved in the sieve that they were retained before the five cycles and the material retained in the sieve was weighed to determine the soundness value of the aggregates, as shown in equation 3.12.

$S=\frac{M2}{M1} * 100$ ……………………………………………………………………………….Eqn (3.12)

Where, $M1$ is the initial mass of the test specimen (in g); and

$M2$ is the mass of material retained on the 10 mm test sieve at the end of the test (in g).

Figure 3.5: Immersion of the sample in sodium sulphate solution and oven drying phase

3.1.6.8 Determination of unconfined compressive strength

Unconfined Compressive Strength (UCS) stands for the maximum axial compressive stress that a specimen can bear under zero confining stress. Due to the fact that stress is applied along the longitudinal axis, the Unconfined Compression test is also known as Uniaxial Compression test. The test samples were retrieved by coring cylindrical samples (Figure 3.6) from rock blocks collected from the field and were selected according to ASTM.D4543-19.And the area of the samples is calculated. Then the test specimen was placed in the compression where the load was applied until it was deformed. The maximum load that caused the deformation is recorded for the determination of the compressive strength, as shown in equation 3.13**.**

$$\sigma = \frac{P}{A} \quad \text{Eqn (3.13)}$$

Where:

σ = Unconfined compressive strength

P = Compressive load of failure and,

A = Cross sectional area

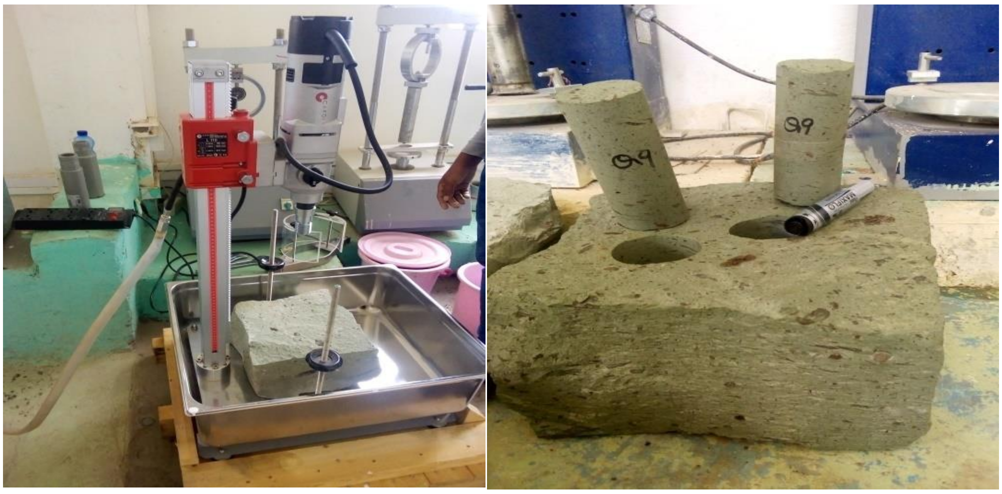

Figure 3.6: Core sample preparation for determination of unconfined compressive strength

3.1.6.9 Petrographic Analysis

The petrographic description of rocks for engineering purposes includes the determination of all parameters which cannot be obtained from a macroscopic examination of a rock sample, such as mineral content, grain size and texture, and which have a bearing on the mechanical behavior of the rock. In this study, thin sections were prepared for the rocks collected from the nine locations at Geological Survey of Ethiopia (GSE), and the thin section was observed by microscope at Addis Abeeba science and technology university (AASTU) to determine the modal mineralogy, texture, and to determine the presence of alkali-silica reactive mineral with the help of an expert in petrography.

Figure 3.7: Optical-microscope used for the examination of the petrography of the samples

CHAPTER FOUR

4. DESCRIPTION OF THE STUDY AREA

4.1 Location and Accessibility

Adama is one of the administrative districts in the East Shewa Zone of the Oromia Regional State of Ethiopia. The study area is located 100 km southeast of Addis Ababa, the capital of Ethiopia, in the northern segment of the main Ethiopian rift valley. Geographically, the area is situated between 39° E to 39°30' E Longitudes and 8°10' N to 8°43' N Latitudes. The study area is accessible by an asphalt road that runs from Addis Ababa to the eastern part of Ethiopia, and that runs from Adama to Asella. The site is also accessible through all weathered and gravel feeder roads from the main road to reach the remaining part of the area.

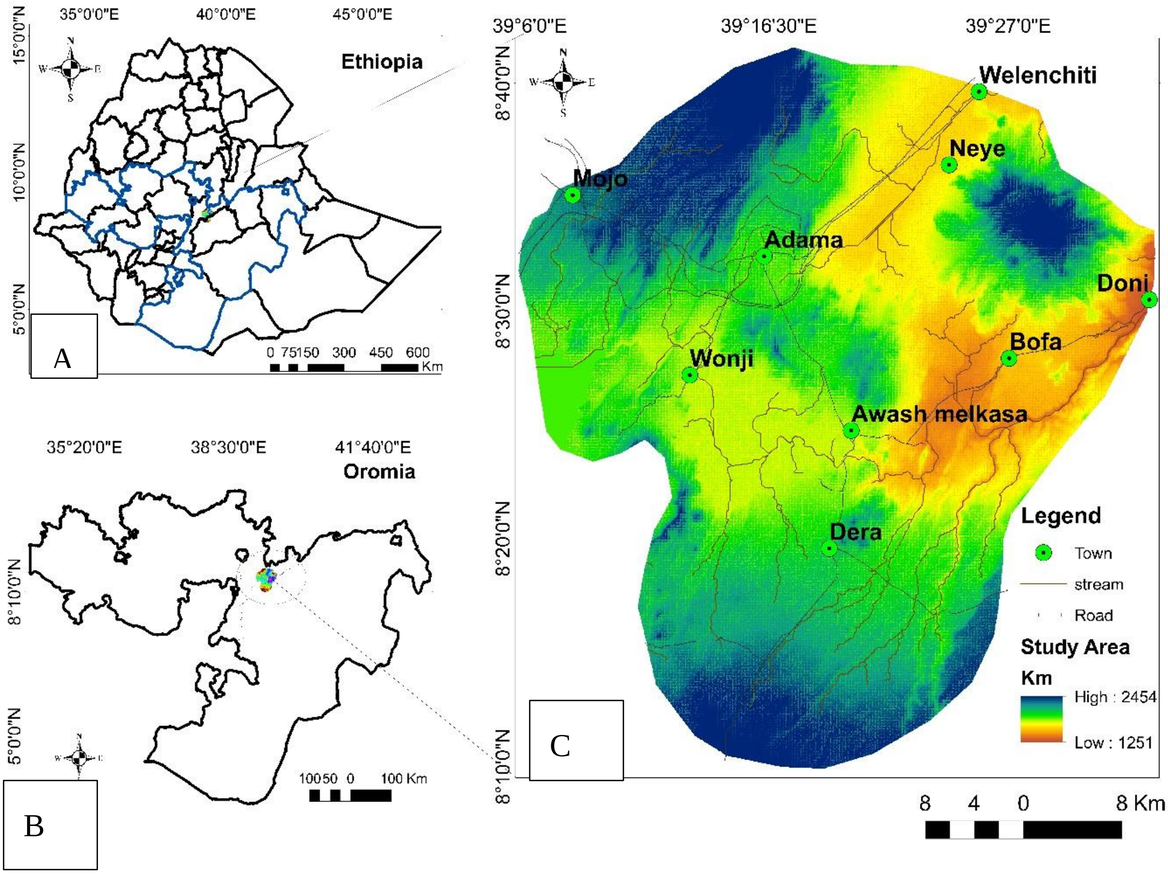

Figure 4.1: a) Ethiopia, b) Oromia, C, study area

4.2 Physiography of the study area

The terrain in the study area is generally rugged, with deeply cut and dissected morphology, undulating topography, and a flat plain with variable slopes. The area's current physiography is primarily the result of past volcano-tectonic activities and the depression of primarily fluvial and lacustrine origin sediments. As a result, fault scarps, fault-controlled grabens that are frequently covered with sediments, horsts, volcanic domes, and cones are the main morphology of the area (which is mostly elongated in the NNE direction).

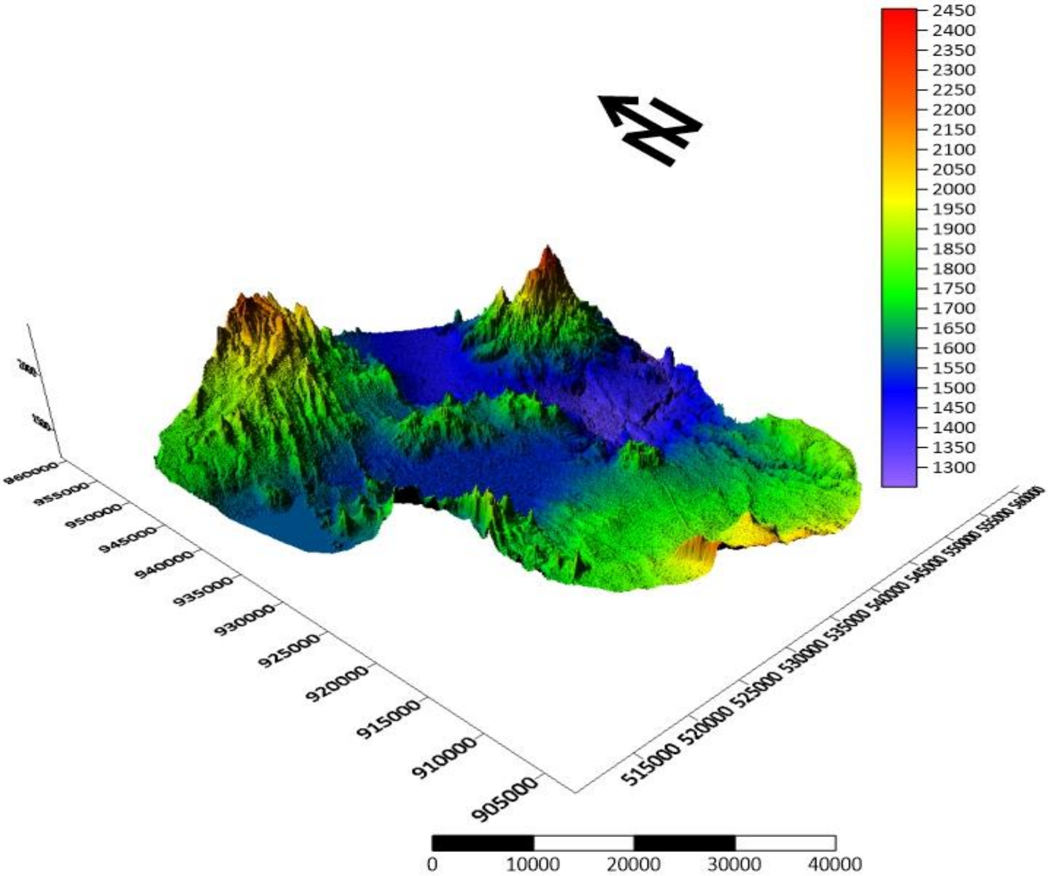

Figure 4.2: Physiography of the study area using DEM

4.3 Climate

The examined area has a warm environment, with an average annual temperature of 21.2 ^{0}C and an average annual rainfall of 881.9mm. The highest temperature occurs during March, April, May, and June, whereas November, December, and January have low temperatures. The Mean monthly average temperature ranges from 19.33°c to 23.54°c, which shows almost the same variation throughout the year. High rainfall occurs in July and August, covering around 50% of the annual rainfall as shown in Figure 4.3. As a result, it can be classified as a semi-arid to semi-humid climatic zone.

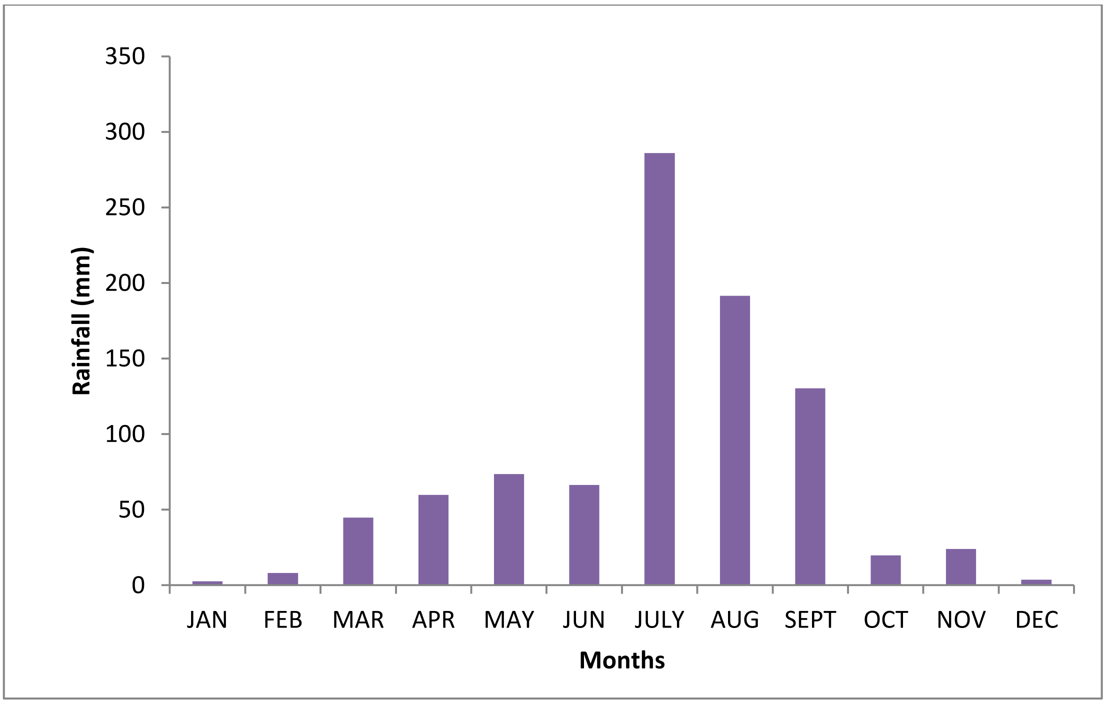

Figure 4.3: Average monthly rainfall in the study area (Ethiopian metrological agency, Adama station)

4.4 Geology

4. 4.1 Regional geology

The Ethiopian Rift Valley is one of the most notable structures of the Great East Africa Rift System, which cuts through the uplifted Ethio-Somali plateau. The Afar triple junction connects the Ethiopian Rift Valley to the Red Sea-Gulf of Aden constructive plate boundary. Many scholars (Di Paola, 1972; Mohr, 1987 and others) believe that the rift was caused by tensional motions that affected the uplifted Ethio-Somalia plateau. The top of the plateau and the bottom of the rift are separated by more than 1000m due to a high number of step-up faults. Almost all of these faults are normal faults (Di Paola, 1972). The MER is a symmetrical graben with steep border faults and uplifted flanks (Woldegabriel *et al*.,1990).

Two main tectonic events have been recognized concerning the tectonic evolution of the Ethiopian Rift System. The first event involved the uplift of the Ethiopian swell, which started in Eocene as part of the Afro-Arabian swell (Mohr, 1967). The second major tectonic event took place across the swell to form the Afar and the Ethiopian Rift of large-scale faulting to form the eastern and western margins of the rift. The eastern margin is morphologically well expressed as compared to the western one, which at places is so sub-dued that the boundary between the rift floor and the plateau is hard to define. According to Kazmin and Berhe, (1978), the initiation of the Ethiopian Rift and the Afar can be traced to 14 Ma ago. Other authors suggest an early Miocene for the Rifts (Berckhemer *et al*., 1975 and others). The last major episode of rift faulting resulted in the formation of the Wonji fault belt (WFB), which is characterized by a number of faults which 15 shattered the rift floor into several relatively small horst and graben structures. The faults are short, normal type, and are oriented in NNE and SSW direction.

The Awash basin is made up primarily of the Ethiopian plateau and the Rift Valley. The rift system is oriented northeast. Tertiary volcanic tuffs and agglomerates from the Paleocene and Miocene, as well as younger, silica-rich rhyolites, trachyte's, tuffs and ignimbrites from the Miocene to Pleistocene and dominate the Ethiopian plateau. The volcanic materials on the Rift Valley floor are mostly Miocene to Pleistocene basalts and ignimbrites, with Holocene lavas found around active volcanic sites. During the Pleistocene pluvial period, large lakes formed on the Rift Valley floor and the flat plains of Wonji and Metehara. Thick lacustrine deposits cover the lower Awash plains. The Rift Valley's flat bottom is often broken by fault scarps and the effect of Pleistocene and Holocene volcanic activity (Taye, 2007).

From a magmatic viewpoint, the area is marked by the presence of numerous volcano-tectonic features such as calderas, composite volcanoes, spatter cones, and fissures, all of which produced massive volumes of ignimbrites and subordinate basaltic lava flows ranging in age from 5 to 0.06 Ma (Meyer, *et al*., 1975 ; Morton *et al*., 1979 and Bigazzi *et al*., 1993). In the northern half of the rift system, Meyer et al., (1975) identified two primary volcanic units. These volcanic units include the older Nazareth group, which dates from 5-2 Ma ago, and the younger Wonji group, which dates from the Pleistocene to the Holocene. A Nazareth faulting phase, active 1.6 to 1.8 million years ago, separates the two components.

The Nazareth series, composed of a thick succession of ignimbrites, rhyolites, trachytes, and pumice, forms the larger part of the rift floor and outcrop in the rift escarpments and on the adjacent plateau margins. According to the authors, the succession in the Nazareth region consists of light rhyolites and ignimbrites. Because it was collected in previously created basins and grabens, light pumice on top of the Nazareth series has more thickness than normal in some areas. In the pumice breccias, tuff and yellow loam alternate. Fissures and vents are thought to be the primary source of this phase's eruptions; however, local centers do occur.

In terms of tectonics, a tensional force created the tectonic pattern within the main Ethiopian rift (MER) in the first phase during the deposition of the stratified Nazareth series, with cracks, fissures, and dykes running NE-SW and NNE-SSW. With the Nazareth faulting period, tectonic activity came to a stop. The pattern can be referred to as tensional tectonics perpendicular to the direction of the main Ethiopian rift (MER) (Taye, 2007).

In the second and main part of the Nazareth faulting phase, a fundamental and completely different evolution began with the wonji fault belt. Meyer *et al*., 1975, suggested the name the wonji series for the volcanic related to the belt. As pointed out by many authors (Mohr, 1967; Hepworth & Gibson, 1970; Meyer *et al*., 1975 and others), the latest volcanism in the Ethiopian Rift is related to its axial extensional zone, the wonji fault belt. The bulk of the Pleistocene to recent volcanism is undoubtedly controlled by this tectonic feature even though some eruptions of basalts and central volcanoes occur outside the belt.

The Wonji group includes all the rift volcanic formed after the last major episode of rift faulting. Groups of fractures, open fissures, and dykes show north-northeast, south-southwest, and north-south direction. A summary of the youngest phase of volcano-tectonic development within the study area is given by Bigazzi *et al.*, (1993). He stated that the collapse of the Gedemsa caldera is younger than 0.2 Ma, and the post-caldera perlites and pumice inside Gedemsa were erupted between 0.2 and 0.1 Ma.He presumed the ages of the great number of faults affecting these products are younger than 0.1 Ma and the aphyric hawiites, mildly alkali-basaltic flows and spatter cones have the age of 0.06 Ma.

Finally, the tectonic of the rift system is analyzed by Boccaletti *et al*., (1999)and state that strike-slip tectonics has played a major role in the development of the rift and oblique extension along major northeast-southwest trending strike-slip faults is responsible for the upwelling and differentiation of most of the acidic volcanic products known to occur, whereas basaltic lava flows and associated volcano-tectonic features are derived from a development of north-south trending extensional features. The authors conclude that the strike-slip system plays a major role in the development and evolution of the post-ignimbrite tectonic history of the main Ethiopian rift (MER), while it is a possibility that this mode of deformation might have also been important for the earlier tectonic phases.

4.4.2 Local geology

The study area is covered by a variety of volcanic rocks of various ages and occurrences, as well as lacustrine and alluvial sediments, which are primarily found between the Wonji and Awash Melkasa areas (Alula *et al*., 1992). The various rock types outcropping in the study area are subdivided into nine units: Alluvial and lacustrine deposits; Wonji unit; Boset unit; Gedemsa unit; Dera-Sodere unit; Bofa unit; Boku-Tede unit; Keleta unit; Nazret unit; and Eastern Margin unit.

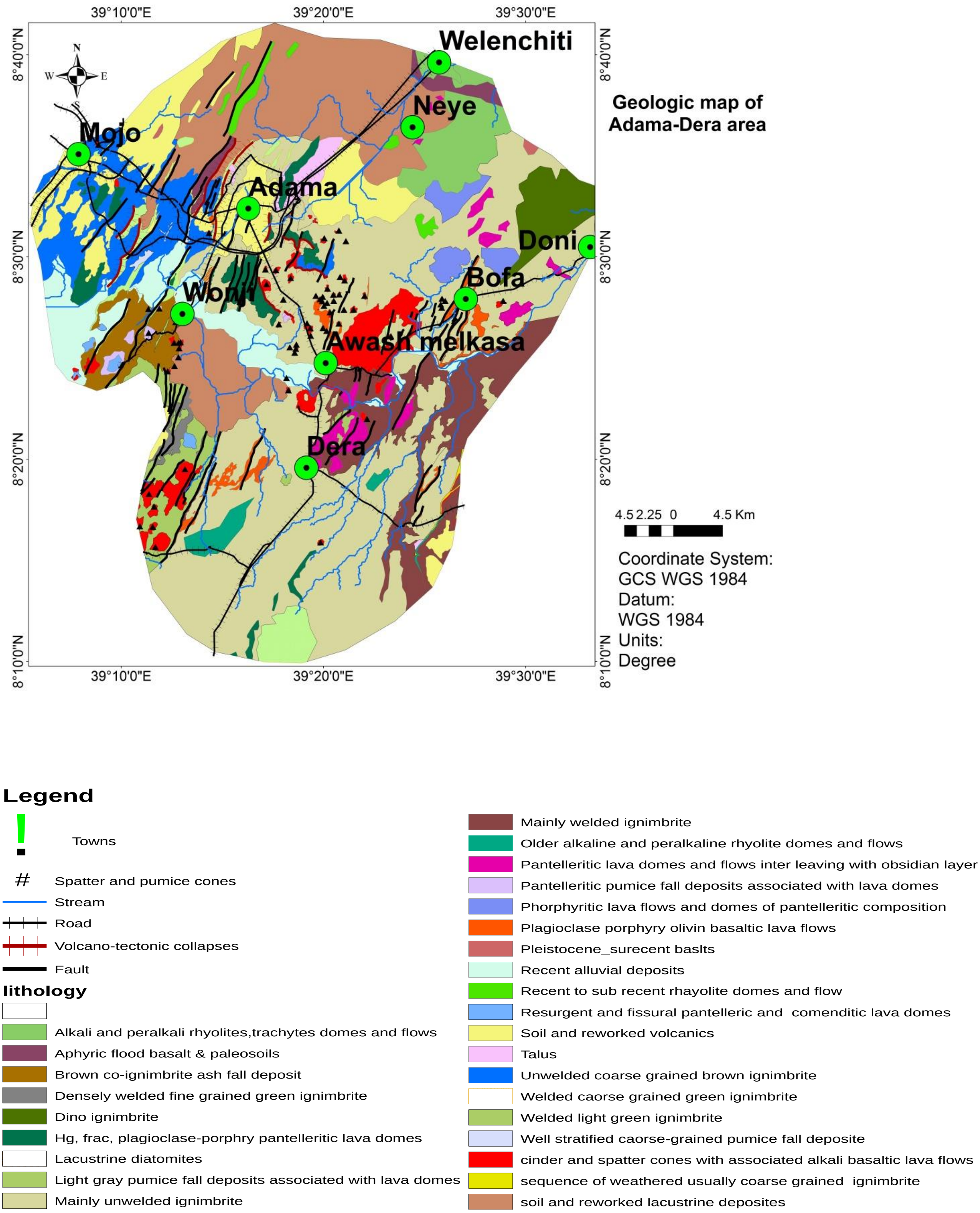

Figure 4.4: Geological map of the study area modified after Alula *et al*., (1992)

4.4.2.1 Wonji unit

These are the area's youngest units, linked to basaltic lavas that erupted from several emission centers. These cones are mostly found in the SE and SW of Adama town (near Wonji).. These cones exhibit north northeast alignment along young fissures usually known as the Wonji Fault Belt, starting north of the Gedemsa rim and Dera (Mohr & Gouin, 1960). Rhyolites, trachytes, obsidian, and recent fissural basalts are the major components of this volcanic unit (Dechasa, 1999).

Cinder and spatter cones with associated alkali basaltic lava flows with porphyritic to subaphyric lavas with phenocrysts of plagioclase, olivine, clinopyroxene, and opaque mineral composition are widely present in the study area. These units are dominantly outcropped in the south along the Adama-Asela main road (Figure 4.6).

Figure 4.5: Scoria cone located southern part of the study area along Adama-Asela main road

4.4.2.2 Boseti unit

This lithological unit is linked to the central volcanic complex event, which occurred northeast of Awash Melkasa in the Tatesa area and took the form of a typical dome structure. It is present in the northeastern part of the study area. It is characterized by porphyritic lava flows and domes of pantelleritic composition with 180m thickness. According to Morton *et al*., (1979) the age of this lava flow is about 0.21 Ma.

4.4.2.3 Gedemsa unit

This unit is dominantly outcropped in the southwest of the study area. The Gedemsa volcano is located in the Ethiopian Rift Valley's central sector, some 25 Km southwest of Adama town and near the eastern Rift boundary. These groups are linked to the study area's most recent intra-rift acidic event, which was related to a huge central volcano that eventually collapsed, forming a 7-Km-wide caldera bordered by a vertical wall of 150-200 m in height (Taye, 2007). The stratigraphy of this group from the bottom to the top starts with basal Rhyolite Lavas Lower, pumice fallouts, upper obsidian lavas, ignimbrites, and upper pumice fallouts intra-calderic lava, domes and pyro-clastic, intra-calderic lacustrine sediments phreatomagmatic tuffs , cinder cones and basaltic lavas (Gdemssa) (Taye, 2007).

Along the northern border, the stratigraphy of this group begins with a thick pyroclastic flow, and ignimbrites, followed by rhyolites and obsidian lava flows from post-caldera activity, and lastly, a pumice fall deposit. A pumice fall deposit may be seen within Gedemsa and along the Wonji road near the Awash River Bridge. Gedemsa is distinguished by a 20-m thick grayish, coarse-grained layer. The clasts are typically angular, with fragments of obsidian red and green lava shards and 2.5cm thick grey fine ash deposits. The fall deposit at the Awash River bridge is three meters thick and shows fine-grained grey ash-flow intercalation. In comparison to the outcrop within Gedemsa, the pumice clasts are smaller.

Densely welded, fine-grained green ignimbrite with pantelleric dark glass fiamme and rhyolitic lava domes are found in the southwest half of the study area. Unwelded or poorly welded facies are seen in the upper part of the ignimbrite sequence. This deposit is 50 m thick and is 0.2-0.25 Ma old. The out crops present has clasts of plagioclase crystals, sanidine, quartz, aegiri-nea-audite, and the matrix flows eulaxtic texture. And an abundant of welded light-green ignimbrite-rich juvenile clasts or pantelleritic and basaltic composition followed by unwelded pumice-rich pyroclastic flow (eastern slope of the Gedemsa caldera). Near Lake Koka are lava domes with a 10m thick brown ash co-ignimbrite ash fall deposit and panterlleritic pumice fall deposit. There are also resurgent pantelleritic, fissural, and comenditic lava domes.

4.4.2.4 Dera-Sodere unit

Dera-Sodere unit is the most widely exposed ignimbrite volcano-stratigraphic unit in the southern part of the study area, particularly near Dera town and Sodere. This unit is made up of manly unwelded ignimbrite, pumice fall deposits, and lava domes and flows. The unwelded ignimbrites units are characterized by fine-grained brown, pink matrix containing small pumice clasts and lithic fragments and are interbedded with paleosol. The light grey pumice fall deposit associated with lava domes with a thickness of up to 4m is found in the area.

At Dera and Bodecha, this unit is exposed along northeast elongated ridges or a typical dome structure, but at Sodere, it forms a north-northeast elongated ridge. The majority of it is seen in the Dera-Sodere area. It is weakly welded, highly weathered, and friable (Taye,2007).

4.4.2.5 Bofa unit

They are generally sub-aphyric flood basalts that are locally vesicular and fresh, with many flows separated by scoria strata. This unit is exposed under the ignimbrite along the scarp west of Nazareth, divided by a 30cm thick red-brown paleosol and a one-meter thick fine-grained brown ash-flow deposit. It's also seen in the study area along the Nazareth-Awash-Melkasa major road. This 2.5-meter-thick rock is predominantly fine-grained, dark in color, and has flow lamination. Under the thin section has a fine-grained texture with plagioclase and olivine micro phenocrysts. Twenty microcrystals of olivine’s, plagioclase pyroxenes and numerous opaques make up the groundmass. This unit's volcanic eruption and flow occurred 0.4 million years ago (Alula *et al*.,1992). This unit also consists of plagioclase porphyry olivine basaltic lava flow. It occurs in a successive layer in which one layer is red in color and fragile due to oxidation and weathering. The other layer is a massive basalt which is strong and has the potential suitability to be used as an aggregate, as shown in the figure below (Taye,2007).

Figure 4.6: Massive and highly oxidized layers of Basalt rock formations near Awash Melkasa

4.4.2.6 Boku-Tede unit

The rocks of this group are connected with huge central volcanoes and are marked by collapsed calderas, one of which, the Boku Caldera, is located in the MER's southern area of Nazareth city. The volcanic eruption and product placement occurred 0.8 Ma ago (Alula *et al*., 1992). Alkaline and peralkaline rhyolite lava domes, flows, and pyroclastic falls, which cover the floor complex ignimbrite layers, are the volcanic products of the Boku volcano. Then, intra-caldera products such as scoria cones and accompanying basaltic lava flows cover the central caldera once these products are ejected, the caldera collapses. The recent deep and extensive late Quaternary faults, which are part of the WFB, have repeatedly dissected this young volcano (Mohr, 1971). In this sense, the temporal coverage for faulting at the Boku stretches as far back as the age of the volcano (0.8 million years, Alula *et al*., 1992) or perhaps earlier, given that the WFB occurred 1.6 Ma ago (Meyer *et al*., 1975). The unit is composed of highly fractured plagioclase-porphyry pantelleritic lava domes with associated obsidian layer and pumice fall deposits. From oldest to youngest, the following lithological units have been recognized in the area. Ignimbrites on the rift floor; somewhat welded tuffs; un-welded tuffs; rhyolitic lava flows; pumice fall deposits; obsidian flows; and basaltic lava flows, scoria. These lithologic units do not run parallel to one other and show differences in lithology (Haile *et al*., 2002).

4.4.2.6.1 Rift floor ignimbrites

The rift floor ignimbrites are the region's oldest outcropping unit. The main outcrops, which have elongated outcrops and are surrounded by faults, are actually located west of Nazareth town. The ignimbrites are large and tightly welded, which is favorable as an aggregate. Alula *et al*., (1992) found a total thickness of roughly 100 m with a K/Ar age of 1.7 Ma. Rift floor ignimbrites are thought to be the basal rocks beneath the Boku volcanic products, based on regional stratigraphy. The out crops present in the area has a grey color with porphyritic texture in which the phenocrysts of feldspar lie on the ground mass of volcanic glass fine-grained feldspar, and opaque minerals (Fe-oxides).

Figure 4.7: Existing quarry site of an ignimbrite out crops in Adama town

4.4.2.6.2 Slightly welded tuffs

Pumice clasts and lithic fragments are abundant in this unit. The tuff is brown in color and outcrops around the Boku caldera's eastern rim. The unit is approximately 80 m thick. (Haile *et al*., 2002). This rock has a grey color with a porphyritic texture in which phenocryst of feldspar lie on the ground mass of volcanic glass, fine-grained feldspar, and opaque minerals (Fe-oxide).

Figure 4.8: An outcrop of ignimbrite in the Boku ridge

4.4.2.6.3 Rhyolitic lava flows

On the caldera's western rim, rhyolitic lava flows occur as a basal layer. The color of these flows is grey, having fine to medium texture, or microscopically, they have porphyritic texture. The pumice fall and obsidian flows are confined by this unit, which generates steep slopes surrounding the rim, as shown in Figure 4.10. The sample Q8 is taken from this rock unit and has shown a good strength due to the sampling, which is of good quality as an aggregate.

Figure 4.9: Rock mass of rhyolite at Boku ridge

4.4.2.6.4 Pumice fall deposits

The deposit is stratigraphically widespread and covers the lowest rhyolitic lava flow. It is completely transformed in hydrothermally active places. Even far out from the caldera, the pumice fall deposit produces a gentler slope, with an exposed thickness of roughly 4.5 m.

4.4.2.6.5 Obsidian flows

These flows are restricted near the caldera rim and are black in color. The flows are highly fractured and, in some spots, worn to a perlite-like form.

4.4.2.6.6 Unwelded tuffs

The region's plains are completely covered in unwelded tuffs. The unit contains a minor amount of pumice fragments and some dark-colored rock fragments up to 4 cm in diameter and ash. The surface runoff has developed deep gullies all across the farmlands due to the unit's looseness. This unit is found on the western side of the study area and seems to be discolored due to weathering, as shown in Figure 4.11.

Figure 4.10: Unwelded tuff observed near Mojo town

4.4.2.6.7 Basaltic lava flows and scoria

These units are located within the caldera and are the consequence of a post-caldera eruption. The texture of basaltic lava flows is vesicular, and some are packed with secondary minerals. Basaltic lava flows exist beneath the scoria layers in some sites.

4.4.2.7 Keleta group

The Keleta Group is a large pyroclastic flow deposit that is thought to be the earliest true rift floor deposit in the studied area. This type of formation is located in the study area's southeast corner. Welded ignimbrite sequences with dark vitrophyritic fiamme and lithic fragment interleaving with aphyritic flood basalt and paleosol can be seen in this location. Throughout the area, the entire pyroclastic section can be divided into a lower unit of proximal facies and an upper unit of distant facies (Taye, 2007).

The lower pyroclastic flow deposit starts with a grey ash-flow covered by glassy ignimbrite and a thick ignimbrite. A 20 cm thick coarse-grained sandy paleosol containing glass chips, pumice pieces, and underlying rocks separates the yellow tuff unit from the underlying ignimbrite. The upper pyroclastic deposit is exposed on the Keleta River's upper reaches. It is made up of unconsolidated brown and grey ash-flow deposits with paleosol intercalation on various levels. The overall thickness is about 10m (Taye, 2007). The ash units are fine-grained and contain small pumice fragments, particularly in the grey ash unit; silicified fossil plants and gas escape routes with fine depleted coarse lenses of pumices are also present. This group's uppermost unit is represented by a fine-grained brown ash-flow deposit that covers huge regions, including the Dera domes, the Awash Melkasa area, and the east-south of Gedemsa Caldera.

The Keleta group's products are also well exposed in the Feyiso intermittent river. The section begins with a yellow ignimbrite unit containing large pumice clasts and lithic fragments, which is overlain by an 8 m-thick brown ash-flow deposit with weak stratification, which is then overlain by a 10 m-thick reworked volcanoclastic deposit with crude stratification marked by stone lines of rounded pebbles. At the top 2-3m thick well-welded ignimbrite carrying large lenses of dark glass is found. This unit's base is glassy and is separated from the underlying reworked volcanoclastic unit by a thin layer (20cm) of fine-grained ash-flow deposit. Petrographically, the ignimbrite shows a eutaxitic texture with glass shards and collapsed pumice containing crystals of plagioclase, quartz, pyroxene, and lithics of trachytic nature. Even though the unit of this section is similar to the ones exposed at the Keleta river liner, the correlation between them is not impossible.

4.4.2.8 Nazret unit

4.4.2.8.1 Aphyric flood Basalt

This form of basalt can be found on the Kimbibit ridge, at the base of the Tedecha cone, and on the road to Sodore near the Melka Woba junction. Vesicular black, fine-grained basalts with sparse plagioclase phenocrysts are representative of these rocks. It has a sparsely porphyritic texture that is placed over a micro-granular groundmass of olivine plagioclase and pyroxene. Zoned plagioclase and pyroxene are the only phenocrysts found.

Figure 4.11: Outcrop of aphyritic flood basalt quarry near police college that is being quarried for an aggregate

4.4.2.8.2 Ignimbrite

This unit is mostly exposed on the western side of the study area. It is represented by pale green, well-welded ignimbrite with many dark glass lenses (fiamme) ranging in size from 3 to 20cm. The unit's thickness ranges from 2 to 40 m, with the ignimbrite becoming less welded and containing more lithic particles as it gets closer to the top. The rock mass near mojo has greenish-gray color, a light grey colour as shown in Figure 4.13. This rock unit has a flowing texture in which the groundmass is composed of mainly volcanic glass, feldspar, and a minor amount of opaque minerals. This ignimbrite unit is also present in Adama town around the Gendehara area, and this formation is light grey in color as shown in Figure 4.14 and is densely welded, which has the potential to be a source for an aggregate apparently, this formation is very near settlement area which is unfavorable as a quarry site. A similar ignimbrite unit with an exposure thickness of 20-25m was discovered along the route to Sodere. It has a base of gray well-welded ignimbrite with "fiamme" of dark glass, with an ignimbrite comprising peches of glass, pumice clasts, and plentiful lithics forming the upper 1.5 meters. These rocks are petrographically eutaxitic, with collapsed partially crystalline pumice, quartz, plagioclase, amphibole, and pyroxene crystals, and lithic pieces of basalts and trachytes.

Figure 4. 12: An outcrop of Medium grained ignimbrite near Mojo town

Figure 4.13: An outcrop of ignimbrite forming columnar joints in Adama, Gendehara area

The sequence of weathered, usually coarse-grained densely welded varicolored ignimbrites containing vitrophyric fimme and lithic fragment with associated lava domes flows interleaving with subaphyric flood basalt, and paleosol are seen in the SE portion of the study area.

4.4.2.9 Soil and reworked volcanics

These units occupy the whole central part of Nazareth and west of Nazareth. Coarse grains are contained as reworked volcanic material of different sizes. They exclude recent lacustrine, alluvial, and colluvial sediments, representing the only volcanic deposits in the study area. These units developed from the weathering of the volcanic rocks. The type and development of soil within the study area is a function of the nature of volcanic rocks, the climate to which it is subjected, and the time of subaerial exposure, which determine the degree of weathering and the rainfall intensity.

4.4.2.10 Talus

Talus is the term that is used for rock fragments that are usually coarse and angular and lying at the base of a cliff or steep slope from which they are derived; also, the mass of such broken rock is considered as a unit. Talus occupies the area at the flanks of Dibibisa ridge, which is east of Adama, and at the escarp of the northwest of Adama.

4.4.2.11 Recent alluvial deposits

These lithological units occupy both nearby sides along the course of the Awash River. At Melka Hida, it has a maximum thickness of 25m overlying tuffs, ignimbrite and volcanic ash. Away from Wonji plain thickness of this unit shows variation from 6-25m.The grain size ranges from clay to silt to gravel, sometimes to cobble, where gravel dominates at the bottom of river channels. They are mainly medium-grained in the floodplain of Awash. The alluvial deposits in the study area's central awash plain were accumulated due to the erosion of the surrounding uplifted areas. They are unconsolidated materials consisting of sand, silt, and clay beds with brown color. Fine ash material is interbedded with the alluvium at places in the central Awash River plain. The thickness of this deposit varies considerably from place to place.

4.4.2.12 Lacustrine deposit

The area between Wonji and Awash Melkasa is covered with an extensive and thick lacustrine deposit. These compact lacustrine deposits are made up of clay, silt, fairly welded travertine, ashes, diatomite, and pumice intercalation. 24 These subracial sedimentary layers have a maximum thickness of 90m in Wonji, according to shallow drill data. They primarily cover the middle main Wonji floodplain and some low-lying flat land in the study area's northern region. Drilling data has revealed that these deposits are located over the ignimbrite and scoria. This unit has a varying thickness of 6-25m away from the Wonji plain. It has a maximum thickness of 25 m overlaying tuffs, ignimbrite, and volcanic ash at Melka Hida. The majority of the lacustrine deposit is fine to medium-grained. Within the thick layer of lacustrine deposit, fine sand lenses are prevalent. Lake deposits in minor graben within Wonji faults make up this unit of the Wonji area. Lacustrine deposits are thought to have been deposited in the lake during the Holocene period, according to Di Paola (1972). These strata are not tectonically disturbed and have not been subjected to extensive periods of sub-aerial denudation, resulting in a large and relatively level land area.

4.4.3 Structures

The study area is in the northern segment of the main Ethiopian rift (MER), and the principal geological features found there include faults, joints, fissures, fractures, and other meso-structures associated with silicic lavas such as flow stacking and folding. A distinct characteristic of the area is Pantelleritic volcanic cones, and domes are good examples of lineaments. Most joints in the study area are of columnar type, particularly associated with welded ignimbrites, as shown in the Figure 4.15.

Figure 4.14: Columnar joints associated with welded ignimbrite.

The Wonji Fault Belt, which forms the axial component of the MER, has a significant impact in the study area. A number of minors and main normal types of faults run virtually parallel to one another in an NNE-SSW direction, commonly in a right stepping fashion. These faults are frequently linked to volcanic activity, generally younger in the center and older as they approach the rift borders (Skutan *et al*., 1987).

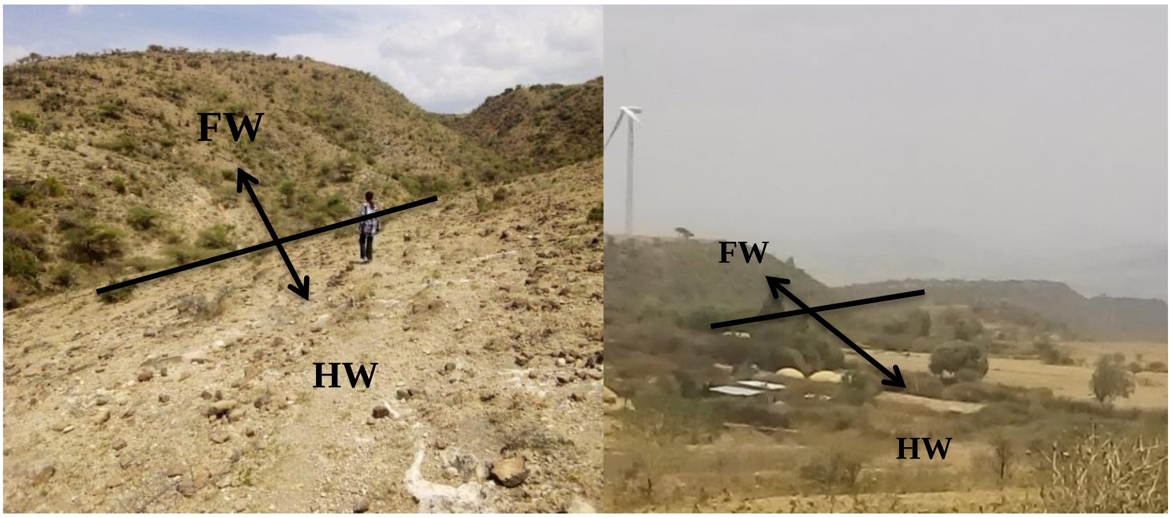

Figure 4.15: Normal Fault observed in the study area

Basaltic spatter cones are located along a NNE oriented strip that runs from the eastern side of Gedemsa to the Boku area with a right "an echelon" displacement. Some of the spatter cones were later disrupted, resulting in a new 'AA' type of lava flow near Melkasa. (Skutan and colleagues, 1992)

Figure 4.16: Cone structures present near Awash melkasa area

CHAPTER FIVE

5. Results and Discussion

5.1. Suitable quarry site selection

Two stages were considered for selecting suitable areas for quarry sites. In the first stage, seven factors, which influence the economic and environmental aspects of quarry sites, were considered, which include land-use and land-cover, distance to built-up areas, depth to groundwater table, distance to water bodies, distance to road, relative relief and slope angle to prepare preliminary suitable quarry sites. In addition to the environmental and economic aspects, the availability of quality materials is an important factor. Therefore, in the second stage, lithology is considered to select the final suitable quarry site with suitable lithology for crushed stone aggregate. These criteria and their classification and rating based on suitability are discussed below:

5.1.1. Suitability of each thematic layer for a quarry site

The thematic maps produced for each criterion that were geo-processed and converted into raster maps were reclassified to give the least and most favorable conditions for quarry site for each criterion, as shown in Table 5.1.

Table 5.1: Classification of each thematic layer and the suitability rating of each class

Criteria	Classes	Description	Suitability	Rating	Area (Km^2)	Area%
Lithology	Soil	Friable, easily disintegrated, highly weathered materials, and weak materials	Unsuitable	0	1426.7	72.43
	Rock	Consolidated, dense, durable, and strong material.	Highly suitable	1	542.44	27.54

Criteria	Classes	Description	Suitability	Rating	Area(km^2)	Area(%)
Land use land cover	Settlement	Housings, commercial buildings, artifacts, and project areas	Unsuitable	0	156.5	7.9
	Dense forest	Thickly vegetated land	Very low suitable	1	65.8	3.3
	Waterbody	Rivers, lakes, streams, and ponds	Low suitable	2	33.4	1.7
	Cropland	The agricultural area where crops are cultivated	Moderately suitable	3	1065.3	54.1
	Shrubs	Scattered vegetation in the form of wild grass, bushes, and small trees	Highly suitable	4	642.3	32.6
	Grass	Land used for grazing	Very highly suitable	5	1.154	0.058
	Bare land	Bare land with no vegetation cover	Extremely suitable	6	4.2	0.214
Distance to build up area (m)	<1000	Extremely close	Unsuitable	0	815.05	41.39
	1300-1000	very close	Very Low suitable	1	177.61	9.01
	1300-1600	Close	Low suitable	2	151.09	7.67
	1600-1900	Not too close	Moderately suitable	3	123.17	6.25
	1900-2200	Fair distance	Highly suitable	4	100.73	5.11
	2200-2500	Good distance	Very highly suitable	5	83.47	4.23
	>2500	At a very good distance	Extremely suitable	6	518.05	26.3
Depth to ground water	<25	Extremely shallow	Unsuitable	0	145.59	7.39
	25-50	Very shallow	Very low suitable	1	178.93	9.08
	50-100	Shallow	Low suitable	2	190.12	9.65
	100-150	Moderate depth	Moderately suitable	3	1011.06	51.34
	150-200	At a fair depth	Highly suitable	4	343.74	17.45
	200-250	Deep	Very highly suitable	5	79.89	4.05
	>250	Very deep	Extremely suitable	6	19.83	1.007

Criteria	Classes	Description	Suitability	Rating	Area(Km^2)	Area (%)
Distance to water body	<150	Close	unsuitable	0	140.40	7.12
	150-300	Very close	Very low suitable	1	127.61	6.48
	300-450	Intermediate	Low suitable	2	121.51	6.17
	450-600	Far away	Moderately suitable	3	115.11	5.84
	600-750	Very far away	Highly suitable	4	111.53	5.66
	750-900		Very highly suitable	5	106.27	5.39
	>900		Extremely suitable	6	1246.72	63.3
Distance to roads	<500	Extremely close	unsuitable	0	288.76	14.66
	>10,000	Very far away	Very low suitability	1	20.48	1.04
	7500-10,000	Far	Low suitability	2	154.61	7.85
	5000-7500	Moderate	Moderately suitable	3	353.06	17.92
	3200-5000	Fair distance	Highly suitable	4	373.91	18.93
	1600-3200	At an economic distance	Very highly suitable	5	418.25	21.23
	500-1600		Extremely suitable	6	361.09	18.33
Relative relief	<5	Extremely low	Unsuitable	0	0.0268	0.0013
	>300	Extremely high	Very low suitable	1	288.49	14.7
	200-300	Very high	Low suitable	2	734.54	37.302
	100-200	High	Moderately suitable	3	853.49	43.34
	50-100	Moderate	Highly suitable	4	87.68	4.45
	25-50	Low	Very highly suitable	5	4.5	0.23
	5-25	Very low	Extremely suitable	6	0.46	0.0234

Criteria	Classes	Description	Suitability	Rating	Area(km$^{2)}$	Area (%)
Slope angle	<5	Extremely gentle	Unsuitable	0	1033.494	52.48
	>60	High escarpment	Very low suitable	1	0.0037	0.00018
	45-60	Escarpment or Cliff	Low suitable	2	0.66	0.0333
	35-45	Steep	Moderately suitable	3	6.56	0.333
	25-35	Moderately steep	Highly suitable	4	32.1	1.63
	15-25	Gentle	Very highly suitable	5	103.8	5.3
	5-15	Moderately gentle	Very highly suitable	6	792.57	40.24

5.1.1.1 Lithology

The main parameter for the selection of a suitable quarry site is the presence of source material in that area. A massive, high cohesion, and homogenous rock is most suitable for the crushed aggregate (Langer & Knepper, 1998; Leroye *et al*., 2017;BGS, 2019). Highly weathered, weak, and Low cohesive rocks such as volcanic ash, pumice, scoria, alluvium, and eluvium products are, on the other hand, absolutely unsuitable (Gudessa *et al*., 2021). Thus, the lithology was grouped into two groups that are cohesive or hard rocks (such as basalt, rhyolite, ignimbrite and etc.) and soil or non-Cohesive material (such as pumice, ash, alluvial deposit, highly weathered rocks and etc.). The cohesive material covers about 542.44Km^2 or 27.69% of the whole area and was given a rating of 1, meaning potentially suitable material to be used as an aggregate in that area. The rest of the study area (1426.7Km^{2}or 72.43%) is covered with non-cohesive material that is unsuitable to be used as a crushed stone aggregate; therefore, it is regarded as unsuitable, as shown in Figure 5.1.

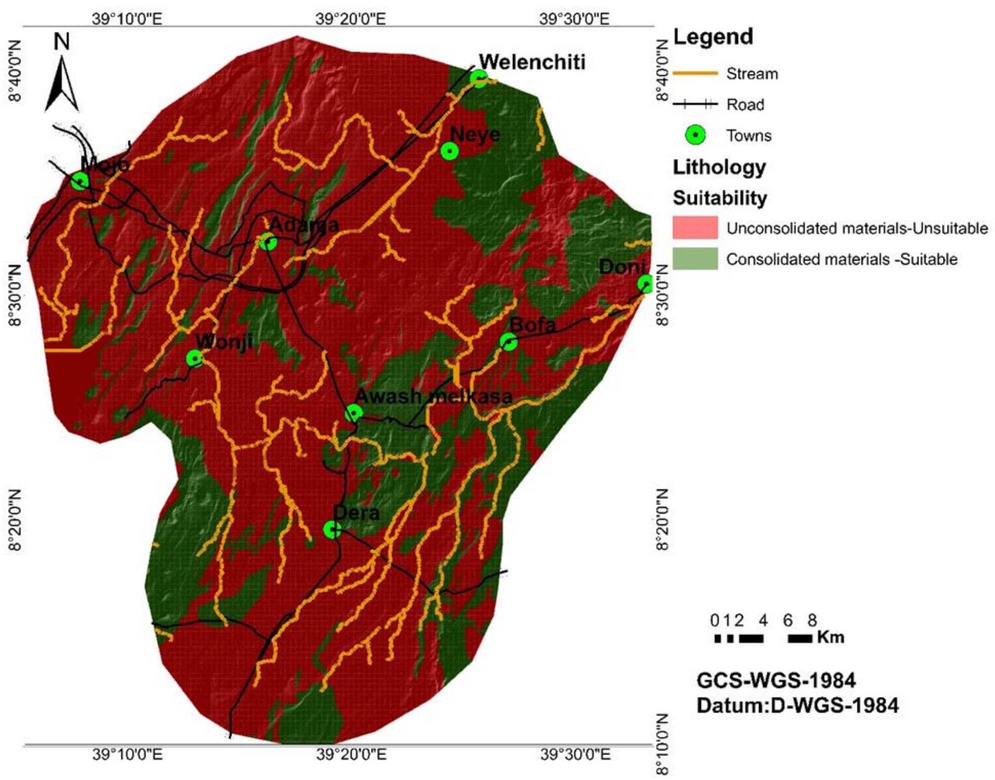

Figure 5.1: Lithologic map reclassified based on the suitability of each lithology as a crushed stone aggregate

5.1.1.2 Land use land cover

Modern techniques of mining using heavy equipment can produce dramatic alternations in land cover, both ecologically and hydrologically (Turner & Ruscher, 2004; Singh, 2007). Further mining activities result in change of topography (Manna & Maiti, 2014)and drainage pattern (Akiwumi & Butler, 2008; Khan & Javed, 2012; Manna & Maiti, 2016) (Akiwumi and Butler, 2008; Khan and Javed, 2012; Manna and Maiti, 2016), and the principal environmental impact comes out as physical disturbances such as landscape change and degradation (Bajocco *et al*., 2012; Tadesse *et al*., 2017), soil erosion and degradation (Singh *et al*., 1997) and general environmental changes (Dhar *et al*., 1991; Prakash & Gupta, 1998). Land use/ land cover (LULC) maps play a significant and prime role in planning, management, and monitoring programs at local, regional, and national levels. This type of information, on the one hand, provides a better understanding of land utilization aspects, and on the other hand, it plays an important role in the formation of policies and programs required for development planning.

In this study, land use, land cover map is used to assess environmentally sensitive land cover such as forest, water bodies, and land use such as settlements, artifacts, archeological sites, etc.that can easily be affected by quarrying operations. Thus land use and land cover were reclassified into seven classes settlement, dense forest, water body, cropland, shrubs, grassland, and bare land, as shown in Table 5.1, and each class were given a rating based on the intensity of collateral damage that quarrying may cause to that specific land use.

Settlement is where residential, commercial, and industrial sites are present, having an area coverage of 156.5 Km^2 which is 7.9% of the total study area. It is part of the study area where a large number of population are present thus, it is the most sensitive of all the other classes to a quarrying activity thus, it was given a rating of 0 since it is unsuitable as a quarry site.

Reducing tropical deforestation to conserve biodiversity and regulate climate is a globally significant goal, yet deforestation rates remain high. Thus dense forest should be protected from activities that cause deforestation, such as quarrying or mining, and in this study thickly vegetated area or a dense forest covers, 65.8 Km^2 which is 3.3% of the study area which was given a rating of 1, meaning it has very low suitability. The water body covers 33.4 Km^2 or 1.7% of the study area during its sensitivity to being polluted it is rated as 2 meaning low suitability. The abundant land use present in the study area is cropland or cultivated land covering about 1065.3Km^2 or 54.1% of the total area. It is an area where crops are cultivated to provide a food source; thus, due to the collateral damage that quarrying may cause relative to the classes mentioned above. It was given a rating of 3 as moderately suitable. Shrubs are scattered vegetation in the form of wild grass, bushes, and small trees. This class covers 642.3 Km^2, which is 32.6% of the total area, and it was rated as highly suitable relative to the other classes. Grassland covers a very small part of the study area, 1.154 or about 0.058% of the whole study area. Grasses can easily be grown within a short period of time, taking that into account, it is classified as very highly suitable for quarry site since the damage done by quarrying activity to this land use is very little relative to the other land uses. Finally, the last one is bare land which is land with no vegetation cover and which is most likely not being used for any other purpose such as housing , cultivation and etc. thus, it was categorized as extremely suitable as a quarry site. Bare land covers 4.2 Km^2 or 0.214% of the total study area. The distribution of each land use land cover class in the study area is shown in Figure 5.2.

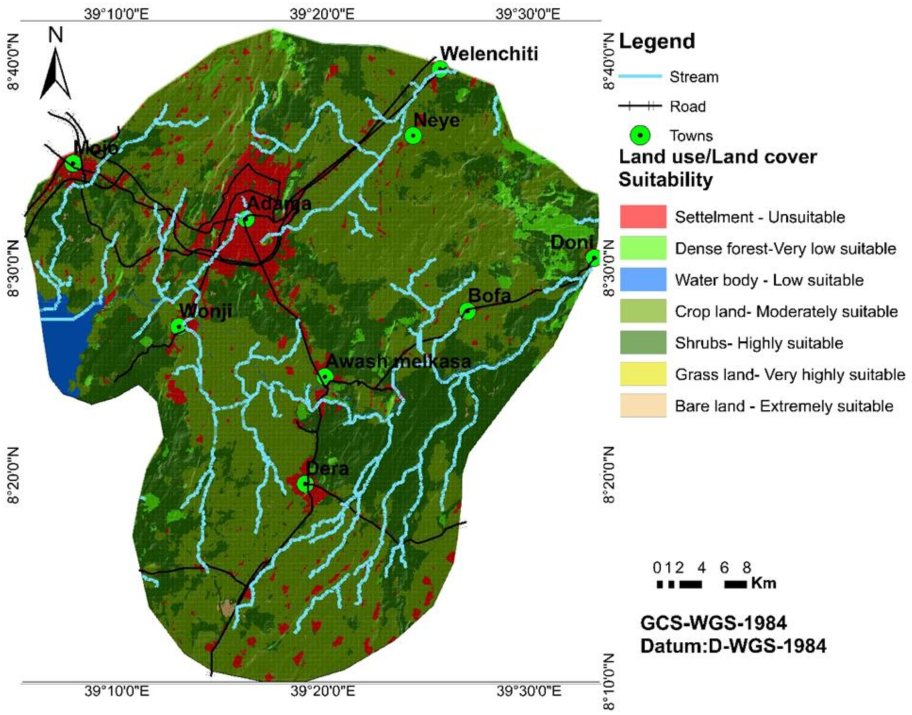

Figure 5.2: Reclassified thematic map of land use /land cover of the study area based on its relative suitability as a quarry site

5.1.1.3 Distance to build up area

A map of distance to build up areas helps to measure the vulnerability of the adjoining community to dust, noise and vibration hazards (Subhasis *et al*., 2018). Gudessa *et al*., (2021) suggested that if a quarry site is within 1000 m away from settlements, it is very close to the population centers, which means they have a higher health hazard. In the contrary, quarry sites more than 2500 m from the build-up area are far away from consumers and will have market problems with higher transportation costs. Due to the rapid population growth, cities such as Adama is expanding, and infrastructures such as roads, housing, and commercial buildings are being constructed, developing the demand for more construction material given this reason, the area bounded within the study area was considered to be at an economical distance. Thus in this study, the previous classification done by Gudessa *et al*., (2021) was modified in which thematic map of distance to build up area was classified into seven classes based on the relative suitability of each subclass for a quarry site. The area within 1000m away from built-up area within 1000m-1300m range, from 1300m-1600m,1600-1900,1900-2200,2200-2500 & >2500 and they were given a suitability rating 0,1,2,3,4,5& 6 respectively. About 815.05 Km^2 or 41.39% of the study area is covered within the unsuitable area, and 518.053km^2, or 26.3% of the study area is extremely suitable regarding its distance to buildup area. The distribution of each class is shown in the figure below.

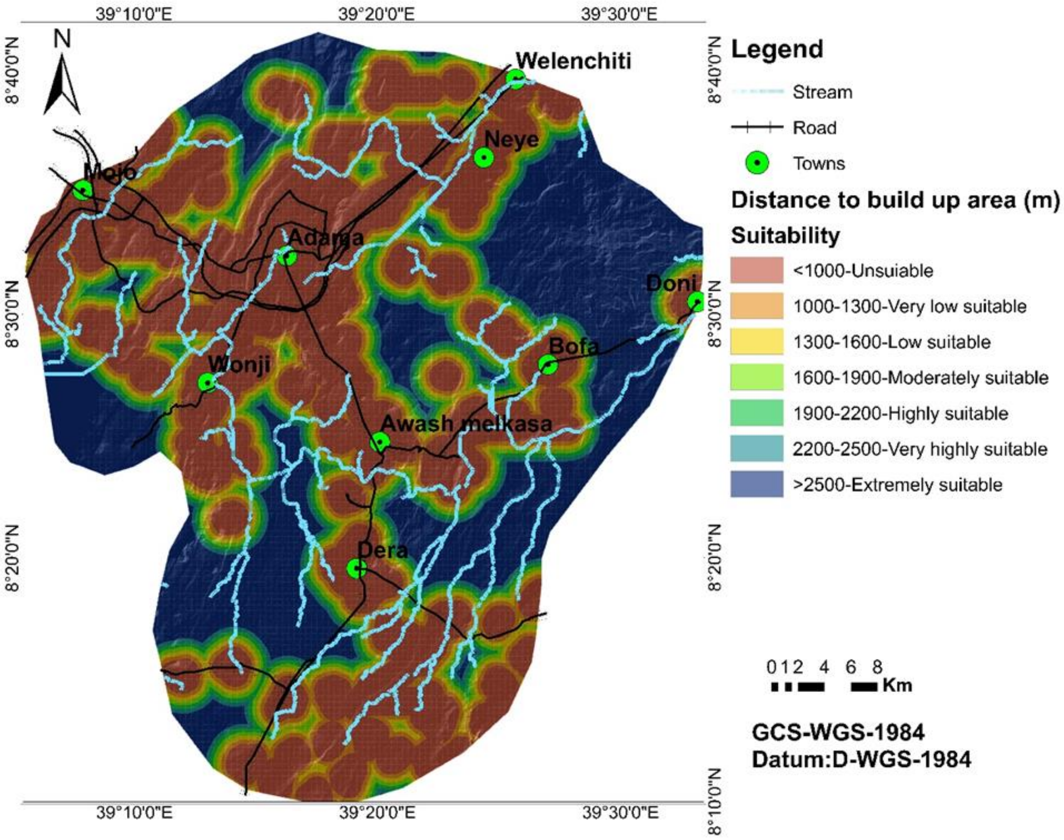

Figure 5.3: Reclassified thematic map of distance to build-up areas based on its suitability as a quarry site

5.1.1.4. Depth to groundwater

The other environmental effects of quarry development are on the quantity and physical and chemical properties of groundwater. Regardless of the small amount of quarried rock compared to the volume of an outcrop, the result of removing the protective rock cover of an aquifer may cause severe pollution of the groundwater and may change groundwater flow patterns (Ekmekci, 1990). Dust, residues from explosives, and runoff from quarries may change the groundwater flow and can affect the quality of water recharging an aquifer (Ekmekci, 1990; Geological survey of Ireland, 2004).Hence, a quarry site should be located where groundwater is sufficiently deep. Thus in this study the thematic map of depth to groundwater is reclassified into seven class ranges rated from unsuitable to extremely suitable. The dominant class (50-100), covering 1011.06 Km^2 or 51.34% of the study area, is widely distributed along with the NE and SW parts of the study area, as shown in Figure 5.4. The zone having a greater groundwater depth (>80 m) are considered suitable as a quarry site (Sadat-Noori *et al*., 2014). In this case based on the SWL present in the area, a relative suitability rating of 3 meaning moderately suitable, was given to this class. About 7.39% or 145.59Km^2 of the study area had an SWL< 25, which was distributed in the SW and NW part of the study area; given most of the water supply in Adama comes from groundwater, it should not be polluted by quarrying activity thus it was rated as an unsuitable area for quarry site. In the study area, the groundwater is deeper in the NE and SE parts of the study area than that in the SW and NW parts of the study area, as shown in the figure below.

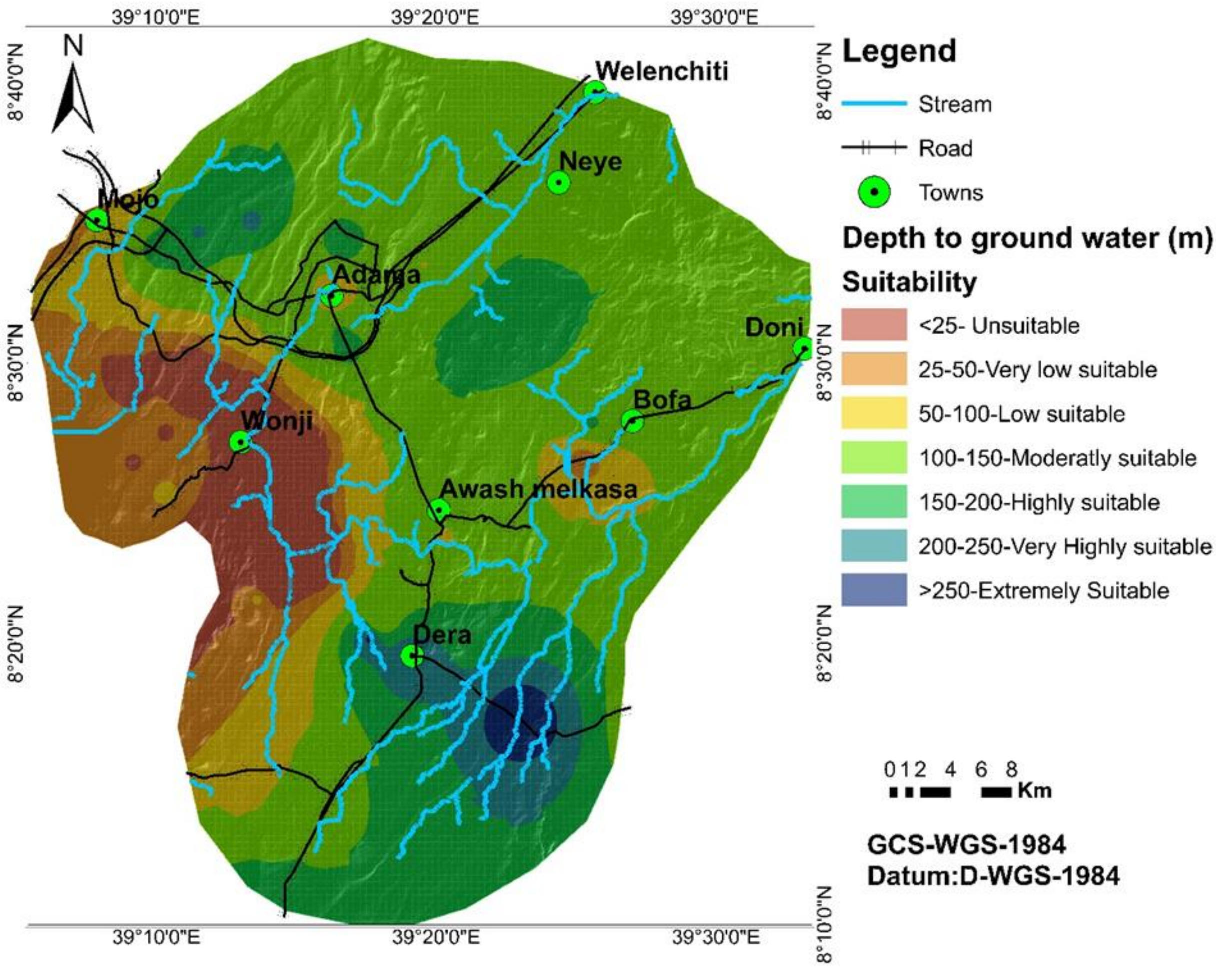

Figure 5.4: Reclassified thematic map of groundwater depth based on its suitability as a quarry site

5.1.1.5. Distance to water body

Quarrying activity near the water body causes pollution of the water; thus quarry site should be at a reasonable distance from water bodies. According to Gudissa *et al*., (2021) the water bodies within 150m distance from the quarry site is very close and may pose difficulty in managing effluents from the quarry activities. However, a quarry site more than 600m away from the water bodies is relatively far away, and pollution from the quarry activities can be managed. Thus the distance of 150m away from the water body, having an area of coverage of 140.4 Km^2 or 7.12% of the total area, was rated as an unsuitable area to perform quarrying operations. The class rang with an extreme suitability rating (>900m), covers most part of the study area, that is 1246.7Km^2 (63.3%) of the total area. The rest of the classes that are between 150m-900m were given a rating as specified in Table 5.1, and their distribution is present in the figure below.

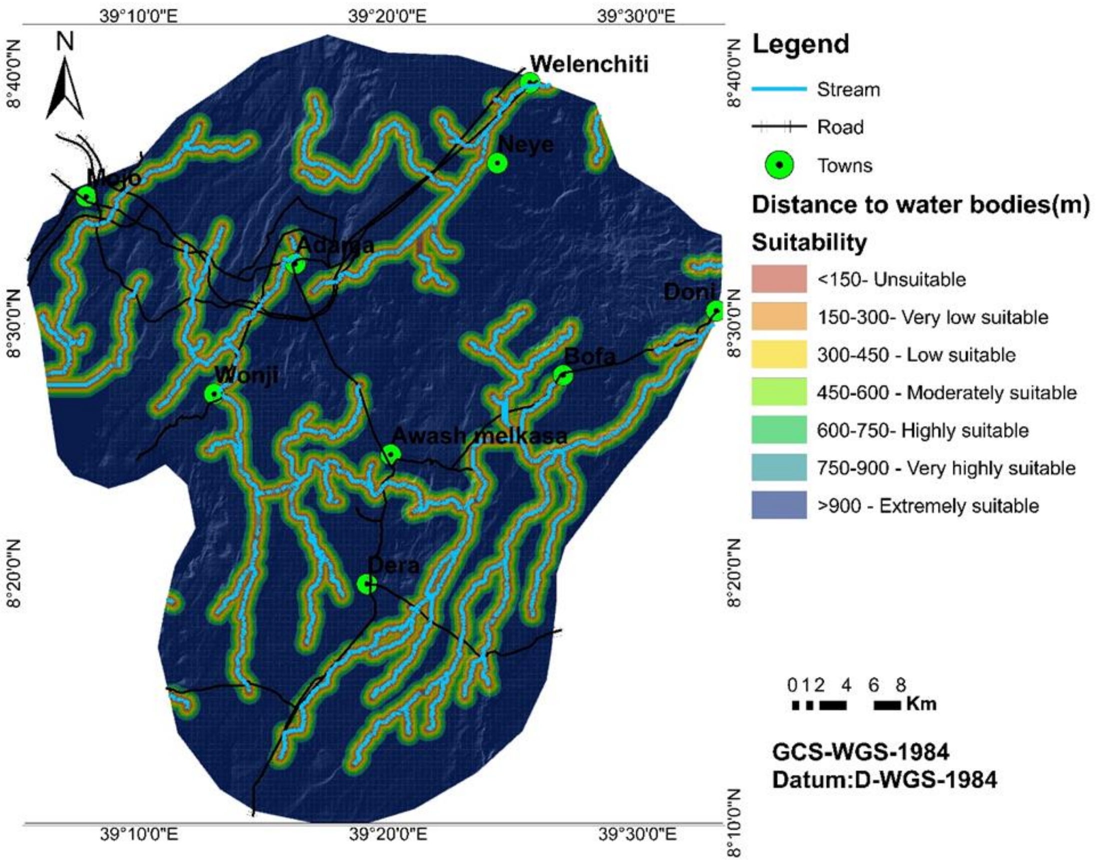

Figure 5.5: Reclassified thematic map of distance to water body based on the suitability as a quarry site

5.1.1.6. Distance to road

The proximity of aggregate resources to the major roads is generally regarded as more suitable because it allows easy access to the road network for the delivery of finished products and helps reduce the cost of the construction and maintenance of access to the necessary rock and quarries (Barakat *et al*., 2016). However, quarrying operation should be at a reasonable distance from the road so as not to disturb or destroy the road with the waste produced from the quarry. Thus proximity to roads was reclassified in seven classes by taking into account that quarry sites should not be too close and too far from the road. In this study area within 500m away from the road (or where the distance from the road is < 500) is considered too close and may disturb the road and the environment associated with it, so it was classified as unsuitable, and the area ranging in the distance from the road from 500m-1600 which covers

361.09 or 18.33% of the total was rated as an extremely suitable since it present at a reasonable distance that allows ease for the transportation of the product to the demand area and far enough so that road is not disturbed by quarrying activity and their by-products such as dust, therefore, it is extremely suitable as a quarry site. About 20.48Km^2(1.04% of the total study area) is located at uneconomic distance greater than 10000m which was given a rating of very low suitability because the long distance makes it hard for the quarry site to be accessed and generates the demand for the construction of a new road which is uneconomical. The rest of the class ranges are specified in the table, and the distance to road and their distribution within the study area is illustrated in the Figure 5.6.

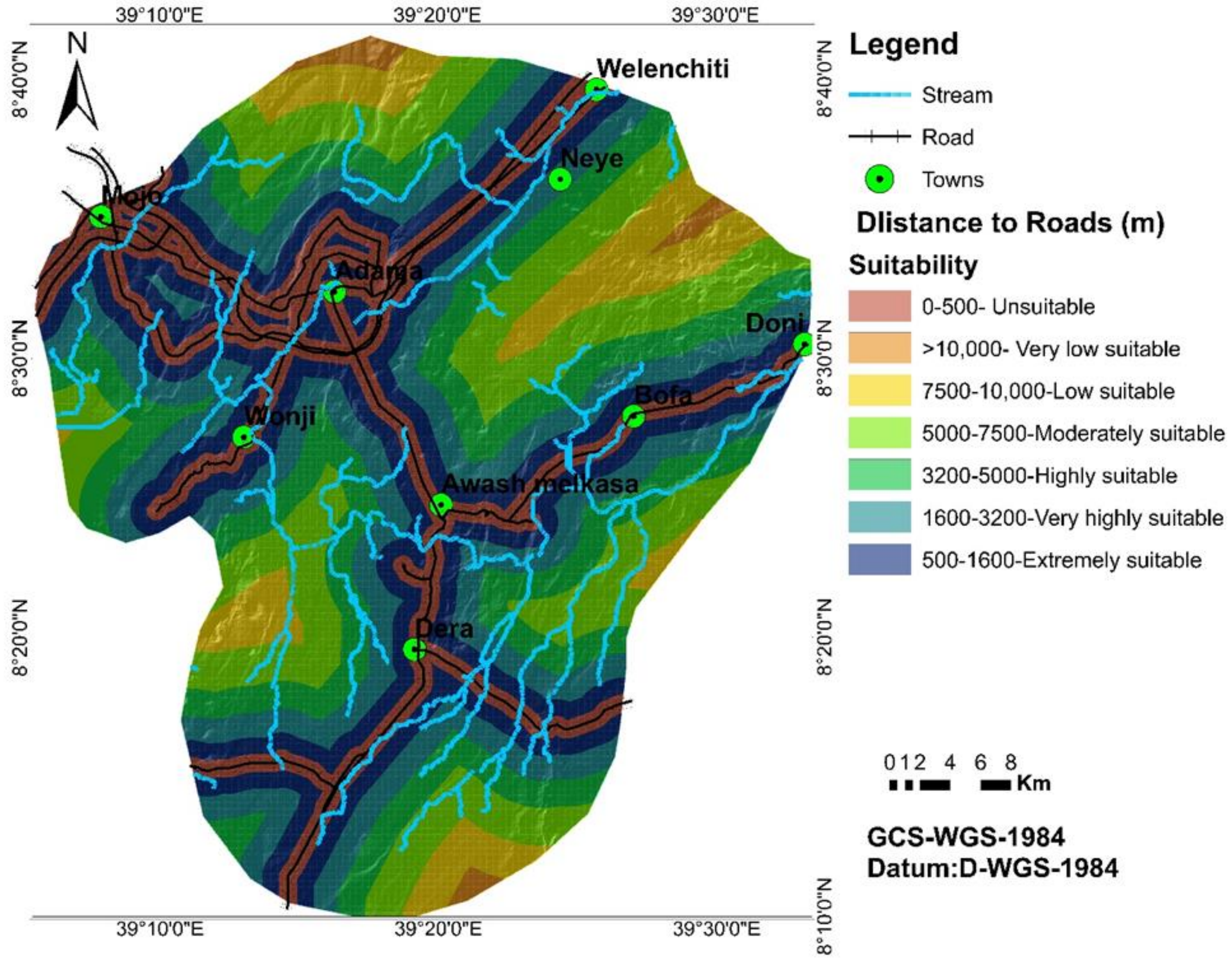

Figure 5.6: Reclassified thematic map of distance to road based on the suitability as a quarry site

5.1.1.7. Relative relief

Relative relief defines the elevation difference within a given slope (Anbalagan, 1992; Raghuvanshi *et al*., 2014; Ermias *et al*., 2017). It can influence the accessibility of quarry operation, potential for flooding, and difficulty in excavation (Gudissa *et al*., 2021). Considering the aforementioned issues, the relative relief is reclassified into seven classes based on the relative suitability of each relative relief range as zone having a relative relief <5 m (extremely low relative relief),>300 m(extremely high relief), 200 m-300 m (very high), 100 m-200 m(high), 50 m-100m(moderate), 25 m-50 m (low) and 5 m -25 m(very low) as shown in the Table 5.1. The area with extremely low relative relief (<5 m) was rated as unsuitable because the area having low relative relief is prone to flooding, and the excavation process in this area is very difficult, which makes it unfavorable to quarrying activity. The area having a relative relief > 300 m was rated as very low suitable because it cannot easily be accessed to perform quarrying activity. The distribution of each relief range shown in Figure 5.7.

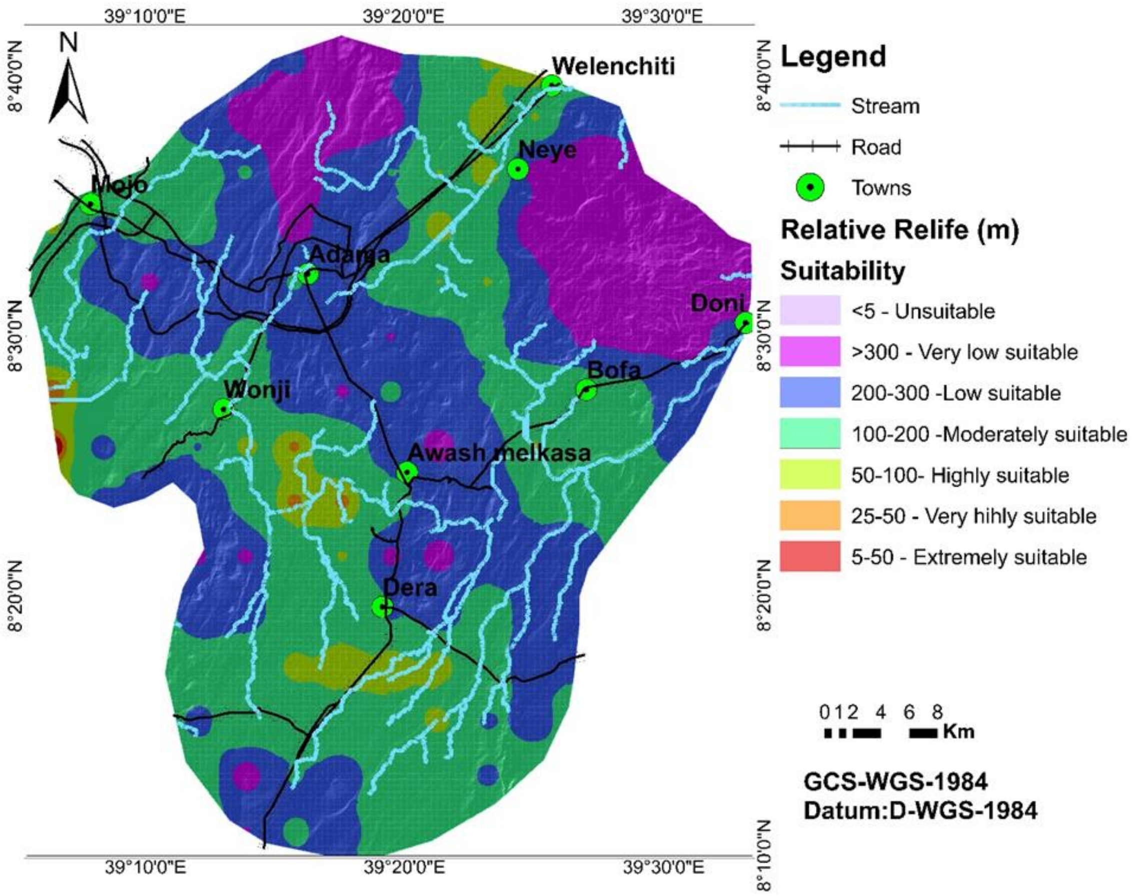

Figure 5.7; Reclassified thematic map of relative relief based on its suitability as a quarry site

5.1.1.7. Slope angle

Slope geometry that affects its stability includes its height and angle (Raghuvanshi *et al*., 2014; Chimidi *et al*., 2017). The Steeper slopes, the more susceptible they are to slope instability (Girma *et al*., 2015; Raghuvanshi *et al*., 2015; Chimidi *et al*., 2017). For safe quarrying activity, a gentle slope angle with less probability of slope failure or rock slide is favorable than a steep slope (Bayisa *et al*., 2015). The slope inclinations $<5^{o}$ may pose difficulties in quarry operations due to poor drainage, water logging, pitting for excavation, and slopes with angles 45^{o} and above will be lower in their suitability owing to difficulties in accessibility and quarry operations (Gudissa *et al*., 2021). Thus slope angle map is reclassified into seven classes in which the slope with $<5^{0}$(Extremely gentle),$>60^{0}$(High escarpment) & 45^{0}-60^{0}(escarpment or cliffs) were rated as unsuitable, very low suitable, and Low suitable. Moreover, the area having 5^{0}-15^{0}(Moderately gentle), 15^{0}-25^{0}(Gentle),25^{0}-35^{0}(Moderately steep), and 35^{0}-45^{0}(steep) slope angle ranges were given a rating of 6,5,4 and 3, as stated in Table 5.1 regarding their distribution in the study area as shown in Figure 5.8.

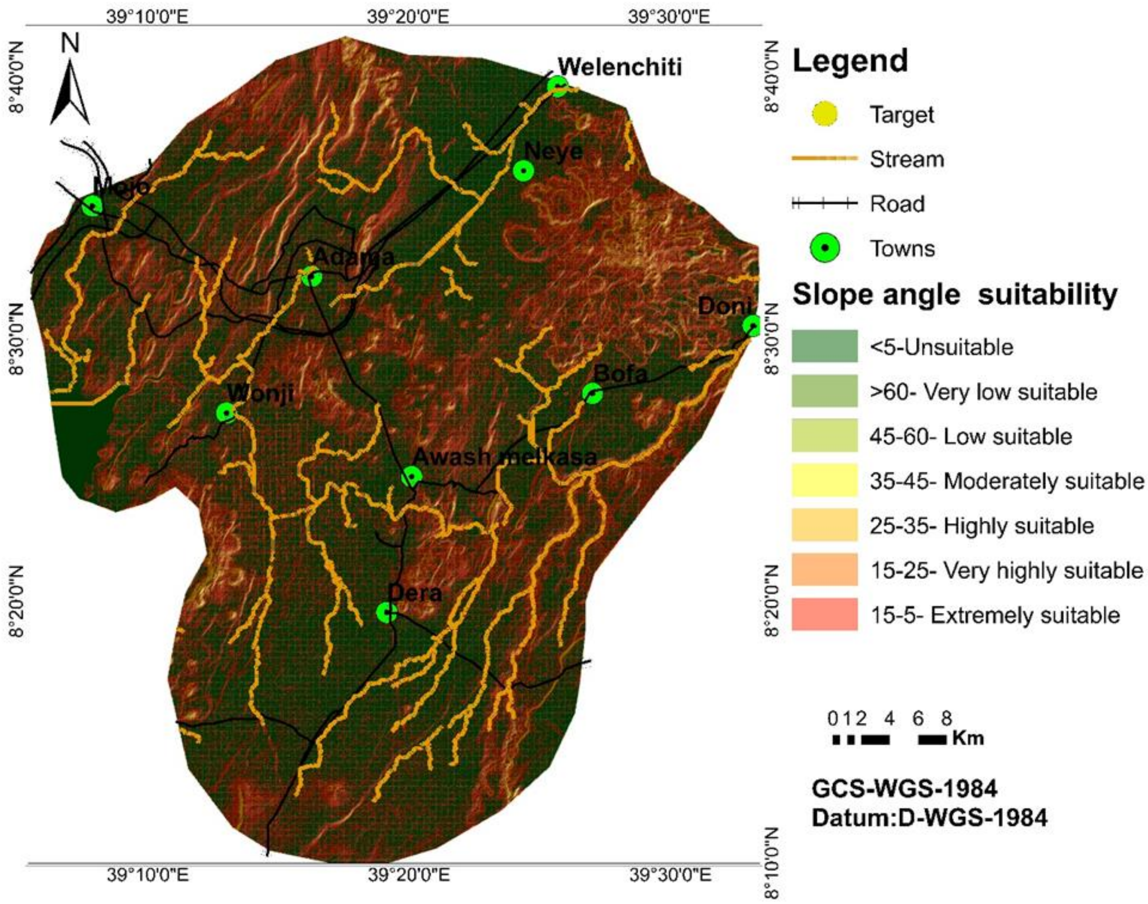

Figure 5.8:Reclassified slope map based on their suitability as a quarry site

5.1.2. Preliminary suitability map

In this study, preliminary site suitability analysis was done using a weighted overlay of the thematic map of the seven criteria, and the order of importance of the seven layers is then converted to a percentage as shown in Table 3,and then, the reclassified maps are added to the model builder and then linked to the weighted overlay tool. The weight of each layer calculated using AHP were inserted, and the layers are overlaid to produce the preliminary quarry site suitability map which is presented in fig 3. In this map, the suitable sites represent the area where quarrying operations can be carried out economically and without significant impact on the environment. Considering the seven criteria about 30.5% (601.6km^2) of the total study area is highly suitable as a quarry site if suitable material is available. Most of the highly suitable area is located away from the buildup area and mostly in an area covered by shrubs. Where dense populations are located and crops are cultivated is shown as an unsuitable area covering about 110.12Km^2 (5.59%) of the study area since those land uses are prone to be highly affected by quarrying activity. The rest of the area covered has low to moderate suitability, that is 383.23km^2 (19.46%) of the study area has low suitability as a quarry site because it is very close to build-up area and water bodies that can easily be disturbed or polluted by quarrying activity. The area having a moderate distance to build up area, water body, road and where the land is covered by shrubs is present as moderately suitable in the map covering 868.43Km^2 or 44.1% of the total area as shown in the figure below.

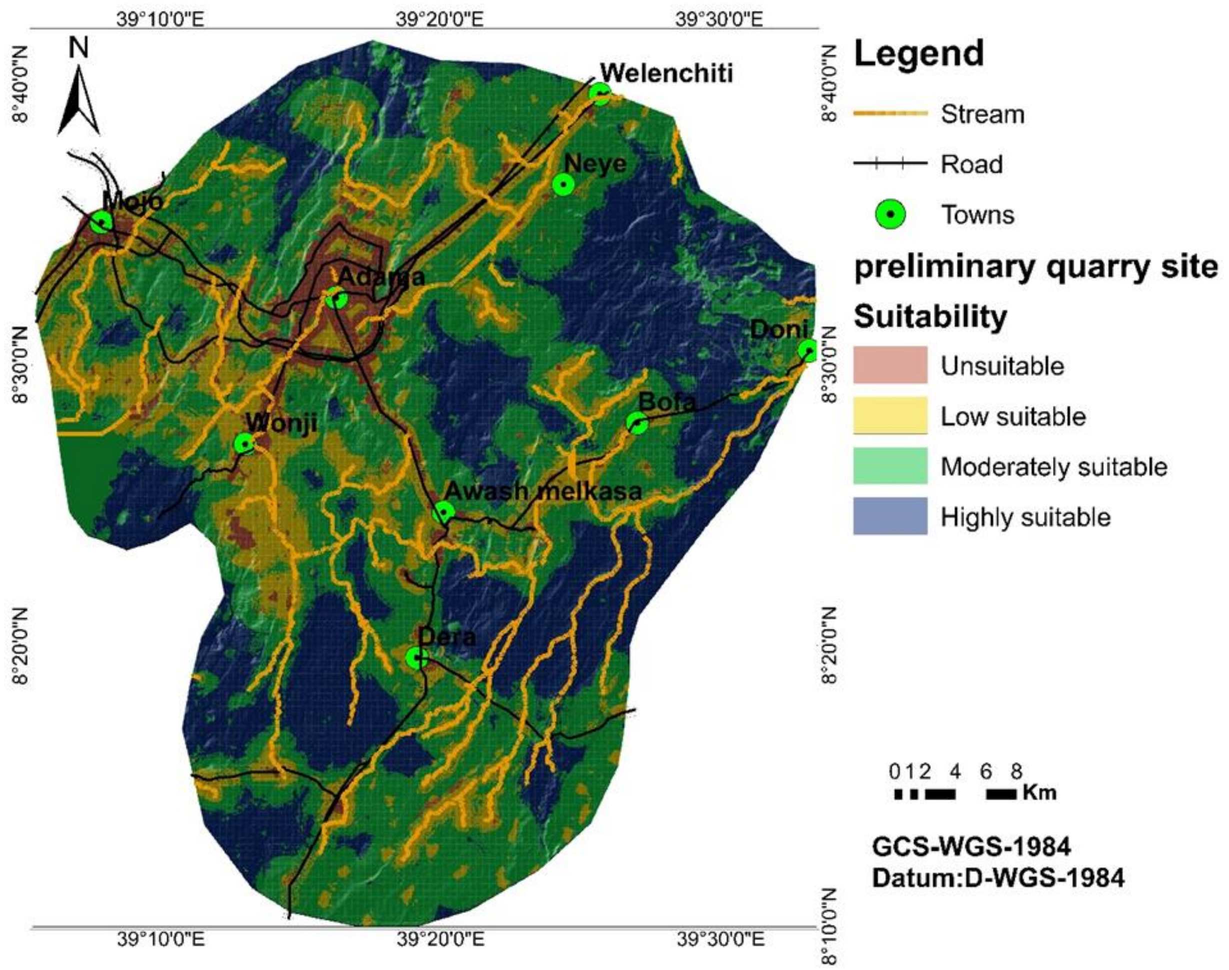

Figure 5.9: Preliminary quarry site suitability map

5.1.3. Final quarry site suitability analysis

In this stage of suitability analysis, the availability of suitable lithology for crushed stone aggregate is considered in addition to the environmental and economic aspects of the quarry operation. For this purpose, the lithology of the study area was classified into two classes soil, unconsolidated and highly weathered material (alluvial soil, volcanic ash, pumice, scoria, and weakly welded ignimbrite (tuff)), and consolidated /cemented) rock (Basalt, welded ignimbrite, etc.) based on their suitability as a crushed stone coarse aggregate for concrete as shown in Figure 5.1**.** Then, using map algebra, specifically multiplication of the preliminary map and lithology map, was used to find the overlapping area of the pixels suitable in the preliminary quarry site suitability map and the suitable lithology (consolidated or cemented rock) for crushed stone aggregate. Finally, the final suitability map is produced and was classified into four classes as unsuitable, covering 1412.9km^2 (72.5%) of the study area. It is an area where a large amount of population is settled and where competent material for aggregate is absent. About 10.515Km^2(0.53%) and 63.73Km^2(3.24%) of the study area were found to have low suitability and moderate suitability, respectively. The area having competent material that is found at a reasonable location based on the preliminary suitability maps was found to be highly suitable, having a total area coverage of 464.18Km^2 that is 23.64 % of the whole studied area, as shown in figure 5.10.

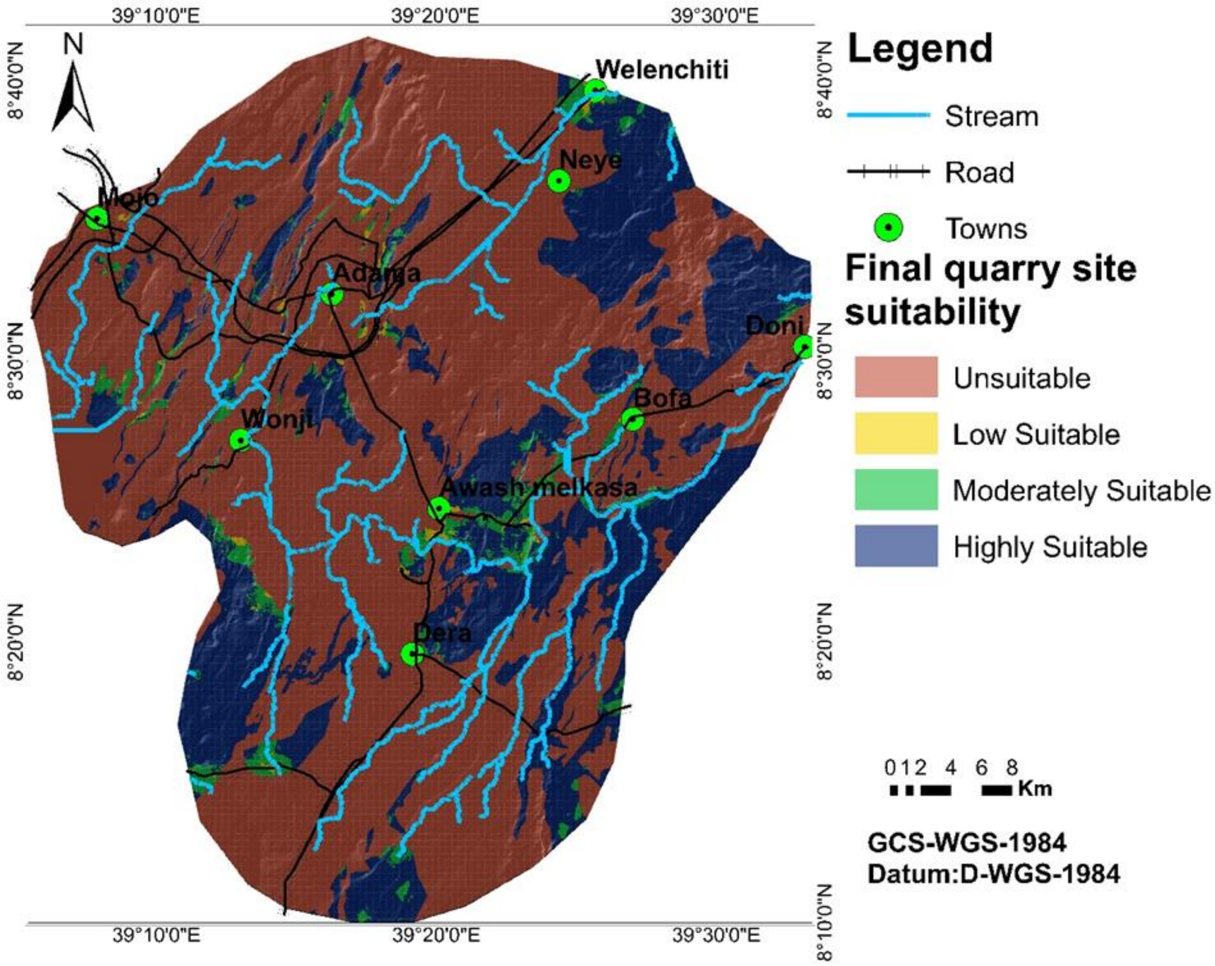

Figure 5.10: Final quarry site suitability map

5.2. Potential quarry site description

Aggregate quality assessment is important to ensure the good performance of aggregate for the intended use. Therefore, following the selection of a suitable quarry site, the physco-mechanial property of the material present at the site should be examined to determine their suitability for aggregate. In this study, nine sites were randomly targeted from highly suitable quarry sites closer to major roads for further evaluation of their physio-mechanical and petrographic property, as shown in Figure 5.11.

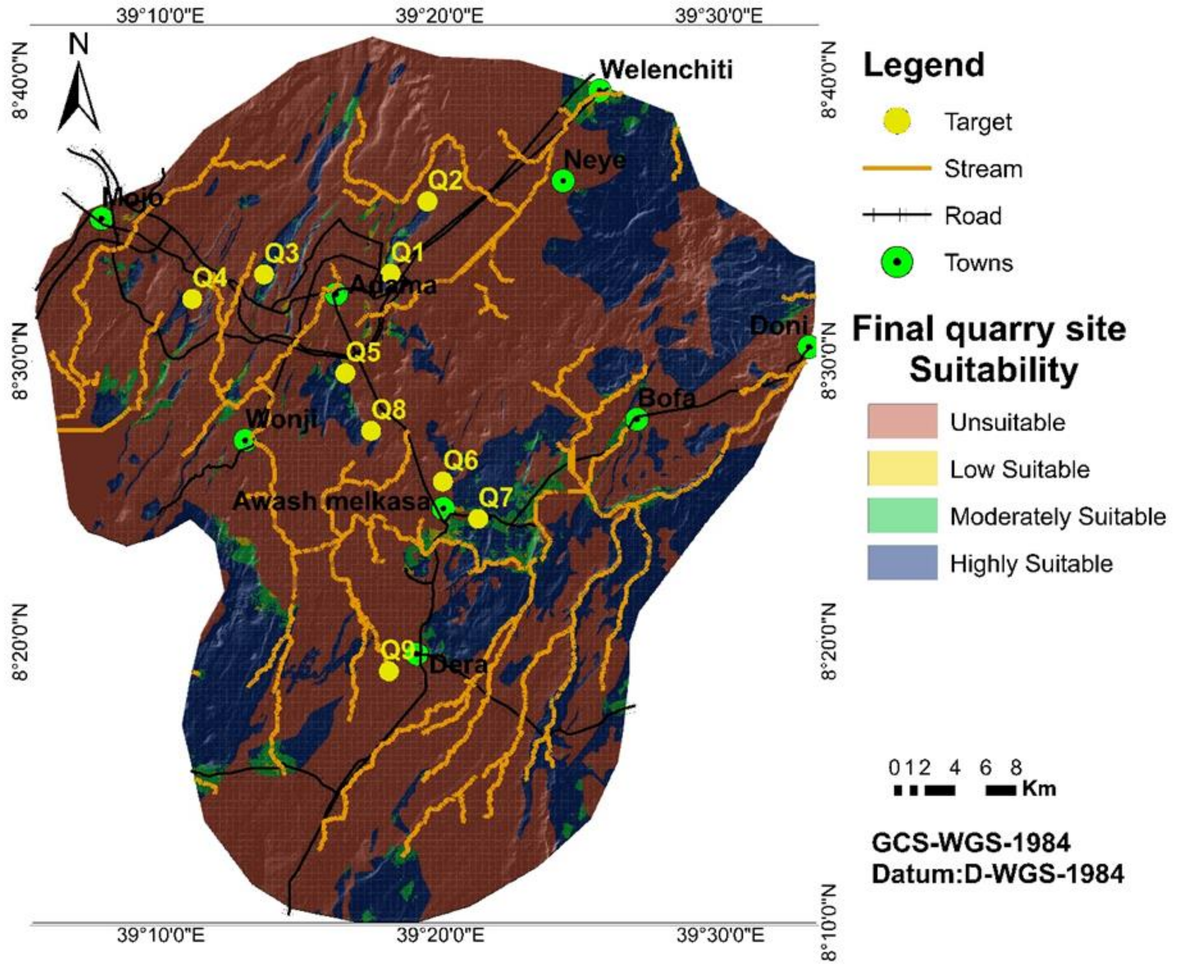

Figure 5.11: Sampling locations

Q1 is an existing large quarry located on the SW side of the study area at 533425m E longitude and 9455235m N latitude, which is an area mostly covered by shrubs. The overburden thickness at the site is less than 10cm which is favorable for quarrying operations. The material present on this site is Ignimbrite having a fine-grained texture. The site is located reasonably far from the road and built up, making it favorable for quarrying operations. This quarry supplies most of the aggregate demand for Adama town without prior knowledge of the physio-mechanical behavior of the rock at the site.

Q2 is located at 535854mE longitude and 949968mN latitude in the northeastern part of the town. The site is at a 3.39km distance from the built-up area, which favors quarrying operations. The overburden thickness in the area is less than 0.5m, making quarrying operations economical. The rock of the area is ignimbrite having a light grey color with fine to medium texture.

Q3 is located at 525123mE and 945183 N of the town around the police college that is about 2.44 Km distance from the built-up area. In this site, moderately weathered basalt having dark grey color and fine to medium texture are present. The site has an over burden thickness of less than 0.2m and is covered by scattered shrubs, making it fit for a quarry site.

Q4 is located at 520417m E and 943574m N, having a 6.69 km distance from the city. The site is easily accessible by a gravel road that intersects with the main road, which is favorable for the transportation of the product. This site possesses ignimbrite greenish-gray in color, having fine to medium texture.

Q5 is found near the city at exact locations 5304627 m E and 938700 m N at the tip of Boku ridge. It has an overburden thickness of 2m which is moderately suitable for quarrying operation (Bayisa *et al*., 2015) based on its economic value. This site has an outcrop that has a grey color and medium texture of ignimbrite and is covered by scattered shrubs which are highly suitable, as shown in Figure 5.11.

Q6 is found near Awash Melkasa at a 10Km distance from Adama exactly at 536862m E and 931601m N. This site has an overburden thickness of 2m which is moderately suitable for a quarry site due to its economic challenge (Bayisa *et al*., 2015). The top layer of this site is highly oxidized and weathered, which is unsuitable for an aggregate, but the layer beneath it is a massive basalt that is dark and has a fine to medium-grained texture.

Q7 is located along the road to Sodere at a distance of 12.9Km from Adama city exactly at N 539184 m E and 929154.5 m. The outcrop present in this area is porphyritic basalt that is dark and has a fine-grained texture with secondary fillings. This site has a very thin overburden thickness, which is economical for quarry development.

Q8 is located at 532151.5m E and 934928 m N south of Adama at a distance of about 4.8 Km. The site has no overburden, and the materials are available at the ridge's surface, making it economical to develop a quarry. The material present in this site is gray Rhyolite with medium to fine texture. This site is easily assessable since it is approximately 650m from the road that runs to Awash Melkasa, which makes the transportation of the material from the quarry to the demanded area easy.

Q9 is an existing open pit quarry near Dera located at 53331mE and 919156mN. The material present in this site is a greenish-gray with fine to medium-grained texture ignimbrite. This site has an overburden thickness of 1m which is good for quarry development.

5.3 Physico-mechanical property

The pysico-mechanical properties such as shape, UCS, crushing value, impact value, Los Angeles abrasion value, water absorption, density, and sodium sulfate soundness of the material present at the target sites were examined following BS and ASTM as discussed below.

5.3.1 Water absorption

It is a measure of the amount of water absorbed by aggregate. It affects the specific gravity of the aggregate as well as in-service behavior of concrete. It is considered an indirect measure of the permeability of aggregate that affects other physical characteristics such as mechanical strength, soundness, and general durability (Smith & Collis, 1993; Neville, 2000; Korkanç & Tuğrul, 2004). The water absorption value of the samples in the nine sites ranges from a minimum value of 0.77% obtained from Q3 to a maximum value of 8.94% obtained from Q2. BS5337:1976 and ASTM C 127-01 standards stated the maximum allowable value of water absorption of concrete aggregate is 3 and 2.5, respectively. Aggregates with low water absorption values are in high demand for quality concrete manufacturing (Fookes, 1980). Hence the studied samples Q1, Q3, Q5, Q6, and Q7 have shown a good water absorption quality that meets the standard specification as stated in Figure 5.12. Apparently, Q2, Q4, Q8, and Q9 has high water absorption value greater than the standard specification (>2.5). Aggregates with high water absorption are more porous and generally considered unsuitable (Schmidt and Graf, 1972).

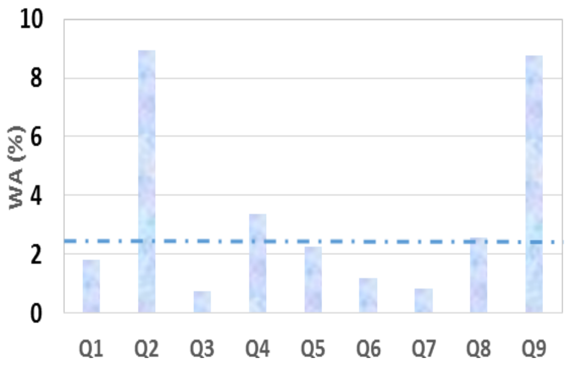

Figure 5.12: Water absorption value of aggregates of the target areas

5.3.2. Density and specific gravity

As summarized in Figure 5.13, the density of test samples ranges from 1940to 3690 kg/m3. The sample Q7 (3690Kg/m3) exhibits maximum density relative to the others, while Q2 (1940Kg/m3) has the minimum density. The relative density (specific gravity) of an aggregate is the ratio of its mass to the mass of an equal absolute volume of aggregates in order to meet the water requirement of the mix design accurately. The specific gravity of aggregates normally used in road construction ranges from about 2.4 to 3.0, with an average of about 2.68 (Neville, 2011; Arumugam, 2014; Nemati, 2015). In this study, specific gravity is computed from the ratio of density of the material per density of water, and the result obtained ranges from 1.94to 3.7. The rock samples Q3, Q4, and Q7 are in the specified range while the materials from Q1, Q2, Q5, Q6, Q8, and Q9 have a specific gravity that is not as per the recommendation. Relative density is not generally used as a measure of aggregate quality, though some porous aggregates exhibiting accelerated freeze-thaw deterioration and have low specific gravities. It is used in certain computations for mixture proportioning and control such as the volume occupied by the aggregate in the absolute volume method of mix design.

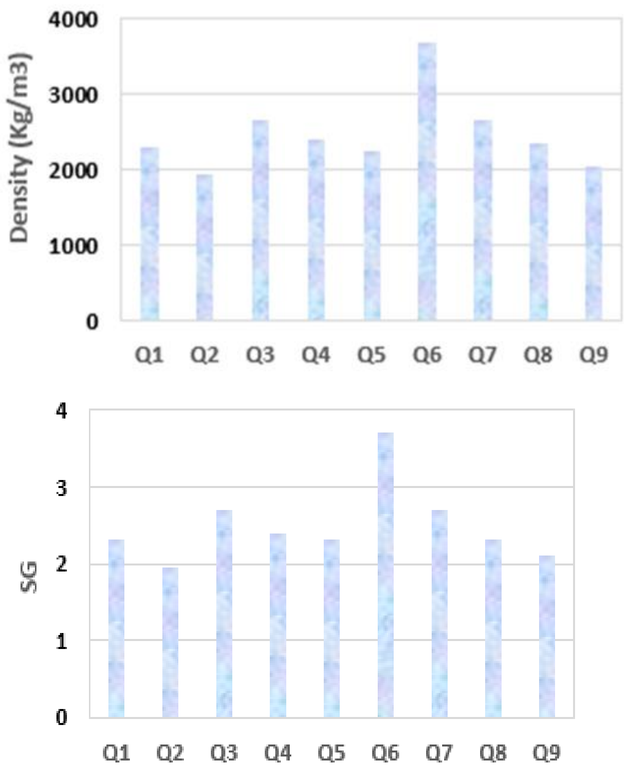

Figure 5.13: a) Density and b) specific gravity of the target area

5.3.3. Flakiness index (FI) and elongation index (EI)

The degree of packing or inter-locking of an aggregate sample depends on the shape of the particles in the mix; therefore, too many flaky or elongated particles can prove an obstacle in achieving the desired packing of aggregates. Flaky and elongated particles tend to lower the workability of concrete mixes. This is because these particles have a very large surface area to volume ratio value. These particles are inherently friable when subjected to heavy loading. Therefore, these are not desirable when preparing concrete mixes for structures that have to bear substantial loads. Particle shape and size distribution also influence the water content necessary to obtain a mix of suitable resistance, which in turn affects the compressive strength, drying. shrinkage and durability of the resulting concrete (Engidasew, 2014). Thus flaky and elongated particles should be limited to the standard specification.

FI values of the samples from the target area range from 11-25%, and the value for EI ranges from 9-24%. The minimum FI and EI are observed in Q4 (11%), and Q7 (9%), respectively, and the maximum value of FI and EI are observed in Q1 (25%) and Q8 (24%), respectively, as shown in Figure 5.14. According to BS-1241, the maximum permissible limit for flakiness index is 30%, and for the elongation index is 45%. The result states that all of the samples collected from each site are within the permissible limit. Therefore, the aggregate shape is suitable for use in concrete. Apparently, IS; 383 2016 clause no 53 specifies that the combination of flakiness and elongation index shall not exceed 40% for crushed and uncrushed aggregate. In that case specification, Q8 fails to meet the standard.

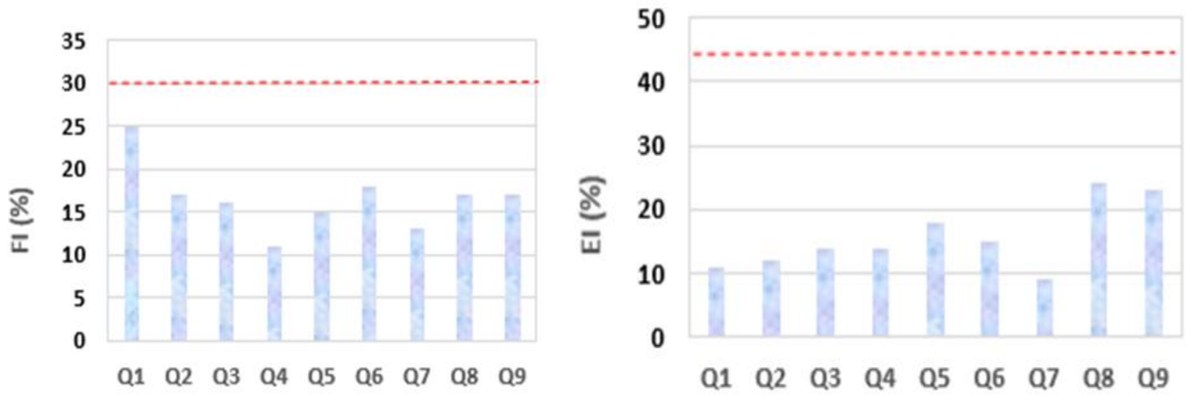

Figure 5.14: Flakiness index and elongation index of the study area

5.3.4. Uniaxial compressive strength (UCS)

UCS test is performed to determine the strength of the intact rock. The results of the UCS value of the samples range from a minimum value of 24.9 MPa to a maximum value of 99 Mpa. The International Society for Rock Mechanics (ISRM) standard terminology for UCS is very low (< 5 MPa), low (5–25 MPa), moderate (25–50 MPa), medium (50–100 MPa), high (100–250 MPa), and very high (> 250 MPa). Therefore, the strength of the sample based on ISRM is low to medium that is Q1 (93.83MPa), Q6 (76.6MPa), Q7 (99.0MPa), Q8 (98.3MPa), and Q9 (52.4MPa) are of medium strength, while Q2 (32.76MPa), Q3 (40.19MPa) and Q4 (27.74MPa) are moderate. The samples from Q5 (24.9) have low strength. Apparently, according to the Instruction manual on concrete test hammers, as cited in Tawake (2007), the rock with UCS value > 20 MPa can be accepted as a suitable aggregate source rock. The result obtained from the UCS test of the rock samples is within the range 24.9-99.6MPa in this case, the rock samples are suitable for an aggregate.

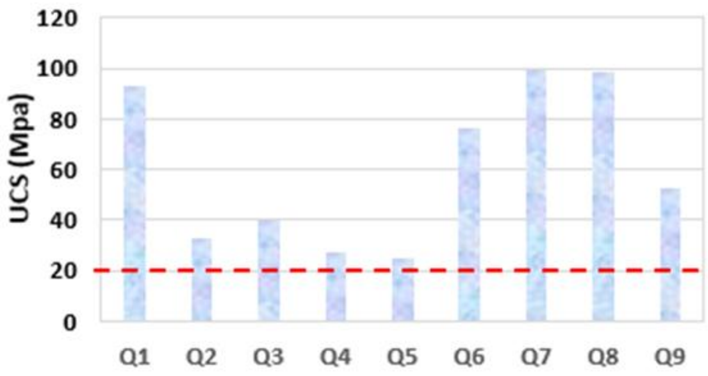

Figure 5.15: Uniaxial compressive strength of the sample from the target areas

5.3.5. Aggregate impact value (AIV)

The proportion of material passing BS 2.36-mm sieve after loading is calculated as a percentage of the original sample weight and expressed as the aggregate impact values for shock loading. AIV is used as a measure of resistance to sudden impact. A low numerical value means a resistant rock. Values obtained from the tests are given in Figure 5.16. The aggregate impact value of the samples varies from 11.73% to 37.25%. According to IS:383, (2016)clause no5.4.2, aggregate to be used for other than wearing surfaces should have an impact value limited to a maximum of 40%, while aggregates to be used in concrete for wearing surfaces like a runway, roads, pavements, tunnel lining carrying water, spillways, stilling basins, the impact value should be <30%. Therefore, all the aggregates from target areas are suitable for use in a concrete work other than wearing surface, while all the samples except Q2, Q4, and Q5 are suitable for a concrete work used for wearing surface.

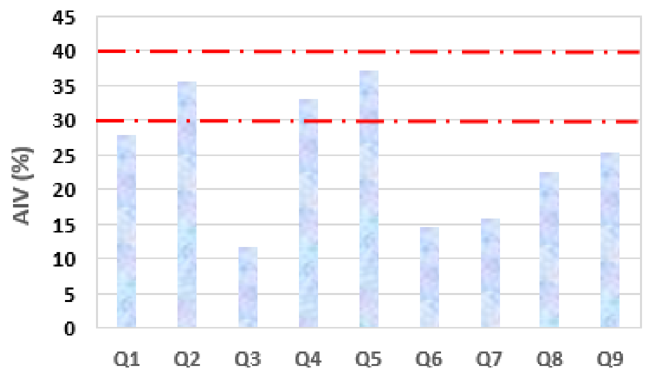

Figure 5.16: Aggregate impact value of the target areas

5.3.6. Aggregate crushing value (ACV)

The proportion of material passing BS 2.36-mm sieve after loading is calculated as a percentage of the original sample weight and expressed as the aggregate crushing values for static loading. The value indicates the ability of an aggregate to resist the gradually applied load. The lower the value, the stronger the aggregate is. For the samples of this study, the aggregate crushing value ranges between 15% and 34%. The maximum value is recorded for Q5 and the minimum value for Q3. According to BS EN 1097-6 (2000), the crushing value of an aggregate should be limited to 30% maximum. Thus all the materials except Q5 satisfy the standard limit and are therefore acceptable.

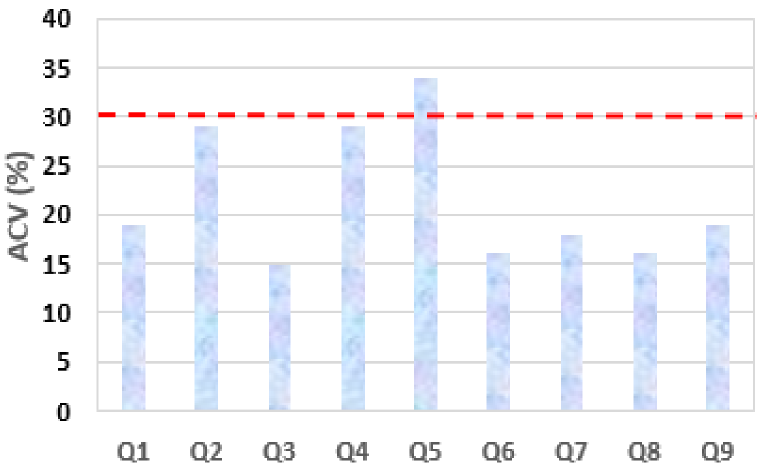

Figure 5.17: Aggregate crushing value of the target area

5.3.7. Los Angeles abrasion value (LAAV)

The abrasion resistance of an aggregate is often used as a general index of its quality. Abrasion resistance is essential when the aggregate is to be used in concrete subject to abrasion, as in heavy-duty floors or pavements. As seen in Figure 5.18, the Los Angeles abrasion values (after 500 cycles) range between 15.05% and 51.10%. According to IS:383, (1970), the abrasion value should not be more than 30% for wearing surface and not more than 50% for concrete other than wearing surface, and according to EN standards, the maximum allowable value is 35 %. The aggregate samples Q1, Q3, Q6, Q7, Q8, and Q9 have a good abrasion value, therefore can be used for concrete work of a wearing surface and the aggregates of Q2, Q4 and Q5 exhibits low abrasion value comparative to the others and can only be used in a concrete work other than wearing surface unfit for concrete as a wearing surface. Because low abrasion resistance of an aggregate may increase the quantity of fines in the concrete during mixing; consequently, this may increase the water requirement and require an adjustment in the water-cement ratio.

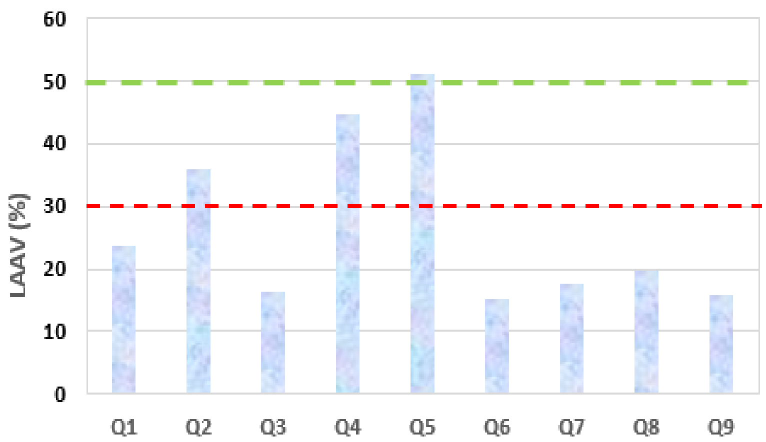

Figure 5.18: Los Angeles abrasion value of the target areas

5.3.8. Soundness

Soundness is the term used for the ability of an aggregate to resist excessive volume changes as a result of changes in the physical environment, e.g. freeze-thaw, thermal changes at temperatures above freezing, etc. (Smith and Collis, 2001). The extent of the disruption is dependent upon the soundness of the aggregate. According to ASTM C88-83(1989), the permissible limit of aggregate soundness value is 12%. The result of this study demonstrated from the test, as shown in Figure 5.19, means that Q1 (6.6%), Q5 (4.7%), Q6 (10.6%), Q7 (3.1%), Q8 (9.4%), and Q9 (1.2%) has a good soundness value within the permissible limit while the result of Q2, Q3 and Q4 has a soundness value that does not meet the standard requirements.

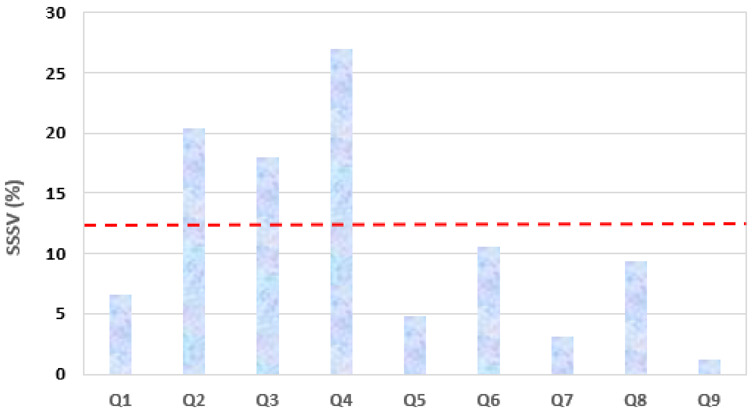

Figure 5.19: Sodium sulphate soundness value of the target in the study area

5.4. Petrography of the aggregates

Representative rock thin sections from each site were used for a detailed petrographic investigation, including structural/textural characteristics and determination of a modal mineralogical composition through microscopic investigations. The petrographic analysis was also carried out to identify the alkali-silica reactive minerals if present in the rock samples. Table 5.2 summarizes the main petrographic features observed at the microscopic scale in the analyzed samples.

Table 5.2: Petrography of the aggregates

Sample ID	Rock texture	Mineral composition					
		Quartz	Pyroxene	Opaque minerals (Fe-oxides)	Feldspar	Olivine	Volcanic glass
Q1	Porphyritic	-	2	3	30	-	65
Q2	Porphyritic	-	2	5	20	-	73
Q3	Porphyritic	-	20	5	71	-	5
Q4	Flow texture	-	1	3	32	-	65
Q5	Porphyritic	-	1	3	21		75
Q6	Porphyritic	-	10	5	80	1	4
Q7	Porphyritic	-	30	1	50	-	19
Q8	Porphyritic	48		7	15		30
Q9	Vitrophyritic			3	5	-	92

The different petrographic properties such as grain size, mineral dispersion, and texture affect the mechanical properties of aggregates. As shown in Figure 5.20 Q1 has a fine to medium texture in macroscopic view and has a porphyritic texture in which the phenocrysts of feldspar lie on the groundmass of volcanic glass, fine-grained feldspar, and opaque minerals (Fe-oxide) in microscopic level.

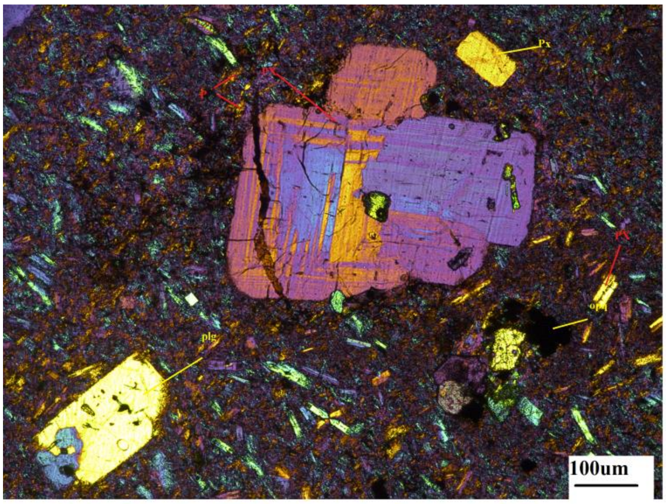

Figure 5.20: Microphotograph of the thin section Of ignimbrite rock (Q1)

The hand specimen of Q2 has a light grey color, and fine to medium grains and thin section analysis (microscopic view) of Q2, as shown in Figure 5.20, demonstrate that it has a porphyritic texture in which the phenocrysts of feldspar and pyroxene lie on the groundmass of volcanic glass, fine-grained feldspar and fine-grained Opaque minerals. As shown in Fig5.21b, Q3 has dark gray in color and fine tomedium-grained texture. Microscopically it has a porphyritic texture in which phenocrysts of feldspar lie on the groundmass of fine-grained pyroxene, feldspar, volcanic glass, and opaque minerals (Fe-oxide).

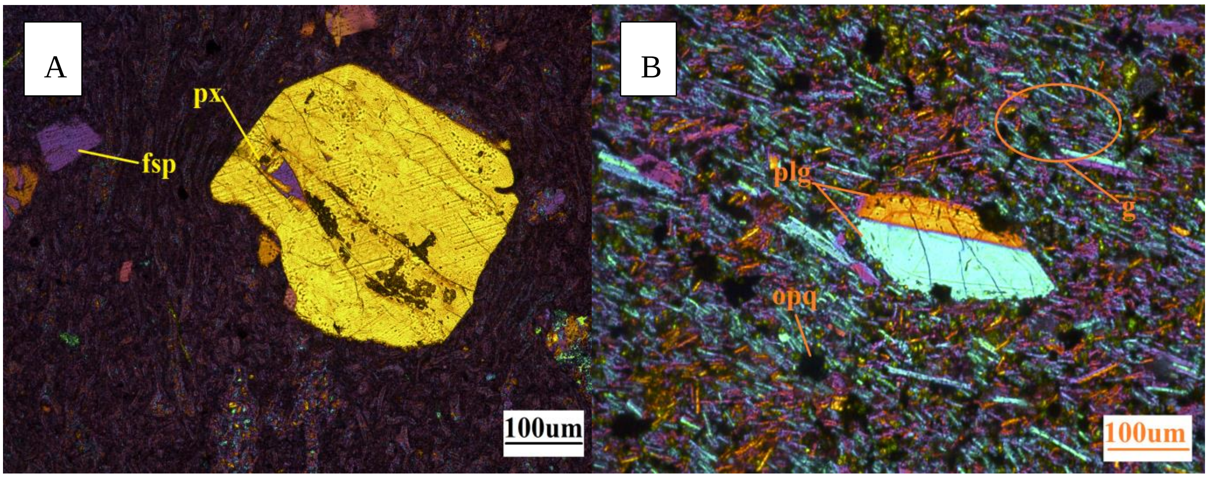

Figure 5.21: Microphotograph of the thin section of the ignimbrite in Q2 (a) and the basalt Q3 (b)

Figure 5.22 demonstrate the macroscopic view of the ignimbrite Q4, which has a greenish-gray color with fine to medium grain texture while figure 5.22a shows the microscopic texture of Q4 is a flowing texture in which the ground mass composed of mainly volcanic glass, feldspar, and minor amount of opaque mineral. The ignimbrite in Q5 has a grey color medium-grained texture as shown in figure 5.22b and has a mineral composition of volcanic glass, feldspar, opaque, and pyroxene. Microscopically Q5 has a porphyritic texture in which the phenocrysts of feldspar lie on the groundmass of volcanic glass, fine-grained feldspar and opaque minerals.

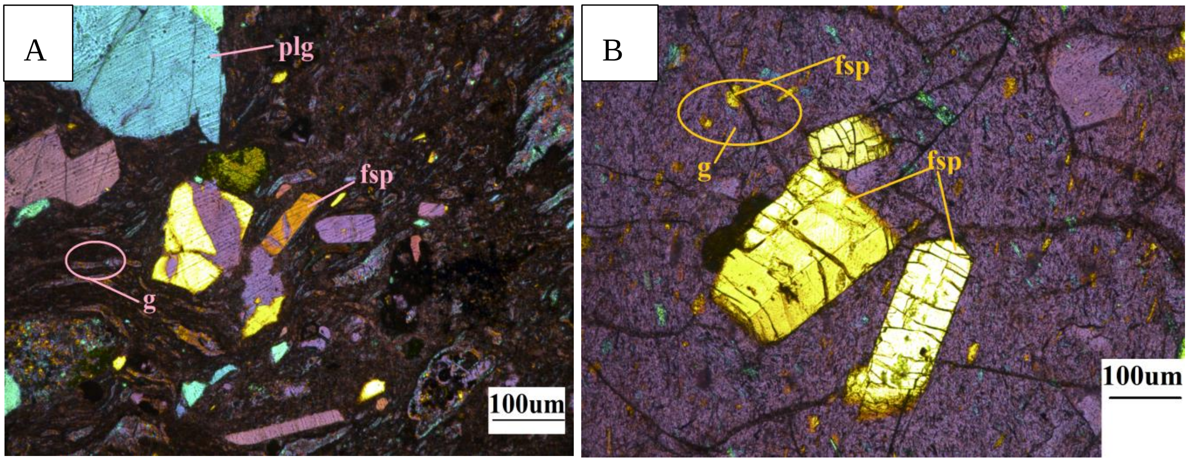

Figure 5.22: Microphotograph of the thin section of the ignimbrite in Q4 (a) and Q5 (bQ6 is andesite having a grey color and fine to medium grain sized and microscopically, it has a porphyritic texture with phenocrysts of plagioclase lie on the groundmass of fine-grained feldspar, pyroxene, and opaque minerals (iron oxides) as shown in the figure 5.23a. Q7 in the hand specimen has a similar appearance to that of Q6 and has a mineral composition of feldspar, pyroxene, volcanic glass, opaque mineral with porphyritic texture in which phenocrysts of feldspar lie on the groundmass of pyroxene, fine-grained feldspar, volcanic glass and opaque minerals as shown in figure 5.23b.

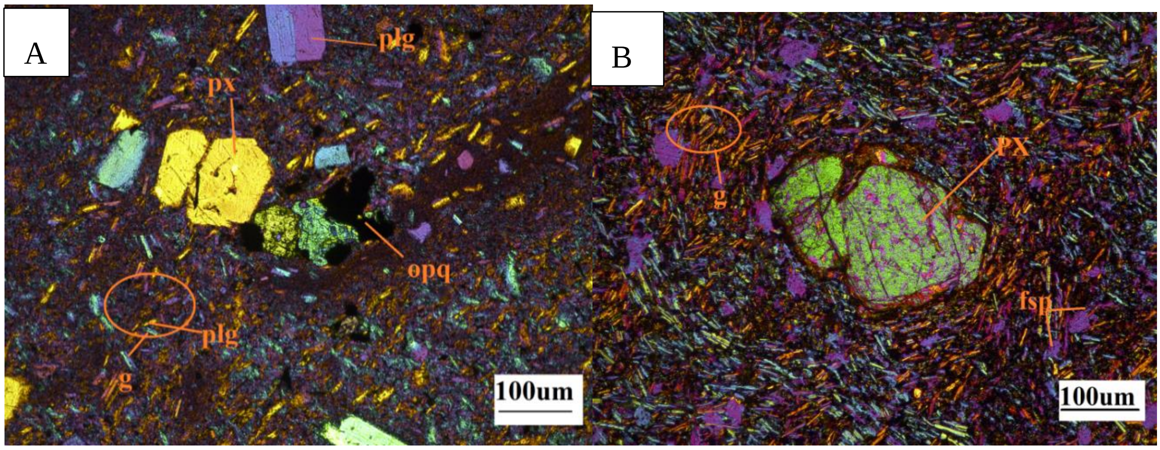

Figure 5.23**:** Microphotograph of the thin section of the basalt in Q6 (a) and Q7 (b)

The hand specimen in Q8 and in Q9 has dark grey and grey colure, respectively, with fine to medium-grained texture. As shown in figure 5.24a, the mineral composition of Q8 is abundantly Quartz (48%) and volcanic glass (30%) which is the groundmass in which phenocrysts of feldspar lie on along with opaque minerals. Moreover, Q9 has a vitrophyric texture in which phenocryst of feldspar lie on the groundmass of volcanic glass, which is abundantly found, as stated in table 4.3 fine-grained feldspar and opaque mineral.

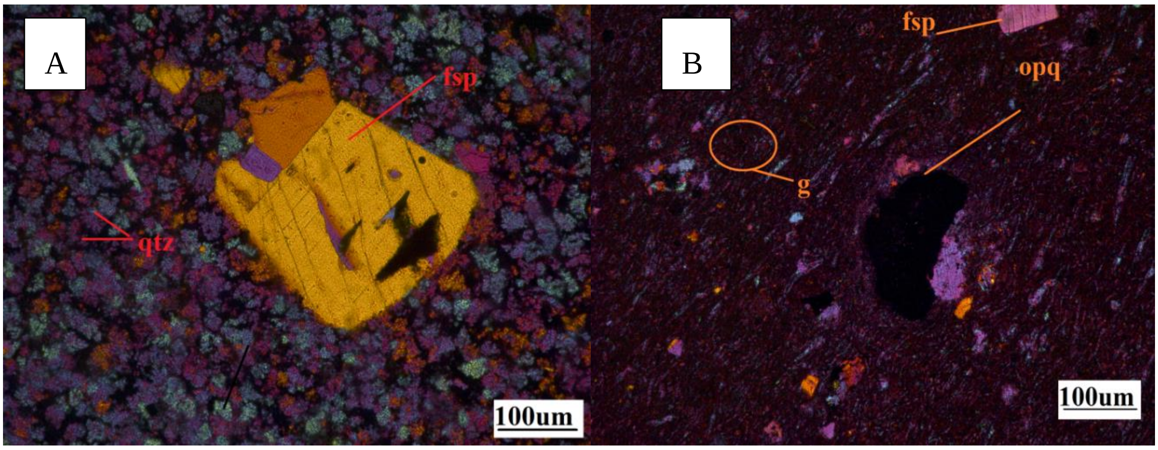

Figure 5.24: Microphotograph of the thin section of the rhyolite in Q8(a) and the ignimbrite in Q9(b) thin section

Finally, alkali-silica reactive minerals such as opal, chalcedony, chert, cristobalite, etc. we're not identified in all rock samples. The olivine identified in Q6 is also within an acceptable limit as it is not greater than 1%. Therefore, the target sites' aggregates are considered not potentially susceptible to alkali-silica reaction. However, for accurate determination of alkali-silica reactivity of aggregates, alkali-silica reactive tests such as the mortar bar test shall be carried out.

5.5. Correlation between physico-mechanical and petrographic properties of the aggregates

In this study correlation analysis was conducted to determine the relation between physico-mechanical and modal mineral composition of the rock (Table 5.3).

Table 5.3: Correlation matrix of the physico-mechanical and modal mineralogy of the aggregates.

	FI (%)	*EI (%)*	*ACV (%)*	*AIV (%)*	*LAAV (%)*	*WA(%)*	*D(kg/m3)*	*SG*	*SSSV (%)*	*UCS(Mpa)*
FI (%)	1									
EI (%)	-0.030	1								
ACV (%)	-0.341	-0.087	1							
AIV (%)	-0.038	0.092	0.894	1						
LAAV (%)	-0.342	-0.080	0.963	0.857	1					
WA(%)	0.004	0.299	0.333	0.516	0.137	1				
D(kg/m3)	-0.014	-0.196	-0.471	-0.675	-0.410	-0.625	1			
SG	-0.027	-0.206	-0.464	-0.681	-0.411	-0.622	0.998	1		
SSSV (%)	-0.346	-0.273	0.287	0.188	0.376	0.076	-0.004	-0.035	1	
UCS(Mpa)	0.419	-0.046	-0.715	-0.530	-0.673	-0.398	0.311	0.296	-0.523	1
fsp	-0.051	-0.493	-0.448	-0.730	-0.381	-0.660	0.869	0.875	0.197	0.142
g	0.091	0.240	0.654	0.853	0.547	0.722	-0.781	-0.773	-0.081	-0.441
ol	0.140	-0.040	-0.302	-0.411	-0.317	-0.258	0.884	0.878	-0.031	0.192
Opq	0.211	0.487	-0.255	-0.125	-0.177	0.071	0.115	0.073	0.320	0.019
Px	-0.278	-0.558	-0.448	-0.726	-0.455	-0.520	0.438	0.465	-0.128	0.320
Qtz	0.043	0.612	-0.302	-0.090	-0.186	-0.097	-0.100	-0.141	-0.078	0.451

As shown in Table 5.3, even though the correlation is weak, the uniaxial compressive strength is positively correlated to the abundance of feldspar, olivine, pyroxene, and quartzes. On the other hand, it is negatively correlated with glass content. Other tests used to determine mechanical properties of aggregate, such as ACV, LAAV, and AIV, are negatively correlated with the abundance of feldspar, pyroxene, and quartz, as shown in Table 5.1, which means that the more these minerals are present, the less the aggregate is likely to be crushed or impacted. According to previous work conducted by Yusof & Zabidi, (2016), quartz and feldspar have high control and influence on rock strength. The presence of volcanic glass is positively correlated with ACV, AIV, LAAV, and water absorption, which means that the higher the volcanic glass, the lower the aggregate quality. The presence of pyroxene and olivine has a positive correlation with the strength or mechanical property of the rock, as stated in the table.

According to Table 5.3, the physical property of the rock, such as SG and density, has a strong positive correlation with the abundance of feldspar and a negative correlation with volcanic glass, indicating that rock density is very sensitive to the minerals that compose a particular rock type. Specific gravity and density has a strong negative correlation with the abundance of volcanic glass.

The water absorption of the rock has a negative correlation with feldspar, and pyroxene, meaning the presence of these minerals, especially feldspar and pyroxene, strongly influence the water absorption may be due to the capacity of the minerals to interlock and form less porosity in the rock. On the other hand, the abundance of volcanic glass has a strong positive correlation with water absorption.

6. Conclusion

For development of a country specifically in the study area where population growth is rapid and where the demand for additional infrastructures is escalating, allocation of potential quarry sites for use as a source of aggregate is very important for the development and sustainable use of available mineral aggregate resources, the protection of natural resources and the reduction of environmental impact.

In this study, site suitability analysis using integrated GIS and AHP techniques was used to select a suitable quarry sites for use as an aggregate source. The suitability analysis was done in two stages, one in which quarry site is selected based on its favorability for land use and land cover, distance to build-up area, depth to groundwater, distance to water body, distance to road, relative relief, and slope angle which resulted in the preliminary suitability map. The preliminary suitability map shows that about 30.5 of (601.6Km^2) of the study area is highly suitable if competent material is available. The final quarry site suitability map was done by including lithology. The result shows that about 464.18 Km2 (23.64%) of the study area is highly suitable, which means competent material is available in the area that facilitates sustainable use of the resource with minimum possible impact on the environment. Moreover, 63.73Km^2 (3.24%) of the study area is moderately suitable, 10.515Km^2(0.53%) of the studied area has low suitability, and 1412 Km^2 (72.5%) is unsuitable.

Following the suitable quarry site selection, nine sites were targeted from the highly suitable sites in the suitability model for geo-mechanical characterization and to validate their suitability as aggregate for concrete. Water absorption, density, specific gravity, shape test, UCS, aggregate crushing value, aggregate impact value, Los Angeles abrasion value, and sodium sulphate soundness of the aggregates was tested. And their results were compared with the standard and indicate that the sample Q1, Q6, and Q7 are suitable in every aspect of the tested property i.e., satisfies the standard limit of each test and are therefore suitable as an aggregate source. The sample Q8 and Q9 has a good quality that satisfies the standard limit in every aspect of their property except for the water absorption.

According to the correlation analysis, there is a relatively strong inverse correlation between aggregate mechanical properties (ACV, AIV, LAAV) and UCS of intact rock. Quartz, pyroxene, and volcanic glass content strongly influence rock strength more than other mineral content. Volcanic glass content relatively strongly controls the aggregate mechanical properties (ACV, AIV, LAAV), water absorption, and density of aggregate. Generally, the higher the volcanic glass, the lower the quality of aggregate, while the more the content of quartz, feldspar, and pyroxene minerals are present, the less the aggregate is likely to be crushed or impacted. Therefore, petrographic analysis of source rock can be considered a good indication of the quality of aggregate.

7. Recommendation

Based on the present study, the following recommendations are forwarded:

- Identification process of a suitable quarry sites for a large area where economical extraction with low environmental degradation is possible, requires a huge amount of money, time, and effort as the suitability of a quarry site is influenced by various factors. Thus, integrated AHP and GIS used in the present study can be followed to economically select quarry sites with suitable material that can be extracted economically and with the lowest possible environmental degradation.
- For the present study, all efforts were made to systematically identify suitable quarry sites as a potential source of aggregate for the study area. Thus, further screening potential suitable site in regards to the recoverable reserve , degree of weathering slope stability analysis to ensure safe extraction of the is highly recommended and detail geo-mechanical property of the material present at the suitable site is strongly recommended.
- In the present study petrographic analysis were carried out, however, due to time constrains further analysis of the rock was not conducted. Thus, it is highly recommended to conduct major rock composition analysis.
- The correlation that was made between physico-mechanical and petrographic properties of the aggregates in this study is based on limited data (9 samples), which need to be considered indicative rather than accurate. Therefore, it is strongly recommended to carry out a further study with more samples.
- The alkali-silica reactivity of the aggregate in this study was evaluated based on petrographic analysis to identify alkali-silica reactive minerals. However, for accurate alkali-silica reactivity evaluation, it is recommended to carry out alkali-silica reactive tests such as the mortar bar test in future studies.

Reference

A.M., N. (2011). *Properties of Concrete* (5th edition ed.). Pearson Education Limited.

Abate, Z. (2016). Impacts of Stone Quarrying on Environment and Livelihood of Local Community in Addis Ababa Peri-Urban Areas. *Unpublished MA Project, Addis Ababa University*.

Abd, E., & Ahmed. (2015). *Engineering Evaluation of Some Lower Eocene Carbonate Rocks as Raw Materials.* sohag Governorate Egypt in Civil Engineering.

Abera, T. .. (2007). *Hydrogeological and Hydrogeochemical Assessment in Adama (Nazareth) - Dera Area, Central Ethiopia.* Masters thesis, Addis Ababa University.

Aburas, M. M., Abullah, S. H., Ramli, M. F., & Ash'aari, Z. H. (2015). A review of land suitability analysis for urban growth by using the GIS-based analytic hierarchy process. *Asian Journal of Applied Sciences, 3*(6).

Adewumi, J. R., Ejeh, O. J., Lasisi, K. H., & Ajibade, F. O. (2019). A GIS–AHP-based approach in siting MSW landfills in Lokoja, Nigeria. *SN Applied Sciences, 1*(12), 1-18 .

Adinkrah-Appiah, K., Kpamma, E. Z., Nimo-Boakye, A. N., Asumadu, K. T., & beng-Ankamah, N. (2016). Annual consumption of crushed stone aggregates in Ghana. *Journal of Civil Engineering and Architecture Research, 3*(10), 1729-1737.

Ajagbe, W. O., Tijani, M. A., & Oyediran, I. A. (2015). Engineering and geological evaluation of rocks for Concrete Production. *LAUTECH Journal of Engineering and Technology, 9*(2), 67-79.

Akanwa, A. O., Okeke, F. I., Nnodu, V. C., & Iortyom, E. T. (2017). Quarrying and its effect on vegetation cover for a sustainable development using high-resolution satellite image and GIS. *Environmental earth sciences, 76*(14), 1-12.

Akiwumi, F. A., & Butler, D. R. (2008). Mining and environmental change in Sierra Leone, West Africa: a remote sensing and hydrogeomorphological study. *Environmental Monitoring and Assessment, 142*(1), 309-318.

Ali, S., Lee, S. M., & Jang, C. M. (2017). Determination of the most optimal on-shore wind farm site location using a GIS-MCDM methodology: Evaluating the case of south korea. *Energies, 10*(12), 2072.

Alkaradaghi, K., Ali, S. S., Al-Ansari, N., Laue, J., & Chabuk, A. (2019). Landfill site selection using MCDM methods and GIS in the Sulaimaniyah Governorate, Iraq. *Sustainability, 11*(17), 4530. doi: https://doi.org/10.3390/su11174530

Alula, D., Getaneh, A., Mazzuoli, R., & Tortorici, L. (1992). Geological map of the Nazareth-Dera region(Main Ethiopian rift)1:50,000 cartgraphy SELCA,florence.

Anbalagan, R. (1992). Landslide hazard evaluation and zonation mapping in mountainous terrain. *Engineering geology, 32*(4), 269-277.

Arumugam, B. (2014). Effect of Specific Gravity on Aggregate Varies the Weight of Concrete Cube. *International Journal of Civil Engineering, 1*, 1-9.

Asante, F., Abass, K., & Afriyie, K. (2014). Stone quarrying and livelihood transformation in Peri-Urban Kumasi. *Journal of Research in Humanities and Social Sciences, 4*(13), 93-197.

ASTM.C88-99a. (1999). Standard Test Method for Soundness of Aggregates by Use of Sodium Sulfate or Magnesium Sulfate.

ASTM.D4543-19. (n.d.). Standard Practices for Preparing Rock Core as Cylindrical Test Specimens and Verifying Conformance to Dimensional and Shape Tolerances.

ASTM-D5030. (n.d.). Standard Test Methods for Density of In-Place Soil and Rock Materials by the Water Replacement Method.

Ataei, M., Jamshidi, M., Sereshki, F., & Jalali, S. M. (2008). Mining method selection by AHP approach . *Journal of the Southern African Institute of Mining and Metallurgy, 108*(12), 741–749.

Awoke, E., Endalew, T., & Solomon, T. (2018). Environment and Social Impacts of Stone Quarrying: South Western Ethiopia, in Case of Bahir Dar Zuria Wereda Zenzelma Kebele. *International Journal of Research in Environmental Science, 5*(2), 29-38.

Aydin, N. Y., Kentel, E., & Duzgun, H. S. (2013). GIS-based site selection methodology for hybrid renewable energy systems: A case study from western Turkey. *Energy conversion and management, 70*, 90-106.

Bajocco, S., De Angelis, A., Perini, L., Ferrara, A., & Salvati, L. (2012). The impact of land use/land cover changes on land degradation dynamics: a Mediterranean case study. *Environmental management*, *49*(5), 980-989.

Barakat, A., Ouargaf, Z., & Touhami, F. (2016). Identification of potential areas hosting aggregate resources using GIS method: a case study of Tadla-Azilal Region, Morocco. *Environmental Earth Sciences, 75*(9), 1-16.

Bayisa, R., Kumar, R. T., & Seifu, K. (2015). Quarry site selection and geotechnical characterization of ballast aggregate for Ambo-Ijaji railway project in central Ethiopia: an integrated GIS and geotechnical approach. *In Engineering Geology for Society and Territory, 6*, 329-335.

Berckhemer, H., Baier, B., Bartelsen, H., Behle, A., Burkhardt, H., Gebrande, H., & Vees, R. (1975). Deep seismic soundings in the Afar region and on the highland of Ethiopia. *Afar Depression of Ethiopia, 1,* 89-107.

Bigazzi, G., Bonadonna, F., Di Paola, G. M., & Giuliani, O. (1993). K-Ar and fission track ages of the last volcano tectonic phase in the Ethiopian Rift Valley (Tullu Moye'Area). In: Geology and mineral resources of Somalia and surrounding regions.

Boccaletti, M., Mazzuoli, R., Bonini, Trua, M., & Abebe, T. (1999). Plio-Quaternary volcanotectonic activity in the northern sectorof the Main Ethiopian Rift: relationships with oblique rifting. *Journal of Africa earth sciences, 29*(1), 679-698.

Bolen, W. P., & Tepordei, V. V. (2001). Construction aggregates. *Mining Engineering, 53*(6), 30-31.

Brail, R. K., & Klosterman, R. E. (2001). *Planning support systems: Integrating geographic information systems, models, and visualization tools.* ESRI, Inc.

British, G. S. (2019). Construction aggregates. Mineral Planning Factsheet. *45*, 567–568.

Broesamle, H., Mannstein, H., Schillings, C., & Trieb, F. (2001). Assessment of solar electricity potentials in North Africa based on satellite data and a geographic information system. *Solar Energy, 70*(1), 1-12.

BS 812-110:1990, B. (n.d.). Testing aggregates Methods for determination of aggregate crushing value (ACV).

BS 812-112:1990, B. (n.d.). Testing aggregates. Method for determination of aggregate impact value (AIV) (AMD 8772) (Superseded but remains current).

BS, E.-6. (2000). Tests for mechanical and physical properties of aggregates. Determination of particle density and water absorption.

BS:812--105.1. (1989). Methods for determination of particle shape - section 105.1: flakiness index.

BS:812-105.2:1989. (n.d.). Methods for determination of particle shape - section 105.2: elongation index.

BS:812-113:. (1990). Testing aggregates. Method for determination of aggregate abrasion value (AAV) (AMD 6986) (AMD 8770) (Withdrawn).

BS:812-2:1995. (n.d.). Methods for determination of particle density and water absorption.

Carney, D. (. (1998). *Sustainable rural livelihoods: What contribution can we make?* Department for International Development, London.

Chabuk, A., Al-Ansari, N., Hussain, H. M., Knutsson, S., & Pusch, R. (2016a). Landfill sitting using GIS and AHP (Analytical Hierarchy Process): A case study Al-Qasim Qadhaa, Babylon, Iraq. *Journal of Civil Engineering and Architecture, 10*, 530–543. doi: https://doi.org/10.17265/1934-7359/2016.05.002

Chabuk, A., Al-Ansari, N., Hussain, H. M., Knutsson, S., & Pusch, R. (2016b). Landfill site selection using Geographic Information System (GIS) and AHP: A case study Al-Hillah Qadhaa, Babylon, Iraq. *Waste Management & Research, 34*(5), 427–437. doi:https://doi.org/10.1177/0734242X16633778

Chabuk, A., Al-Ansari, N., Hussain, H. M., Knutsson, S., & Pusch, R. (2017). Landfill sites selection using analytical hierarchy process and ratio scale weighting: Case study of AlMahawil, Babylon, Iraq. *Engineering, 9*(2), 123–141. doi:https://doi.org/10.4236/eng.2017.92006

Chabuk, A., Al-Ansari, N., Hussain, H. M., Laue, J., Hazim, A., Knutsson, S., & Pusch, R. (2019). Landfill sites selection using MCDM and comparing method of change detection for Babylon Governorate, Iraq. *Environmental Science & Pollution Research, 26*, 3. doi:https://doi.org/10.1007/s11356-019-05064-7

Chaudhary, P., Chhetri, K, S., Joshi, K. M., Shrestha, B. M., & Kayastha, P. (2016). Application of an Analytic Hierarchy Process (AHP) in the GIS interface for suitable fire site selection: A case study from Kathmandu Metropolitan City, Nepal. *Socio-economic planning sciences, 53*, 60-71.

Chimidi, G., Raghuvanshi, T. K., & Suryabhagavan, K. V. (2017). Landslide hazard evaluation and zonation in and around Gimbi town, western Ethiopia—a GIS-based statistical approach. *Applied Geomatics, 9*(4), 219-236.

Chizoro, J., Jamare, J., Kanodereka, S., Mkusha, S., & Munyaradzi, C. (1997). *A Study of the Environmental Impacts of Black Granite Quarrying in Mutoko District.* Department of Natural Resources and Department of Ministry of Mines,Environment and Tourism,, Harare.

Coppin, N., & Bradshaw, A. (1982). The Establishment of Vegetation in Quarries and open pit non-metal mines. *Mining journal books*, 112.

Darwish, T., Khater, C., Jomaa, I., Stehouwer, R., Shaban, A., & Hamze, M. (2011). Environmental impact of quarries on natural resources in Lebanon. *Land Degradation & Development, 22(3)*, 345–358. doi: https://doi.org/10.1002/ldr.1011

de Castro Pessoa, J. R., Domínguez, J. S., Wilson, R. E., da Silva Charles, V., de Carvalho, G., & de Assis, J. T. (2015). Calculation of percentage of coarse aggregate present in concrete using processing of digital images obtained with a commercial scanner. *J. Chem, 136-139*, 136-139.

Dechasa, T. (1999). Water balance and effect of irrigated agriculture on groundwater quality in Wonji area/Ethiopian Rift Valley. *Unpublished MSc thesis, Addis Ababa University, Addis Ababa, Ethiopia.*

Dengiz, O., Bayramin, İ., & Yüksel, M. (2003). Geographic information system and remote sensing based land evaluation of Beypazarı area soils by ILSEN model. *Turkish Journal of Agriculture and Forestry, 27*(3), 145-153.

Dey, P. K., & Ramcharan, E. K. (2008). Analytic hierarchy process helps select site for limestone quarry expansion in Barbados. *Journal of Environmental Management, 88*(4), 1384–1395. doi:https://doi.org/10.1016/j.jenvman.2007.07.011

Dhar, B. B., Jamal, A., & Ratan, S. (1991). Air pollution problems in an Indian opencast coal mining complex: A case study. *International Journal of Surface Mining, Reclamation and Environment*, *5*(2), 83-88.

Di Paola, G. M. (1972). The Ethiopian Rift Valley (between 7 00′ and 8 40′ lat. north). *Bulletin Volcanologique, 36*(4), 517-560.

Dimopoulou, E., Tolidis, K., Orfanoudakis, Y., & Adam, K. (2013). Spatial multi-criteria decision analysis for site selection of sustainable stone waste disposal. *Fresenius Environmental Bulletin, 22*(7), 2022-2026.

Ebistu, T. A., & Minale, A. S. (2013). Solid waste dumping site suitability analysis using geographic information system (GIS) and remote sensing for Bahir Dar Town, North Western Ethiopia. *African Journal of Environmental Science and Technology, 7*(11), 9.

Egesi, N., & Nwosu, J. I. (2018). Crushed rocks and dimension stone: Exploration, evaluation, and exploitation in parts of Igarra Area, Southwestern Nigeria. *International Journal of Sciences, 7,* 10–20. doi:https://doi.org/10.18483/ijSci.1398

Ekmekci, M. (1990). Impact of quarries on karst groundwater systems.

Emil, M. K. (2010). *Land degradation assessment for an abondoned coal mine with geospatial information technologies.* Master's thesis , Middle East Technical University.

Engidasew, T. A. (2014). Engineering geological characterization of volcanic rocks of Ethiopian and Sardinian highlands to be used as construction materials.

Engidasew, T., & Abay, A. (2016). Assessment and Evaluation of Volcanic Rocks Used as Construction Materials in the City of Addis Ababa. *Momona Ethiopian Journal of Science, 8*, 193-212.

FAO. (1976). A framework for land evaluation. Food and Agriculture Organization of The United Nations. *Soils Bulletin No. 32*. Retrieved from http://www.fao.org/docrep/x5310e/x5310e00.htm

Fookes, P. G. (1980). An introduction to the influence of natural aggregates on the performance and durability of concrete. *Quarterly Journal of Engineering Geology and Hydrogeology, 13*(4), 207-229.

Fookes, P. G. (1991). Geomaterials. *Quarterly Journal of Engineering Geology and Hydrogeology, 24*(1), 3-15.

Gabarrón, M., Zornoza, R., Acosta, J., Faz, Á., & Martínez-Martínez, S. (2019). 157–205. *Elsevier*, 157–205.

Gamal El-Dine, H., Sadek, R. R., Zayet, H. H., & Refaat, T. M. (2009). Respiratory Problems among Workers Exposed to Quarries dusts in El-Mina Governorate. *EL Mina Med. Bull, 20*(2), 360.

Girma, F., Raghuvanshi, T. K., Ayenew, T., & Hailemariam, T. (2015). Landslide hazard zonation in Ada Berga District, Central Ethiopia–a GIS based statistical approach. *J Geom, 9*(1), 25-38.

Gudissa, L., Raghuvanshi, T. K., Meten, M., & Chemeda, Y. C. (2021). TES analysis for crushed stone aggregate quarry site selection: the case of limestone terrain around Harer-Dire Dawa towns, Eastern Ethiopia. *Arabian Journal of Geosciences, 14*(4), 1-21.

Gudissa, L., Raghuvanshi, T., Meten, M., & Chemeda, Y. C. (2021). A GIS-AHP based approach for optimization of quarry site location around Harer and Dire-Dawa towns, Eastern Ethiopia. *Journal of Environmental Engineering and Landscape Management, 30*(1), 151-164. doi:https://doi.org/10.3846/jeelm.2022.16280

Haile, G., & Suryabhagavan, K. V. (2019). GIS-based approach for identification of potential rainwater harvesting sites in Arsi Zone, Central Ethiopia. *Modeling Earth Systems and Environment, 5*, 353–367. doi:https://doi.org/10.1007/s40808-018-0537-7

Haile, T., Alemayehu, T., & Fisseha, S. (2002). Integrated geophysical investigations to study thermal zones at Boku volcanic Centre, Main Ethiopian Rift. *SINET :Ethiopian Journal of Science, 25*(2), 253-262.

Hepworth, J. V., & Gibson, I. L. (1970). The Structure of Afar and the Northern Part of the Ethiopian Rift: Discussion. *Philosophical Transactions of the Royal Society of London Series A, 267*(1181), 338.

Ireland, G. S. (2004). Quarries and ancillary activities. guidelines for planning authorities, Department of the Environment; Heritage and Local Government. 46.

Irfan, T. Y. (1996). Mineralogy, fabric properties and classification of weathered granites in Hong Kong. *Quarterly Journal of Engineering Geology and Hydrogeology, 29*(1), 5-35.

IS:383. (1970). Indian Standard specification for coarse and fine aggregate from natural souurces for concrete.

Is:383. (2016). Coarse and fine aggregate- specification. clause no5.4.2,.

Jablonsky, J. (2015). Analysis of selected prioritization methods in the analytic hierarchy process. *Journal of Physics: Conference Series*, 622. doi: https://doi.org/10.1088/1742- 6596/622/1/012033

Jafari, S., & Zaredar, N. (2010). Land Suitability Analysis using Multi AttributeDecision Making Approach. *International journal of environmental science and development, 1*(5), 441.

Kakulu, S. E. (2003). Trace metal levels in soils and vegetation from some tin mining areas in Nigeria. *Global Journal of Pure and Applied Sciences, 9*(3), 331-338.

Kazmin, V., & Berhe, S. M. (1978). Geology and development of the Nazret area. *Northern Ethiopian Rift sheet NC37–15, Memoir, 3*, 26.

Khaleghi, E. M., Kamani, M., & Ajalloeian, R. (2019). An investigation of the general relationships between abrasion resistance of aggregates and rock aggregate properties. *Bulletin of Engineering Geology and the Environment, 78*, 3959-3968.

Khan, D., & Samadder, S. R. (2015). A simplified multi-criteria evaluation model for landfill site ranking and selection based on AHP and GIS. *Journal of Environmental Engineering and Landscape Management, 23*(4), 267–278. doi: https://doi.org/10.3846/16486897

Khan, I., & Javed, A. (2012). Spatio-temporal land cover dynamics in open cast coal mine area of Singrauli, MP, India. *J. Geogr. Inform. Syst, 4*, 521–529.

Korkanç, M., & Tuğrul, A. (2004). Evaluation of selected basalts from Niğde, Turkey, as source of concrete aggregate. *Engineering Geology, 75*(3-4), 291-307.

Kou, G., Ergu, D., Chen, Y., & Lin, C. (2016). Pairwise comparison matrix in multiple criteria decision making . *Technological and Economic Development of Economy, 22*(5), 738–765. doi: https://doi.org/10.3846/20294913.2016.1210694

Kozul, R., & Darwin, D. (1997). *Effects of aggregate type, size, and content on concrete strength and fracture energy*. University of Kansas Center for Research, Inc.

Lad, R. J., & Samant, J. S. (2014). Environmental and social impacts of stone quarrying-A case study of Kolhapur District. *International Journal of Current Research, 6*(63), 5664-5669.

Langer WH, G. V. (1993). Natural aggregate- building America’s future. *US Geol Survey Circ, 1110*, 39.

Langer, W. (1988). Natural aggregates of the conterminous United States. *US Geol Survey Bull, 1594*, 33.

Langer, W. H. (2001). *Potential environmental impacts of quarrying stone in karst.* Open-File, US Geol Survey.

Langer, W. H., & Knepper, D. H. (1998). Geologic characterization of natural aggregate: a field geologist's guide to natural aggregate resource assessment. *In Aggregate Resources CRC Press.*, 275-293.

Leroy, M. N., Molay, T. G., Joseph, N., Colince, F. M., & Bienvenu, N. J. (2017). A comparative study of concrete strength using metamorphic, igneous, and sedimentary rocks (crushed gneiss, crushed basalt, alluvial sand) as fine aggregate. *Journal of Architectural Engineering Technology, 6*, 1-6. doi:https://doi.org/10.4172/2168-9717.1000191

Lindqvist, J.E, Akesson, U., & Malaga, K. (2007). Microstructure and functional properties of rock materials. *Materials characterization, 58*(11-12), 1183–1188.

Lüttig, G. W. (1994). Rational management of the geo-environment–A view in favour of “Geobased Planning In Aggregates-Raw Minerals’ Giant. 1-34.

Lyu, H. M., Sun, W. J., Shen, S. L., & Arulrajah, A. (2018). Flood risk assessment in metro systems of mega-cities using a GIS-based modeling approach. *Science of the Total Environment, 626*, 1012-1025 .

M, N. A. (2011). *Properties of Concrete* (5th edition ed.). Pearson Education Limited.

Malczewski, J. (2004). GIS-based land-use suitability analysis a critical overview. *Progress in planning, 62*(1), 3-65.

Mandal, S., & Mondal, S. S. (2016). Analytic Hierarchy Process (AHP) approach for selection of open cast coal mine project. *International Journal of Industrial Engineering Research and Development, 7*(2), 1–13. doi:https://doi.org/10.34218/IJIERD.7.2.2016.001

Manna, A., & Maiti, R. (2014). Opencast coal mining induced defaced topography of RANIGANJ coalfield in India-remote sensing and GIS based analysis. *Journal of the Indian Society of Remote Sensing, 42*(4), 755-764.

Manna, A., & Maiti, R. (2016). Alteration of surface water hydrology by opencast mining in the Raniganj Coalfield Area, India. *Mine Water and the Environment, 35*(2), 156-167.

Maponga, O., & Munyanduri, N. (1998). Environmental Impact of Quarrying on Otere Village,Odeda,South Western Nigeria.

Meyer, W., Pilger, A., Rosler, A., & Stets, J. (1975). Tectonic evolution of the northern part of the Main Ethiopian Rift in southern Ethiopia. *Afar depression of Ethiopia*, *14*(1), 352-362.

Ming'ate, F. L., & Mohamed, M. Y. (2016). Impact of stone quarrying on the environment and the livelihood of communities in Mandera County, Kenya. *Journal of Scientific Research and Reports, 10*(5), 1-9.

Mohr, P. (1967). The Ethiopian Rift System. *Bulletin Geophysical Observatory, 11*, 1-65.

Mohr, P. (1987). Patterns of Faulting in the Ethiopian Rift Valley. *Tectonophysics*, 143.

Mohr, P. A. (1971). *The geology of Ethiopia. Haile Selassie I University Press.*

Mohr, P. A., & Gouin, P. (1960). *Report on a geological excursion through southern Ethiopia*.

Morton, W. H., Rex, D. C., Mitchell, J. G., & Mohr, P. (1979). Riftward younging of volcanic units in the Addis Ababa region, Ethiopian rift valley. *Nature, 280*(5720), 284-288.

Mustafa, A., Singh, M., Sahoo, R., Ahmed, N., Khanna, M., Sarangi, A., & Mishra, A. (2011). Land suitability analysis for different crops: A multi criteria decision making approach using remote sensing and GI. *Researcher, 3*(12), 61–84.

Naeem, M., Khalid, P., Sanaullah, M., & ud Din, Z. (2014). Physio-mechanical and aggregate properties of limestones from Pakistan. *Acta Geodaetica et Geophysica, 49*(3), 369-380.

Nartey, V., Nanor, J., & Klake, K. (2012). Effects of Quarry Activities on Some Selected Communities in the Lower Manya Krobo District of the Eastern Region of Ghana. *Atmospheric and Climate Sciences, 2*, 362-372.

Nemati, K. (2015). Aggregates for Concrete . *Concrete Technology*, 1-16.

Neville, A. (2000). Properties of concrete. 4th.

Neville, A. (2011). *Properties of Concrete* (5th edition ed.). Pearson Education Limited.

Ning, X., Ding, L. Y., Luo, H. B., & Qi, S. J. (2016). A multi-attribute model for construction site layout using intuitionistic fuzzy logic. *Automation in Construction, 72*, 380-387.

Ozcan, O., Musaoglu, N., & Seker, D. (2012). Environmental impact analysis of quarrying activities established on and near a river bed by using remotely sensed data. *Fresenius Environ Bull, 21*(11), 3147–3153.

Pal, S., & Mandal, I. (2017). Impacts of Stone mining and crushing on stream characters and vegetation health of DwarkaRiver Basin of Jharkhand and West Bengal, Eastern India. *Journal of Environmental Geography, 10(1–2),* 11-21. doi:https://doi.org/10.1515/jenge

Prajapati, J., & Karanjit, S. (2019). Effect of coarse aggregate sources on the compressive strength of various grade of nominal mixed concrete. *Journal of Science and Engineering, 7*, 52-60.

Prakash, A., & Gupta, R. P. (1998). Land-use mapping and change detection in a coal mining area-a case study in the Jharia coalfield, India. *International journal of remote sensing, 19*(3), 391-410.

Přikryl, R. (2017). Constructional geomaterials: versatile earth resources in the service of humankind—introduction to the thematic set of papers on: challenges to supply and quality of geomaterials used in construction. *Bulletin of Engineering Geology and the Environment, 76*(1), 1-9.

Rabia, H., & Terribile, F. (2013). Introducing a new parametric concept for land suitability assessment. *International Journal of Environmental Science and Development, 4*(1), 15-19.

Raghuvanshi, T. K., Ibrahim, J., & Ayalew, D. (2014). Slope stability susceptibility evaluation parameter (SSEP) rating scheme–an approach for landslide hazard zonation. *Journal of African Earth Sciences, 99*, 595-612.

Raghuvanshi, T. K., Negassa, L., & Kala, P. M. (2015). GIS based Grid overlay method versus modeling approach–A comparative study for landslide hazard zonation (LHZ) in Meta Robi District of West Showa Zone in Ethiopia. *The Egyptian Journal of Remote Sensing and Space Science, 18*(2), 235-250.

Räisänen, M. (2004). Relationships between texture and mechanical properties of hybrid rocks from the Jaala–Iitti complex, southeastern Finland. *Engineering geology, 74*(3-4), 197-211.

Raisanen, M., Mertamo, M., Stenlid, L., & Viitanen, J. (2006). *Laboratory crushing of rock aggregates.* Geological Survey of Finland.

Rajasekhar, M., Sudarsana, R. G., Imran, B. U., Siddi, R. R., Pradeep, K. B., & Ramachandra, M. (2019). Identification of suitable sites for artificial groundwater recharge structures in semi-arid region of Anantapur District: AHP Approach. *Hydrospatial Adrospatial Analysis, 3*(1), 1–11. doi:https://doi.org/10.21523/gcj3.19030101

Saaty, T. L. (1970). How to make a decision: the analytic hierarchy process. *European journal of operational research, 48*(1), 9-26.

Saaty, T. L. (1977). A scaling method for priorities in hierarchical structures. *Journal of Mathematical Psychology, 15*(3), 234– 281. doi:https://doi.org/10.1016/0022-2496(77)90033-5

Sadat-Noori, S. M., Ebrahimi, K., & Liaghat, A. M. (2014). Groundwater quality assessment using the Water Quality Index and GIS in Saveh-Nobaran aquifer, Iran. *Environmental Earth Sciences, 71*(9), 3827-3843.

Sajid, M., & Arif, M. (2015). Reliance of physico-mechanical properties on petrographic characteristics: consequences from the study of Utla granites, north-west Pakistan. *Bulletin of Engineering Geology and the Environment, 74*(4), 1321-1330.

Sati, V. P. (2015). Socio-Economic and Environmental Impacts of Stone Mining in Shivpuri District, Madhya Predesh, India. *Journal of Scientific Research & Reports, 4*, 47-54.

Satty, T. L. (1970). Principle and appliance of analytic hierarchy process. *Management Science*, 11.

Schmidt, R. J., & Graf, P. E. (1972). Effect of water on resilient modulus of asphalt-treated mixes. *In Association of Asphalt Paving Technologists Proc, 41*, 118-162.

Serbu, R., Marza, B., & Borza, S. (2016). A spatial Analytic Hierarchy Process for identification of water pollution with GIS software in an eco-economy environment. *Sustainability, 8*(11), 1208.

Singh, A. (2007). Revegetation of coal-mine spoils using Prosopis julifora in Singraulicoalfield is a harmful practice from an ecological viewpoint. *Curr. Sci, 93*(9), 1204.

Singh, N. P., Mukherjee, T. K., & Shrivastava, B. B. (1997). Monitoring the impact of coal mining and thermal power industry on landuse pattern in and around Singrauli coalfield using remote sensing data and GIS. *Journal of the Indian Society of Remote, 25*(1), 61-72.

Skutan, B., Kidane, A., & Birhanu, B. (1987). *Geophysical Survey for Hydrogeological study in the Nazareth area (sheet NC 37-15).* Unpublised report, EIGS, Addis Ababa. .

Smith, M. R., & Collis, L. (1993). Aggregates. Sand, gravel and crushed rock aggregates for construction purposes. *Engineering geology special publication, 9*, XX-339.

Smith, M., & Collis, L. (2001). *Aggregates—sand, gravel and crushed rock aggregates for construction purposes* (3 ed.). London: The Geological Society.

Sreenivasa, R., & Ravanu, R. (2014). SocioEconomic and Environmental Perception of Inhabitants of a Quarry Area: A Case Study of Bidadi, Bangalore Rural District. *International Journal of Engineering Science Invention, 4*(3), 11-22.

Subhasis, B. S., Giyasuddin, S., & Arindam, R. (2018). Economic importance of stone quarrying in rural livelihood and its impact on environment: A case study of Saltora Block, Bankura, West Bengal. *International Journal of Scientific Research and Reviews, 7*(3), 1045–1062.

Tadesse, L., Suryabhagavan, K. V., Sridhar, G., & Legesse, G. (2017). Land use and land cover changes and Soil erosion in Yezat Watershed, North Western Ethiopia. *International soil and water conservation research, 5*(2), 85-94.

Tanko. (2007). Environmental concerns, assessment and protection procedures for Nigeria's oil industry; Centre for Development studies and the school of Geography. *Geololy. Environment. Science,* 1.

Taye, A. (2007). *Hydrogeological and Hydrogeochemical Assessment in Adama (Nazareth) - Dera Area, Central Ethiopia.* Masters thesis, Addis Ababa University.

Temiz, N., & Tecim, V. (2009). The use of GIS and multi-criteria decision-making as a decision tool in forestry. *OR Insight, 22*(2), 105-123.

Turner, M., & Ruscher, C. (2004). Change in landscape pattrerns in Georgia USA. *Landscape Ecol, 1*(4), 251–421.

Vaidya, O., & Kumar, S. (2006). Analytic hierarchy process: An overview of applications. *European Journal of Operational Research, 169*(1), 1–29. doi: https://doi.org/10.1016/j.ejor.2004.04.028

Vargahan, B., Shahbazi, F., & Hajrasouli, M. (2011). Quantitative and qualitative land suitability evaluation for maize cultivation in ghobadlou region. *Ozean Journal of Applied Sciences, 4*(1), 91-104.

Waltham, T. (1994). *Foundations of engineering geology* (2 ed.). London: Spon Press.

Wei, D., & Faguang, L. (2011). Specification for mix proportion design of ordinary concrete (JGJ55).

WH, L. (2001). *Potential environmental impacts of quarryingstone in karst—a literature review.* US Geol Survey Open-File.

Woldegabriel, G., Aronson, J. L., & Walter, R. C. (1990). Geology, geochronology, and rift basin development in the central sector of the Main Ethiopia Rift. *Geological Society of America Bulletin, 102*(4), 439-458.

Woodfin, T. M. (1993). Design with nature. *Ian L. McHarg, Wiley*, 197.

Xiao, N., Bennett, D. A., & Armstrong, M. P. (2002). Using evolutionary algorithms to generate alternatives for multiobjective site-search problems. *Environment and Planning A, 34*(4), 639-656.

Xu, L., & Yang, J. B. (2001). *Introduction to multi-criteria decision making and the evidential reasoning approach* (Vol. 106). Manchester: Manchester School of Management.

Xu, Z., & Li, Q. (2014). Integrating the empirical models of benchmark land price and GIS technology for sustainability analysis of urban residential development. *Habitat International, 44*, 79-92.

Yoxas, G., T, S., Sargologou, L., & Stournaras, G. (2011). Multiple criteria analysis for selecting suitable sites for construction of sanitary landfill based on hydrogeological data; Case study of Kea Island (Aegean Sea, Hellas). In: Lambrakis, N., Stournaras, G., Katsanou, K. (eds) Advances in the Research of A. *Environmental Earth Sciences, 2*, 97–104. doi:https://doi.org/10.1007/978-3-642-24076-8_12

Yusof, N. Q., & Zabidi, H. (2016). Correlation of mineralogical and textural characteristics with engineering properties of granitic rock from Hulu Langat, Selangor. *Procedia Chemistry, 19*, 975-980.

Zelenović, V. T., Srdjević, Z., Bajčetić, R., & Vojinović Miloradov, M. (2012). GIS and the analytic hierarchy process for regional landfill site selection in transitional countries: A case study from Serbia. *Environmental Management, 49*, 445–458. doi:https://doi.org/10.1007/s00267-011-9792-3

Appendix

Table 1 Density and specific gravity of the samples from the target areas

Density and specific gravity												
Sample code	Initial volume of water		Volume of water + test specimen		Volume of the test specimen		Mass of the test specimen		Density= mass/volume (KG/m^3)		Specific gravity =Density of solid/density of water	
	Determination		Determination		Determination		Determination		Determination		Determination	
	I	II	I	II	I	II	I	II	I	II	I	II
Q1	500	500	750	730	250	230	570	535	2280	2326	2.28	2.32
Q2	500	500	760	730	260	230	480	470	1846	2043	1.85	2.02
Q3	500	500	735	750	235	250	630	665	2681	2660	2.68	2.66
Q4	500	500	720	710	220	210	475	560	2159	2667	2.15	2.66
Q5	500	500	760	730	260	230	590	515	2269	2239	2.26	2.23
Q6	500	500	620	610	120	110	435	415	3625	3770	3.62	3.77
Q7	500	500	700	750	200	250	525	670	2625	2680	2.62	2.80
Q8	500	500	740	760	240	260	565	605	2354	2326	2.35	2.32
Q9	500	500	750	750	250	250	510	515	2040	2060	2.04	2.06

Table2. Aggregate crushing value of the samples from the target area

Aggregate crushing value (ACV)										
Sample code	Size of aggregate used				Passing		14mm			
					Retained		10mm			
	Weight of mold (WA)		Weight of mold +sample taken(WB)		Weight of sample(WC)= WB-WA		Wight of the aggregate passing 2.36mm sieve (WD)		Aggregate crushing value =WD/WC*100	
	Determination		Determination		Determination		Determination		Determination	
	I	II	I	II	I	II	I	II	I	II
Q1	3330	3330	5410	2350	2080	2020	430	360	20.7	17.8
Q2			5360	5360	2030	2030	580	580	28.6	28.6
Q3			5360	5360	2030	2030	310	305	15.3	15.0
Q4			5485	5490	2155	2160	590	675	27.4	31.3
Q5			5360	5360	2030	2030	680	695	33.5	34.2
Q6			5360	5360	2030	2030	320	315	15.8	15.5
Q7			5375	5360	2045	2030	375	360	18.3	17.7
Q8			5390	5365	2060	2035	320	340	15.5	16.7
Q9			5360	5360	2030	2030	390	390	19.2	19.2

Table 3 Aggregate impact value of the samples from the target area

Aggregate impact value (AIV)															
Sample code	Size of aggregate used			No of blows =15			Passing			14mm					
							Retained			10mm					
	Weight of mold (WA)			Weight of mold +sample taken(WB)			Weight of sample(WC)= WB-WA			Wight of the aggregate passing 2.36mm sieve (WD)			Aggregate impact value =WD/WC*100		
	Determination			Determination			Determination			Determination			Determination		
	I	II	III	I	II	III	I	II	III	I	II	III	I	II	III
Q1	2960	2960	2960	3240	3220	3235	280	260	275	75	75	85	26.85	28.85	30.91
Q2				3145	3155	3165	185	195	205	65	70	70	35.14	35.90	34.15
Q3				3285	3285	3275	325	315	295	35	40	45	10.77	12.70	15.25
Q4				3205	3200	3200	245	240	240	80	80	80	32.65	33.33	33.33
Q5				3215	3215	3205	255	255	245	95	95	90	37.25	36.73	36.73
Q6				3260	3230	3220	300	270	260	45	45	50	15.00	16.67	19.23
Q7				3245	3260	3270	285	300	310	40	45	45	14.04	15.00	14.52
Q8				3230	3200	3245	270	240	285	60	65	65	22.22	22.92	22.81
Q9				3150	3145	3150	190	185	190	50	45	50	26.32	24.32	26.32

Table 4 Los Angeles abrasion value of the samples from the target areas

Aggregate Los Angeles abrasion value (LAAV)								
Sample code	Size of aggregate used				Passing		20mm	14mm
					Retained		14mm	10mm
	Grade B Sphere steel ball uses=11		Rate 33rev/sec Total revolution =500		Mass of each size used(g)		2500	2500
	Initial mass of the test specimen(m1)		Mass retained on 1.7mmseive(m2)		Mass passing 1.7mm sieve(m3)=m1-m2		Los Angeles abrasion value	
	Determination		Determination		Determination		Determination	
	I	II	I	II	I	II	I	II
Q1	5000	5000	3810	3815	1199	1185	23.8	23.7
Q2			3420	3000	1580	2000	31.6	40.0
Q3			4275	4075	725	925	14.5	18.5
Q4			2700	2830	2300	2170	46.0	43.4
Q5			2480	2410	2520	2590	50.4	51.8
Q6			4155	4340	845	660	16.9	13.2
Q7			4145	4100	855	900	17.1	18.0
Q8			4060	3955	940	1045	18.8	20.9
Q9			4280	4160	720	840	14.4	16.8

Table 5 Flakiness and Elongation index of Q1

Aggregate Flakiness and Elongation index				Sample ID:Q1					
BIS Sieves Size (mm)		weight of Aggregate Retained on Various Sieves (g) (C)		Weight of Aggregate Passing Various thickness Gauge (g) (D)		Weight of Non-Flaky Aggregate Retained on thickness Gauge (W_3) (g)		Weight of Aggregate Retained on Various Elongation Gauge (g) (E)	
Passing (A)	Retained (B)	Determination		Determination		Determination		Determination	
		I	II	I	II	I	II	I	II
50	37.5	6285	6445	870	1240	6285	6445	40	0
37.5	28	5000	5380	515	695	5000	5380	570	545
28	20	3505	3410	460	670	3505	3410	295	380
20	14	2015	2050	505	260	2015	2050	770	120
14	10	1060	1035	1380	2120	1060	1035	590	145
10	6.3	505	500	225	200	505	500	245	275
Total weight of W_1 (g)		18370	18820	3955	5185	18370	18820	2510	1465
		Flakiness Index = (Total weight of material passing various thickness Gauges/Total weight of Sample taken)X100			Elongation Index = (Total weight of material Retained on various Length Gauges/Total weight of Non-Flaky Aggregate Retained on thickness Gauge)X100				
Flakiness Index = W_2/W_1X100				22	28	Elongation Index = W_4/W_3X100		14	8
Average Flakiness Index in percentage				25		Average Elongation Index in percentage		11	
Combined flakiness and Elongation Index (%) or Flakiness + Elongation						35			

Table 6 Flakiness and elongation index of Q2

Aggregate Flakiness and Elongation index				Sample : Q2					
BIS Sieves Size (mm)		weight of Aggregate Retained on Various Sieves (g) (C)		Weight of Aggregate Passing Various thickness Gauge (g) (D)		Weight of Non-Flaky Aggregate Retained on thickness Gauge (W_3) (g)		Weight of Aggregate Retained on Various Elongation Gauge (g) (E)	
Passing (A)	Retained (B)	Determination		Determination		Determination		Determination	
		I	II	I	II	I	II	I	II
50	37.5	6765	7230	605	460	6765	7230	0	0
37.5	28	5335	5645	1255	1380	5335	5645	290	580
28	20	3855	5535	540	835	3855	5535	475	990
20	14	2160	2270	400	520	2160	2270	595	810
14	10	855	1270	270	390	855	1270	425	455
10	6.3	435	505	190	205	435	505	235	155
Total weight of W_1 (g)		19405	22455	3260	3790	19405	22455	2020	2990
		Flakiness Index = (Total weight of material passing various thickness Gauges/Total weight of Sample taken)X100			Elongation Index = (Total weight of material Retained on various Length Gauges/Total weight of Non-Flaky Aggregate Retained on thickness Gauge)X100				
Flakiness Index = W_2/W_1X100			17	17	Elongation Index = W_4/W_3X100			10	13
Average Flakiness Index in percentage			17		Average Elongation Index in percentage			12	
Combined flakiness and Elongation Index (%) or Flakiness + Elongation						29			

Table 7 Flakiness and elongation index of Q3

Aggregate Flakiness and Elongation index				Sample ID:Q3					
BIS Sieves Size (mm)		weight of Aggregate Retained on Various Sieves (g) (C)		Weight of Aggregate Passing Various thickness Gauge (g) (D)		Weight of Non-Flaky Aggregate Retained on thickness Gauge (W_3) (g)		Weight of Aggregate Retained on Various Elongation Gauge (g) (E)	
Passing (A)	Retained (B)	Determination		Determination		Determination		Determination	
		I	II	I	II	I	II	I	II
50	37.5	7170	7515	1740	1790	7170	7515	210	110
37.5	28	6235	6410	795	600	6235	6410	855	1195
28	20	5090	5130	540	515	5090	5130	1375	1225
20	14	2165	2270	405	245	2165	2270	495	400
14	10	1095	1015	145	175	1095	1015	140	170
10	6.3	510	520	165	170	510	520	170	185
Total weight of W_1 (g)		22265	22860	3790	3495	22265	22860	3245	3285
		Flakiness Index = (Total weight of material passing various thickness Gauges/Total weight of Sample taken)X100			Elongation Index = (Total weight of material Retained on various Length Gauges/Total weight of Non-Flaky Aggregate Retained on thickness Gauge)X100				
Flakiness Index = W_2/W_1X100			17	15	Elongation Index = W_4/W_3X100			15	14
			16		Average Elongation Index in percentage			15	
Combined flakiness and Elongation Index (%) or Flakiness + Elongation						31			

Table 8 Flakiness and elongation index of the sample from Q4

Aggregate Flakiness and Elongation index		Sample ID:Q4							
BIS Sieves Size (mm)		weight of Aggregate Retained on Various Sieves (g) (C)		Weight of Aggregate Passing Various thickness Gauge (g) (D)		Weight of Non-Flaky Aggregate Retained on thickness Gauge (W_3) (g)		Weight of Aggregate Retained on Various Elongation Gauge (g) (E)	
Passing (A)	Retained (B)	Determination		Determination		Determination		Determination	
		I	II	I	II	I	II	I	II
50	37.5	7305	7360	900	1265	7305	7360	415	115
37.5	28	6155	6125	465	405	6155	6125	1450	545
28	20	5040	5195	245	355	5040	5195	715	1585
20	14	2145	2120	315	435	2145	2120	490	355
14	10	1065	1125	105	90	1065	1125	120	105
10	6.3	550	515	105	90	550	515	195	150
Total weight of W_1 (g)		22260	22440	2135	2640	22260	22440	3385	2855
		Flakiness Index = (Total weight of material passing various thickness Gauges/Total weight of Sample taken)X100			Elongation Index = (Total weight of material Retained on various Length Gauges/Total weight of Non-Flaky Aggregate Retained on thickness Gauge)X100				
Flakiness Index = W_2/W_1X100			10	12	Elongation Index = W_4/W_3X100			15	13
			11		Average Elongation Index in percentage			14	
Combined flakiness and Elongation Index (%) or Flakiness + Elongation						25			

Table 9 Flakiness and elongation index of Q5

Aggregate Flakiness and Elongation index		Sample ID:Q5							
BIS Sieves Size (mm)		weight of Aggregate Retained on Various Sieves (g) (C)		Weight of Aggregate Passing Various thickness Gauge (g) (D)		Weight of Non-Flaky Aggregate Retained on thickness Gauge (W_3) (g)		Weight of Aggregate Retained on Various Elongation Gauge (g) (E)	
Passing (A)	Retained (B)	Determination		Determination		Determination		Determination	
		I	II	I	II	I	II	I	II
50	37.5	7170	7350	770	950	7170	7350	1590	1755
37.5	28	6065	6119	970	615	6065	6119	1450	765
28	20	5175	5140	1190	785	5175	5140	405	920
20	14	2080	2070	245	495	2080	2070	395	330
14	10	1015	1035	410	115	1015	1035	140	70
10	6.3	510	525	90	110	510	525	150	75
Total weight of W_1 (g)		22015	22239	3675	3070	22015	22239	4130	3915
		Flakiness Index = (Total weight of material passing various thickness Gauges/Total weight of Sample taken)X100			Elongation Index = (Total weight of material Retained on various Length Gauges/Total weight of Non-Flaky Aggregate Retained on thickness Gauge)X100				
Flakiness Index = W_2/W_1X100			17	14	Elongation Index = W_4/W_3X100			19	18
			15		Average Elongation Index in percentage			18	
Combined flakiness and Elongation Index (%) or Flakiness + Elongation						33			

Table 10 Flakiness and elongation index of Q6

Aggregate Flakiness and Elongation index				Sample ID:Q6					
BIS Sieves Size (mm)		weight of Aggregate Retained on Various Sieves (g) (C)		Weight of Aggregate Passing Various thickness Gauge (g) (D)		Weight of Non-Flaky Aggregate Retained on thickness Gauge (W_3) (g)		Weight of Aggregate Retained on Various Elongation Gauge (g) (E)	
Passing (A)	Retained (B)	Determination		Determination		Determination		Determination	
		I	II	I	II	I	II	I	II
50	37.5	7120	7145	625	950	7120	7145	415	335
37.5	28	6080	6175	940	965	6080	6175	1475	1120
28	20	5035	5090	1155	1275	5035	5090	670	1280
20	14	2035	2085	625	395	2035	2085	355	295
14	10	1045	1075	205	180	1045	1075	245	245
10	6.3	510	505	245	160	510	505	215	145
Total weight of W_1 (g)		21825	22075	3795	3925	3925	22075	3375	3420
		Flakiness Index = (Total weight of material passing various thickness Gauges/Total weight of Sample taken)X100			Elongation Index = (Total weight of material Retained on various Length Gauges/Total weight of Non-Flaky Aggregate Retained on thickness Gauge)X100				
Flakiness Index = W_2/W_1X100			17	18	Elongation Index = W_4/W_3X100			15	15
			18		Average Elongation Index in percentage			15	
Combined flakiness and Elongation Index (%) or Flakiness + Elongation						33			

Table 11 Flakiness and elongation index of Q7

<table>
<tr><td colspan="4">Aggregate Flakiness and Elongation index</td><td colspan="6">Sample ID:Q7</td></tr>
<tr><td colspan="2">BIS Sieves Size (mm)</td><td colspan="2">weight of Aggregate Retained on Various Sieves (g) (C)</td><td colspan="2">Weight of Aggregate Passing Various thickness Gauge (g) (D)</td><td colspan="2">Weight of Non-Flaky Aggregate Retained on thickness Gauge (W_3) (g)</td><td colspan="2">Weight of Aggregate Retained on Various Elongation Gauge (g) (E)</td></tr>
<tr><td rowspan="2">Passing (A)</td><td rowspan="2">Retained (B)</td><td colspan="2">Determination</td><td colspan="2">Determination</td><td colspan="2">Determination</td><td colspan="2">Determination</td></tr>
<tr><td>I</td><td>II</td><td>I</td><td>II</td><td>I</td><td>II</td><td>I</td><td>II</td></tr>
<tr><td>50</td><td>37.5</td><td>7505</td><td>7363</td><td>665</td><td>1310</td><td>7505</td><td>7363</td><td>0</td><td>0</td></tr>
<tr><td>37.5</td><td>28</td><td>6220</td><td>6400</td><td>645</td><td>265</td><td>6220</td><td>6400</td><td>785</td><td>235</td></tr>
<tr><td>28</td><td>20</td><td>5035</td><td>6080</td><td>765</td><td>780</td><td>5035</td><td>6080</td><td>725</td><td>335</td></tr>
<tr><td>20</td><td>14</td><td>2090</td><td>2065</td><td>270</td><td>280</td><td>2090</td><td>2065</td><td>450</td><td>440</td></tr>
<tr><td>14</td><td>10</td><td>1025</td><td>1120</td><td>255</td><td>240</td><td>1025</td><td>1120</td><td>340</td><td>355</td></tr>
<tr><td>10</td><td>6.3</td><td>555</td><td>510</td><td>240</td><td>195</td><td>555</td><td>510</td><td>195</td><td>270</td></tr>
<tr><td colspan="2">Total weight of W_1 (g)</td><td>22430</td><td>23538</td><td>2840</td><td>3070</td><td>22430</td><td>23538</td><td>2495</td><td>1635</td></tr>
<tr><td colspan="2"></td><td colspan="3">Flakiness Index = (Total weight of material passing various thickness Gauges/Total weight of Sample taken)X100</td><td colspan="5">Elongation Index = (Total weight of material Retained on various Length Gauges/Total weight of Non-Flaky Aggregate Retained on thickness Gauge)X100</td></tr>
<tr><td colspan="3">Flakiness Index = W_2/W_1X100</td><td>13</td><td>13</td><td colspan="3">Elongation Index = W_4/W_3X100</td><td>11</td><td>7</td></tr>
<tr><td colspan="3"></td><td colspan="2">13</td><td colspan="3">Average Elongation Index in percentage</td><td colspan="2">9</td></tr>
<tr><td colspan="6">Combined flakiness and Elongation Index (%) or Flakiness + Elongation</td><td>22</td><td></td><td></td><td></td></tr>
</table>

Table 12 Flakiness and elongation index of Q8

Aggregate Flakiness and Elongation index				Sample ID:Q8					
BIS Sieves Size (mm)		weight of Aggregate Retained on Various Sieves (g) (C)		Weight of Aggregate Passing Various thickness Gauge (g) (D)		Weight of Non-Flaky Aggregate Retained on thickness Gauge (W_3) (g)		Weight of Aggregate Retained on Various Elongation Gauge (g) (E)	
Passing (A)	Retained (B)	Determination		Determination		Determination		Determination	
		I	II	I	II	I	II	I	II
50	37.5	7025	7050	1270	480	7025	7050	1905	2005
37.5	28	6035	6130	1150	640	6035	6130	1510	205
28	20	5015	5070	1140	820	5015	5070	1530	420
20	14	2015	2145	385	615	2015	2145	1235	550
14	10	1025	1015	210	210	1025	1015	240	340
10	6.3	515	505	180	245	515	505	205	145
Total weight of W_1 (g)		21630	21915	4335	3010	3010	21630	6625	3665
		Flakiness Index = (Total weight of material passing various thickness Gauges/Total weight of Sample taken)X100			Elongation Index = (Total weight of material Retained on various Length Gauges/Total weight of Non-Flaky Aggregate Retained on thickness Gauge)X100				
Flakiness Index = W_2/W_1X100				20	14	Elongation Index = W_4/W_3X100		31	17
				17		Average Elongation Index in percentage		24	
Combined flakiness and Elongation Index (%) or Flakiness + Elongation							41		

Table 13 Flakiness and elongation index of Q9

Aggregate Flakiness and Elongation index				Sample ID:Q9					
BIS Sieves Size (mm)		weight of Aggregate Retained on Various Sieves (g) (C)		Weight of Aggregate Passing Various thickness Gauge (g) (D)		Weight of Non-Flaky Aggregate Retained on thickness Gauge (W_3) (g)		Weight of Aggregate Retained on Various Elongation Gauge (g) (E)	
Passing (A)	Retained (B)	Determination		Determination		Determination		Determination	
		I	II	I	II	I	II	I	II
50	37.5	7010	7220	390	535	7010	7220	2128	2100
37.5	28	6035	6015	920	1180	6035	6015	520	525
28	20	5010	5075	880	845	5010	5075	1515	870
20	14	2120	2060	600	665	2120	2060	565	500
14	10	1090	1025	480	175	1090	1025	465	360
10	6.3	505	510	445	265	505	510	470	230
Total weight of W_1 (g)		21770	21902	3715	3665	21770	21905	5663	4585
		Flakiness Index = (Total weight of material passing various thickness Gauges/Total weight of Sample taken)X100			Elongation Index = (Total weight of material Retained on various Length Gauges/Total weight of Non-Flaky Aggregate Retained on thickness Gauge)X100				
Flakiness Index = W_2/W_1X100			17	17	Elongation Index = W_4/W_3X100			26	21
			17		Average Elongation Index in percentage			23	
Combined flakiness and Elongation Index (%) or Flakiness + Elongation						40			

Table 14 Sodium sulphate soundness value of the sample taken from the target area

Sample code	Sodium sulphate soundness value							
	Initial weight of the test specimen		Weight of specimen retained after 5 cycle		Weight of passing		Total weight of the specimen passing the 8mm sieves	Sodium sulphate soundness value=(weight of the specimen passing from 8mm sieve /Initial weight of the test specimen)*100
	19mm to 12.5mm	12.5mm to 9.5mm	19mm to 12.5mm	12.5mm to 9.5mm	19mm to 12.5mm	12.5mm to 9.5mm		
Q1	670	330	632	302	38	28	66	6.6
Q2			542	254	128	76	204	20.4
Q3			538	282	132	48	180	18
Q4			487	247	183	87	270	27
Q5			654	299	16	31	47	4.7
Q6			610	285	60	45	105	10.5
Q7			655	314	15	16	31	3.1
Q8			592	314	78	16	94	9.4
Q9			666	322	4	8	12	1.2

Table 15 Water absorption of the sample taken from the target areas

Sample code	Water absorption of the aggregates					
	Weight of the specimen under surface dry saturated condition(C)		Weight of the sample under oven-dry condition(D)		Water absorption =C-D/D*100	
	Determination		Determination		Determination	
	I	II	I	II	I	II
Q1	580	545	570	535	1.75	1.86
Q2	525	510	480	470	9.37	8.51
Q3	635	670	630	665	0.79	0.75
Q4	490	580	475	560	3.15	2.57
Q5	525	600	515	585	1.94	2..56
Q6	525	675	520	670	0.96	0.74
Q7	440	420	435	415	11.14	1.20
Q8	580	620	564	605	2.65	2.47
Q9	555	560	510	515	8.82	8.73